State Estimation for Active Distribution Network

Sara Nanchian

A thesis submitted to

Imperial College London

for the degree of Doctor of Philosophy

Department of Electrical and Electronic Engineering

Imperial College London

February 2016

To my son (Sam)

With Love

Declaration of Originality

I hereby declare that the work presented in this thesis is my own work, and, where appropriate, contributions from other people whom have been acknowledged.

Sara Nanchian

Copyright Declaration

The copyright of this thesis rests with the author and is made available under a Creative Commons Attribution Non-Commercial No Derivatives licence. Researchers are free to copy, distribute or transmit the thesis on the condition that they attribute it, that they do not use it for commercial purposes and that they do not alter, transform or build upon it. For any reuse or redistribution, researchers must make clear to others the licence terms of this work

Abstract

The requirement of accommodating more distributed generations (DGs) at distribution voltage level has encouraged distribution network operators to utilize their feeder capacity more effectively. This requires the availability of the various network measurements such as voltages, currents, loads, voltage control settings and DG outputs. However these quantities are not directly available in the distribution network control centre. Therefore, to control voltage and power flow in the network, the estimations of these quantities are required. This consists of the monitoring and control of the network operation by application of modern distribution management system (DMS) at the primary substation. The state estimator takes all the available network measurement information, together with a parameterized network model and estimates state of the system in operational time scale. The estimator outputs are then fed into the main control functions and other asset management tools.

Although the application of State Estimation (SE) is very common task at transmission system, the practical application are not common at distribution level. This is due to the fact that the operation, topology and design at distribution level differ from those at transmission level. The untransposed three-phase circuits, unbalanced loads, shorter lines with higher ratio of R/X, and the existence of discrete control options such as transformer tap positions illustrates some of those differences.

These specificities have motivated this piece of research to consider some of the key issues in distribution system state estimation and to develop algorithms to tackle them. This thesis investigated in detail the criterion for identifying suitable solvers for the distribution system state estimation (DSSE) while considering the specific characteristic of the distribution network such as discrete tap position by exploring new optimization methods which are likely to be useful for practical implementation. Some of the research findings have already been disseminated through invited conference panel and IEEE journal.

Contents

ABSTRACT 5

CONTENTS 6

LIST OF FIGURES 10

LIST OF TABLES 13

ABBREVIATIONS 15

ACKNOWLEDGEMENTS 17

LIST OF PUBLICATIONS 18

INTRODUCTION 19

1.1 Research motivation and objectives 19

1.2 Literature review 20

1.2.1 Distribution state estimation methodology 20

1.2.2 Transformer tap estimation 23

1.3 Organization of the thesis 25

1.4 Contributions of the thesis 26

STATE ESTIMATION IN DISTRIBUTION NETWORKS 28

2.1 Overview of state estimation in distribution network....30

2.1.1 Input to the DSSE....32

2.1.2 State estimator block....39

2.2 Weighted Least Square (WLS) estimation....44

2.3 Robust state estimation....45

2.4 Bad data detection....45

2.5 Mathematical modelling for three-phase state estimation....46

2.5.1 Equality constraints c(x):....46

2.5.2 Inequality constraints....47

2.6 Case studies....47

2.6.1 The standard IEEE-13 bus test feeder....47

2.6.2 The standard IEEE-123 bus test feeder....48

2.7 Results and discussions....50

2.8 Conclusions....59

THREE PHASE STATE ESTIMATION BY PARTICLE SWARM OPTIMIZATION....60

3.1 Particle Swarm Optimization (PSO)....62

3.1.1 Selection of parameters for PSO and simulation condition....63

3.1.2 Improving the speed of convergence....64

3.1.3 General algorithm for PSO....65

3.2 Hybrid Particle Swarm Optimization (HPSO)....67

3.3 Distribution state estimation by HPSO....68

3.3.1 Network configuration and network data 68

3.3.2 Power flow calculation 68

3.3.3 State estimation based on HPSO algorithm 68

3.4 Results and discussions 71

3.4.1 Case studies 71

3.4.2 Discussions 81

3.5 Conclusions 83

DISTRIBUTION STATE ESTIMATION BY ORDINAL OPTIMIZATION ..84

4.1 Mathematic formulation of the three phase state estimation problems with continuous and discrete variables 85

4.2 Ordinal Optimization 87

4.2.1 Application of OO to complex optimisation problems 87

4.3 Distribution system state estimation by Ordinal Optimization 89

4.3.1 Network configuration & network data 90

4.3.2 Select N designs in search space 90

4.3.3 Evaluate and order *N* designs 91

4.3.4 Select the best subset 92

4.3.5 Good enough solution 92

4.4 Results and discussions 93

4.4.1 Case study 93

4.4.2 Results and comparisons 94

4.5 Conclusions 99

STATE ESTIMATION FOR ACCURATELY COMPUTING LOSSES IN DISTRIBUTION NETWORK....100

5.1 Breakdown of losses in the UK distribution network model....101

5.2 Loss estimation and minimization-proposed strategy....101

5.3 Case studies and discussions....102

5.3.1 Estimation of losses by HPSO for IEEE-123 bus test system....102

5.3.2 Estimation of losses by OO for 129 bus test system....104

5.4 Conclusions....108

CONCLUSIONS AND FUTURE WORK....109

6.1 Summary of thesis contributions....109

6.2 Future work....111

REFERENCES....113

APPENDIX A : IEEE-13 BUS TEST FEEDER....120

APPENDIX B : IEEE-123 BUS TEST FEEDER....125

APPENDIX C : MEASUREMENT JACOBIAN....137

APPENDIX D : ROBUST ESTIMATION....142

List of Figures

Fig. 2.1 Diagram of a classic distribution management system (DMS) 31

Fig. 2.2 Normal distribution curve 33

Fig. 2.3 Conventional OLTC control algorithm [43] 37

Fig. 2.4 On Line tap changer (OLTC) [45] 38

Fig. 2.5 Two-port π-model of a transmission line 40

Fig. 2.6 IEEE-13 bus distribution system 48

Fig. 2.7 IEEE-123 bus distribution system 49

Fig. 2.8 True and estimated voltage for IEEE-123 bus system at phase a by WLS 53

Fig. 2.9 True and estimated voltage for IEEE-123 bus system at phase b by WLS 53

Fig. 2.10 True and estimated voltage for IEEE-123 bus system at phase c by WLS 54

Fig. 2.11 True and estimated angles for IEEE-123 bus system at phase a by WLS 54

Fig. 2.12 True and estimated angles for IEEE-123 bus system at phase b by WLS 55

Fig. 2.13 True and estimated angles for IEEE-123 bus system at phase c by WLS 55

Fig. 2.14 True and estimated voltage for IEEE-123 bus system at phase a by WLS for different switch status 56

Fig. 2.15 True and estimated voltage for IEEE-123 bus system at phase b by WLS for different switch status 56

Fig. 2.16 True and estimated voltage for IEEE-123 bus system at phase c by WLS for different switch status 57

Fig. 2.17 True and estimated angles for IEEE-123 bus system at phase a by WLS for different switch status 57

Fig. 2.18 True and estimated angles for IEEE-123 bus system at phase b by WLS for different switch status 58

Fig. 2.19 True and estimated angles for IEEE-123 bus system at phase c by WLS for different switch status 58

Fig. 3.1 General algorithm for PSO 67

Fig. 3.2 Setting up of HPSO 70

Fig. 3.3 True and estimated voltage for IEEE-13 bus system at phase a by PSO 73

Fig. 3.4 True and estimated voltage for IEEE-13 bus system at phase b by PSO 73

Fig. 3.5 True and estimated voltage for IEEE-13 bus system at phase c by PSO 74

Fig. 3.6 True and estimated voltage for IEEE-13 bus system at phase a by HPSO 74

Fig. 3.7 True and estimated voltage for IEEE-13 bus system at phase b by HPSO 75

Fig. 3.8 True and estimated voltage for IEEE-13 bus system at phase c by HPSO 75

Fig. 3.9 IEEE-123 bus distribution system 76

Fig. 3.10 Proposed penalty function 76

Fig. 3.11 True and estimated voltage for IEEE-123 bus system at phase a by HPSO 77

Fig. 3.12 True and estimated voltage for IEEE-123 bus system at phase a by HPSO 77

Fig. 3.13 True and estimated voltage for IEEE-123 bus system at phase c by HPSO 78

Fig. 3.14 True and estimated voltage for reduced model of 123 bus system at phase a by HPSO 78

Fig. 3.15 True and estimated voltage for reduced model of 123 bus system at phase b by HPSO 79

Fig. 3.16 True and estimated voltage for reduced model of 123 bus system at phase c by HPSO 79

Fig. 3.17 Convergence characteristic of HPSO and PSO 81

Fig. 4.1 General flow chart of OO 89

Fig. 4.2 129 bus distribution system (extended model of IEEE-123 bus distribution network) 94

Fig. 4.3True and estimated voltage with WLS &OO for phase a for 129 bus system (extended model of IEEE-123 bus distribution network) 95

Fig. 4.4 True and estimated voltage with WLS &OO for phase b for 129 bus system (extended model of IEEE-123 bus distribution network) 96

Fig. 4.5 True and estimated voltage with WLS &OO for phase c for 129 bus system (extended model of IEEE-123 bus distribution network) 96

Fig. 5.1 Breakdown of distribution network losses [64] 102

Fig. 5.2 KW losses for HPSO and WLS for 123 bus system 104

Fig. 5.3 KVAr losses for HPSO and WLS for 123 bus system 104

Fig. 5.4 KW losses for OO and WLS for 129 bus system (extended model of IEEE-123 bus system) 106

Fig. 5.5 KVAr losses for OO and WLS for 129 bus system (extended model of IEEE-123 bus system) 107

Fig. A.1 IEEE 13 bus test system 120

Fig. B.1 IEEE 123 bus test system 125

List of Tables

Table 2.1 True and estimated voltages for IEEE-13 bus distribution system by WLS 51

Table 2.2 The true and estimated angle for IEEE-13 bus distribution system by WLS 52

Table 3.1 The true and estimated tap position for 13 bus system at bus 6 80

Table 3.2 True and estimated tap position for 123 bus system.....80

Table 4.1 Value of the objective function and its sensitivity to tap position for 129 bus system (extended model of IEEE-123 bus distribution network).....97

Table 4.2 True and estimated tap position for 129 bus system (extended model of IEEE-123 bus distribution network) by OO &WLS.....98

Table 4.3 Speed of of solution in HPSO and OO for 129 bus system (extended model of IEEE-123 bus distribution network) 98

Table A.1 Overhead line configuration data.....121

Table A.2 Underground line configuration data 121

Table A.3 Line segment data 122

Table A.4 Transformer data.....122

Table A.5 Capacitor data 123

Table A.6 Regulator data 123

Table A.7 Spot load data.....124

Table A.8 Distributed load data 124

Table B.1(a) Line segment data 126

Table B.2(b) Line segment data.....127

Table B.3(c) Line segment data 128

Table B.4(d) Line segment data.....129

Table B.5 Overhead line configurations (Config.) 130

Table B.6 Underground line configuration (Config.) 130

Table B.7 Three phase switch.....131

Table B.8 Transformer data 131

Table B.9 Regulator data 132

Table B.10(a) Spot loads 133

Table B.11(b) Spot loads 134

Table B.12(c) Spot loads 135

Table B.13 Shunt capacitor 136

Abbreviations

DG	Distributed Generation
DMS	Distribution Management System
SE	State Estimation
DSSE	Distribution System State Estimation
VVC	Voltage and Var Control
OLTC	On Load Tap Changer
SCADA	Security Control And Data Acquisition
WLS	Weighted Least Squares
PMU	Phasor Measurement Unit
NN	Neural Networks
GA	Genetic Algorithms
HBMO	Honey Bee Mating Optimization
PSO	Particle Swarm Optimization
HPSO	Hybrid Particle Swarm Optimization
OO	Ordinal Optimisation
MLE	Maximum Likelihood Estimation
pdf	probability distribution function
LS	Least Squares
QC	Quadratic Constant

WLAV	Weighted Least Absolute Value
SHGM	Schweppe Huber Generalised M
SR	Square Root
MINLP	Mixed Integer Non-Linear
EHV	Extra High Voltage
HV	High Voltage
LV	Low Voltage

Acknowledgements

I would like to express my deepest gratitude to my supervisor Prof. Bikash Pal whom I have been fortunate to have known. The completion of this thesis is the outcome of his inspiring guidance, patience and support over the past four years. For that and the opportunity that he has given me I will be forever indebted to him. Thank you!

I would like to thank my examiners Prof. Vladimir Terzija and Dr. David Angeli for their invaluable feedback on my thesis.

I would like to acknowledge the financial support provided by the Power Networks Research Academy (PNRA) under grant EP/F037686/1to carry out this PhD and the technical suggestions provided by people from Scottish and Southern Energy (UK): David Macleman, David Mobsby and Martin Lee.

Thanks to past and present colleagues in the Control and Power Group at Imperial College London for providing an enjoyable working and learning environment: Sara, Ankur, Yousef, Hossein, Yashodhan, James, Georgios and Jose. Also I would like to thank Ankur Majumdar for his influence on this work through the sharing of knowledge.

Words cannot express the gratitude I owe to my parents Zahra and Mahmoud and my sister Samaneh for their unconditional love and support all these years and beyond. Their encouragements and supports are invaluable to me.

I am very grateful to my husband Nima for his support and understanding during my PhD study. A very special thanks goes to Sam my son who is joy of my life. I would have not been able to achieve this without them.

List of Publications

Journal papers:

- **Nanchian, S**.; Majumdar, A.; Pal, B.C., "Three-Phase State Estimation Using Hybrid Particle Swarm Optimization," in *Smart Grid, IEEE Transactions on* , vol.PP, no.99, pp.1-1.
  URL: http://ieeexplore.ieee.org/stamp/stamp.jsp?tp=&arnumber=7110397&isnumber=5446437

- **Nanchian, S.;** Pal, B.C., " Ordinal Optimization Technique for Three Phase Distribution Network State Estimation with Discrete and Continuous Variables," in *Smart Grid, IEEE Transactions on* , Under review.

Conference papers:

- **Nanchian, S**.; Majumdar, A.; Pal, B.C.; Mobsby, D.; MacLeman, D.F., "Transformer tap estimation using hybrid particle swarm optimization," Invited panel paper in *PES General Meeting | Conference & Exposition, 2014 IEEE* , vol., no., pp.1-5, 27-31 July 2014.

  URL: http://ieeexplore.ieee.org/stamp/stamp.jsp?tp=&arnumber=6938992&isnumber=6938773

Chapter 1

Introduction

1.1 Research motivation and objectives

Driven primarily by the need to integrate wind and solar and other sources of renewable distributed generation (DGs), the operation and control of power distribution network are undergoing unprecedented changes in recent times. At the present time, the amount and size of DG connection is restricted by the passive operational philosophy of distribution networks due to dramatic increase of voltage at the point of connection. The network is now required to be more active in terms of dynamically providing voltage and var control (VVC). The intermittency associated with these new forms of generation has made the VVC very challenging. Switchable shunt capacitor/reactor, tapped line voltage regulators, on load tap changer (OLTC) in primary substation are the traditional options of voltage and VAR control. These devices are now required to operate more actively for providing voltage control in coordination with the fast power electronics based reactive power available from the DGs. The control of these devices needs to be coordinated in distribution substation control for optimal operation. So, the operational visibility of the network is required. This is provided by the state estimation (SE).

The state estimation (SE) is described as a process of finding network voltage magnitudes and angles so that all the other network quantities such as transformer and feeder loadings

etc. can be obtained from them. The estimator outputs can then be fed into the main control functions and asset management softwares/tools.

SE is a very standard task included in supervisory control and data acquisition (SCADA) platform for power transmission systems. However, the practical applications are not that common in distribution networks since the topology, planning, design and operation of distribution network are different from those in the transmission network. For instance, at the distribution level, the network is hardly balanced due to the presence of single and two-phase laterals, untransposed three-phase circuits and unbalanced loads with shorter lines and higher ratio of R/X. There are many unmeasured loads points which make the network highly unobservable. Moreover, some of the control options available with voltage regulating devices are discrete such as transformers taps which conventional state estimator of transmission system is not capable of handling the discrete nature of these devices. Therefore, determining suitable state estimator for distribution system is a challenging task as the tools to evaluate the quality of state estimation must consider a number of key issues such as the state estimation algorithms, network reconfigurations and phase unbalance.

The objectives of the proposed research programme reported in this thesis are to explore and develop the new methodologies for distribution system state estimation and address the key issues for its suitability to practical implementation.

1.2 Literature review

Until recently it was not much important to have mandatory state estimation at distribution system. But with growing controllable devices and components, it is now important to have state estimator for efficient operation of the distribution network.

1.2.1 Distribution state estimation methodology

There have been growing literatures in distribution system state estimation.

Li [1] paper proposes a three phase distribution system state estimator based on weighted least square (WLS) method. Also, the deviation of the bus voltages and power flow are obtained in this paper in order to obtain the associated uncertainty of the estimated states.

Chen and others [2] have provided a thorough model of distribution transformer including

core loss to obtain more accurate state estimates. Standard weighted least square (WLS) is suggested.

Since the quality and adequacy of measurements are less than required, several papers focused on accurately estimating the loads through additional measurement placements. References [3] and [4], have proposed the concept of minimum additional measurements for improving accuracy of the SE in WLS framework.

Because of the radial nature of the distribution network it was found computationally much easier to formulate feeder current as state variables [5], [6]. In this method all the measurements such as power and voltage measurements are converted to their equivalent currents. The results are very convincing and with slight modification in the form of inclusion of constraints in the optimisation objective, small meshed network can also be solved. Small meshed network arises from closing normally open point to extend the feed.

Lin and Tang [7] have improved this further by proposing a new fast decoupled state estimator with equality constraints to increase the speed of convergence. This method is based on the equivalent current measurement in rectangular coordinates.

The authors in [8] later extended the branch current based estimation to obtain a desired set of locations where placements of meters provide maximum impact in terms of accuracy.

References [9], [10], [11] and [12] have demonstrated the impact of various degrees of unbalanced in the network loads and parameters and topological uncertainties on the accuracies of SE. Zero injections are taken as constraints in the nodes having no measurement.

The authors in [13] and [14] have demonstrated further the impact of inaccurate parameters, untransposed lines, ignored transformer vector groups etc. not only on the accuracy of the estimated quantities but on the bad data rejection capability as well. This led to the requirement of synchronised phasor measurements at the distribution level.

Recently Haughton and Heydt [15] proposed a linear state estimator for full three phase unbalanced distribution system. It assumes that synchronised Phasor Measurement Unit (PMU) based measurement and other smart demand measurements are available. It is indicated smart meters may record and transmit active and reactive power, energy

consumption over time intervals, e.g., 5, 15, 60 min, so real time state estimation is not possible.

The authors in [16] used graph theory approach to place measurement to guarantee observability and then solve the node current injection equations to obtain node voltage and angle which appears to work as robust approach to obtain the estimates.

The radial nature of the distribution network is exploited by the backward forward sweep method proposed in [17] which is somewhat along the lines of load estimation as performed in radial distribution system power flow computation. It refines the pseudo measurement by power summation at node.

Reference [18] provides faster algorithm for estimating loads. The approach is to reduce the complexity of the network into several load estimation zones connected through physical measurements.

Ghosh and others [19] have proposed a different method for state estimation in distribution network which applies a probabilistic extension of the radial load flow algorithm. In this algorithm the real measurements are treated as solution constraints. Their method has exploited the radial nature of the distribution network. Celik and Liu [20] have applied a Gauss-Seidel load flow algorithm for state estimation in radial distribution networks. In this approach the load profiles which are based on the historical load data are arranged with regards to the actual measurements. Therefore, the total loads as seen at the measurement point matches with the measurement.

None of the above references considered primary distribution transformer on-load tap changing (OLTC) position as estimated variable. The OLTC makes significant impact on the network voltage profile and hence on the feeder current and power flow. The absence of OLTC action as state variable in the state estimation algorithm produces inaccurate estimates of the network quantities thus making network control less effective. The exclusion of transformer tap position as estimated variable from the above references encouraged us to develop a three phase state estimation algorithm including the tap as discrete variable. Therefore, it would obtain the exact position of transformer tap which is not possible by conventional weighted least square (WLS) method.

1.2.2 Transformer tap estimation

The distribution network has another problem of very rapid and severe voltage fluctuation because of the variable infeed from the DGs. The output from DG being not predictable (solar and wind), the voltage variation in the network is very severe. So the voltage control is as important as feeder flow control. In view of such increasing voltage and var control (VVC) requirement, it is required that state estimation include OLTC as discrete variables to provide most effective control set command.

There has not been much literature in tap observability detection. The authors in [21] proposed a robust algorithm based on Givens rotation of the gain matrix to obtain the state and tap position under erroneous zero injection. The method is demonstrated to work well in Brazilian system models of varying complexity.

The authors in [22] used node voltages, angles and tap position as state variables under the assumption that the taps are continuous. However, in practice OLTC has discrete tap positions so inaccurate estimate produces inaccurate computed values of other network quantities such as feeder flows, losses etc. So, the incorporation of the discrete tap variables in SE is required for efficient network operation and control.

SE is commonly formulated as a weighted least squares (WLS) problem. However, transformer tap positions make the problem a mixed integer nonlinear one. So, the solution of the problem through the normal equation framework is not possible as the objective function is not differentiable [23].

Authors in references [24] and [25] have assumed continuous taps instead of discrete and have incorporated rounding technique or sensitivity method to address the complexity of discrete values. However, this assumption reduces the accuracy of the SE and the solution does not represent the actual network taps positions. Therefore, the estimation of the transformer tap positions has to be obtained from the solution of the mixed integer non-linear optimization problem containing continuous and discrete values [26], [27].

There has been growing interest in the application of heuristic algorithms such as neural networks (NN), genetic algorithms (GA), honey bee mating optimization (HBMO), and particle swarm optimization (PSO) in recent years. To overcome the computational difficulty of such complex optimization problem, these algorithms have been successfully applied to a

wide range of optimization problems where they can handle continuous and integer variables in the objective function as they do not need the function to be continuous and differentiable [28].

PSO appears to be an effective method in comparison to the other heuristic algorithms. It has simple concept which it is easy to implement and produces reasonable results for various problems and performs better in comparison to GA and other evolutionary algorithms [29]. However, its weak form of selection which increases the amount of time to get to the effective area in the solution space has motivated some authors to work on hybrid form of this algorithm.

Author in [30] used hybrid form of PSO (HPSO) combining the feature from PSO and GA to estimate the current state of system. HPSO uses a selection method which is based on the evolution from generation to generation. However, it has been only applied in balanced state estimation problem without considering the unbalanced nature of the system and discrete tap as state variables. The assumption of balanced system model which assumes that line parameters and loads are balanced would results in unexpected system performance or undesirable operating situations. Since the analysis is applied on the single phase model, simply using the positive sequence network for estimation of the system states. Therefore, an appropriate three-phase estimator is required to accurately obtain the states of the system including the discrete value of transformer tap positions in an unbalanced distribution network [6], [31]. This has been the main motivation for the application of HPSO algorithm for a comprehensive three phase state estimation in unbalanced distribution network with inclusion of discrete tap as state variable in this study.

However, similar to other heuristic algorithms, the HPSO technique convergence time is long for a reasonably sized network model. This is one of the down sides of application of heuristic algorithm for SE in real time. Therefore, it makes the HPSO result very valuable for network computation used for operational planning purposes such as hour ahead contingency analysis and reactive power control scheduling, loss estimation for dynamic pricing purpose as it generate more accurate estimation of the system states even though the calculation is not done in real time.

In order to reduce the convergence time in this study we have applied the ordinal optimization (OO) algorithm for state estimation in distribution network. The main purpose

of application of OO theory in distribution system state estimation (DSSE) problem is to limit the searching space to the good subset of search space through limited sampling [32]. This is expected to reduce the solution time. This method helps to find a good enough solution with high probability instead of the best in solving problems with vast search space. This is the case in finding the optimal solution for DSSE problem with continuous and discrete variables combined.

The authors in [26] and [33] considered ordinal optimization (OO) and mixed-integer quadratic programming on a balanced three-phase network model without considering the unbalanced nature of the distribution system. However my research proposes a full three-phase state estimator including unbalanced load network model and the discrete taps as additional estimated variables based on OO optimization technique in order to estimate the discrete value of the transformer taps and obtain more accurate value of the losses in the network. Since, obtaining accurate losses in the network assist to develop tools to reduce them and setting more reasonable electricity price for customers.

1.3 Organization of the thesis

Following this introduction and literature review, the remaining chapters of the thesis are organised as follows:

Chapter 2 provides an overview of state estimation in distribution network. Various methods of robust estimation and their strengths and weaknesses have been discussed briefly.

The solution of weighted least squares estimation derived from maximum likelihood estimation concept is discussed in detail.

The mathematical modelling of the three-phase state estimator alongside the three phase model of various components of the distribution network such as distribution lines, transformers, loads and switches have been described in details. Also, various test system models used for simulations and assumptions for the DSSE are described.

Chapter 3 proposes a technique which addresses the transformer taps estimation in the context of distribution system state estimation (DSSE). The mathematic formulation of hybrid particle swarm optimization (HPSO) method for three phase state estimation with inclusion of transformer tap position as state variable is detailed. The state estimation results

utilising the HPSO algorithm are presented. The results of this chapter have been published in [34].

Chapter 4 studies the transformer taps estimation through the ordinal optimization technique in the context of three phase distribution system state estimation (DSSE) with continuous and discrete variables. The formulation of the three phase state estimation problem with continuous and discrete value and its solution through the ordinal optimization technique and the optimality of the proposed technique are discussed in detail.

Chapter 5 proposes the loss estimation in distribution network based on various methods of state estimation which have been studied in the previous chapters of this research such as WLS, HPSO and OO. The loss estimation results utilising the WLS, HPSO and OO algorithm are presented.

Chapter 6 summarises the findings in this work with a brief overview of the future research directions.

1.4 Contributions of the thesis

This thesis attempts to address the DSSE issues discussed in Section 1.2. The contributions of the thesis can be summarised as follows:

1. The DSSE literature is mostly based on adaptation of transmission system SE algorithms (particularly WLS). The issue of the discrete value of transformer tap position is addressed through the assumption of continuous value for balanced system which is not correct representative of the tap positions. Moreover, the performance of the three phase SE algorithms in distribution network with discrete taps is not addressed in the literature. The work presented in this thesis investigates the existing transmission system SE techniques and algorithms and assesses their suitability to the DSSE problem.

2. It is clear from the existing literature that there is no methodology available to estimate the discrete value of transformer tap position in unbalanced distribution networks. The estimation of transformer taps position in unbalanced distribution system can be addressed by application of hybrid particle swarm optimization (HPSO) method which can also improve the quality of voltage and angle estimates

across the network. My research demonstrates the comprehensive modelling, computation and analysis in this context for the first time. I have also made several modifications of traditional PSO and HPSO techniques to obtain solutions faster. The selected algorithm is tested on the IEEE 13-bus and 123-bus distribution network.

3. My research proposes a full three-phase state estimator including unbalanced load network model and the discrete taps as additional estimated variables based on Ordinal optimization (OO) method in order to speed up the convergence time and estimate the discrete value of the transformer taps. The OO algorithm is tested on 129 bus distribution network (extended model of IEEE-123 bus distribution network).

4. The obtained losses from HPSO and OO method proved to be more accurate in comparison with the conventional method of estimation (WLS). Also, obtaining the lower losses has a direct effect in reducing the cost of electricity for customer.

Chapter 2

State estimation in distribution networks

In recent times almost all power networks across the world are undergoing significant transition in respect of planning, design, operation and control because of the need to integrate large volume of renewable sources of generations The nature and location of these generations are such that, sometime it is more economical to be connected to the network at lower distribution voltage rather than feeding through transmission. This means that significant amount of network reinforcement is necessary to accommodate theses distributed generation (DG) at distribution level. Currently, the amount of DG at the distribution level is limited by the passive operating technique of distribution networks. Excessive voltage rise is experienced at the point of generator connection when DG output is high. So the amount of generation that can be absorbed in the network is restricted by the voltage limit violations. As a consequence, advanced power flow and voltage control will be required to guarantee acceptable quality of supply levels [35].

The effective control of the network relies on the availability of the network voltages, currents, loads, voltage control setting and DG output information. Usually in the power distribution context, these quantities may not be directly available at the substation control centre. So the estimation of these quantities will be required to control voltage and power flow in the network. This is a typical state estimation problem. For this, different state estimation (SE) techniques have been developed. State estimation is related to the

conventional load-flow calculations and is designed to handle many uncertainties associated with trying to do on line load flow for an actual system using meter reading telemetered in real time to a digital computer.

State estimation procedures are used from long to assess the network operating conditions of transmission systems where a large number of redundant on-line measurements and reliable communication channels are available. These form a fully integrated Supervisory Control and Data Acquisition (SCADA) system which convey the dispersed measurements to the centralized controller [36]. However, in distribution systems the idea is relatively new and practical applications are not that common because the planning, design and operation philosophy of distribution network are different from those in the transmission network. Distribution systems have many features that are different from transmission systems. These include:

1. Topology

    - Radial topology: Many independent substations supplying several radial feeders.
    - Have multiple short branches with low impedance as well as high R/X ratios. In distribution network the distances between conductors of cables are very small therefore the inductance is small and the ratio of R/X is high. These may cause numerical problems for traditional state estimation algorithms.

2. Phase unbalance

    - The degree of unbalance, at distribution networks, may be quite high and each phase must be considered independently due to the presence of single and two-phase laterals, untransposed three-phase circuits and unbalanced loads while the degree of unbalance in transmission network is appropriately small that it can be ignored and only positive sequence terms analysed.

3. Network size

    - A typical network size ranges from a few 10,000 to 100,000 electrical nodes while in transmission network a typical network size ranges from a few hundred busses to one to two thousand [37].

4. Real-time measurements

- The network is highly unobservable due to limited numbers of real-time measurements. At present, the availability of real time measurements is often limited to the Primary Substation.
- There are many more load points than measurements and the network is highly unobservable and each measurement is counted as a critical measurement [38]. Since the numbers of real measurements are low in distribution network, the implementation of SE tools requires large number of forecasted data to overcome this observability problem.

5. Discrete value of control devices

- Some of the control options available with voltage regulating devices are discrete such as transformers taps. Therefore, the conventional WLS estimator is not capable of handling of the non-Gaussian nature of the measurements and the discrete nature of the objective function.

All of these features make the distribution system state estimation more challenging compared to that in the transmission network. As a consequence, transmission state estimation techniques cannot be applied directly to distribution systems. In order to develop new methods of state estimation in distribution network and improve the quality of estimate in distribution network, the number of issues such as the state estimation algorithms, modeling of pseudo measurements, placement of phasor measurement units (PMUs), network reconfigurations and phase unbalance should be considered [5], [13].

The objectives of this research are to study and develop new techniques for distribution system state estimation (DSSE) while considering the specific characteristic of the distribution network and investigating the new optimization method which can estimate the discrete position of transformer taps efficiently and accurately.

2.1 Overview of state estimation in distribution network

The state estimation is a data processing algorithm which takes the network measurement information, together with a parameterized network model and instantaneously identifies the overall system operating state. This involves collection of voltage magnitudes, current

injections, and real and reactive power flows such that there are more measurements than state variables, thus forming an over-determined system. These measurements are assigned a weight based on their accuracy and inserted into load flow-like equations which are non-linear and required multiple iterations to arrive at a solution. The outcome of this minimization is the system state .The static state of an electric power system is defined as the vector of the voltage magnitudes and angles at all network buses. The estimator outputs can then be fed into the main control functions and asset management software [39].

The operators can utilize this information to make decisions regarding the control and operation of their system.

This section explains the various components of the DSSE functional block in a typical distribution management system (DMS). Fig. 2.1 shows the diagram of a classic distribution management system (DMS) design. The configurations of these components are as follows:

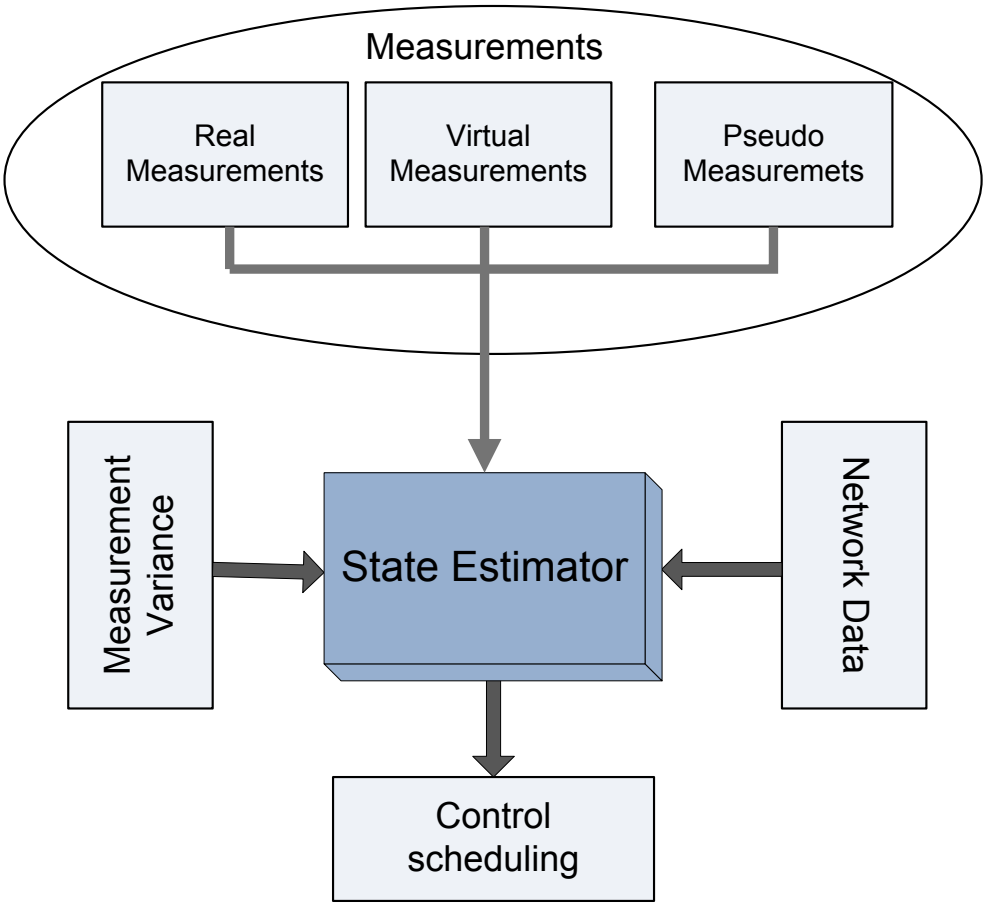


Fig. 2.1 Diagram of a classic distribution management system (DMS)

2.1.1 Input to the DSSE

DSSE consists of all the inputs to the DSSE block and it consists of following components:

Measurements

- Actual measurements: These are all the telemetered values from metering devices which include magnitude of voltages, line currents, real and reactive power injections and real and reactive power flows $(v, \delta, I, P, Q, P_{ij}, Q_{ij})$.
- Pseudo measurements: These are the estimated value of loads. In distribution system it is very difficult to get exact load information in real time since the major part of the MV-LV networks are poorly monitored and supported by weak communication facility. Therefore, the availability of required measurement is not practical due to the massive size of the system and the associated costs [40]. As a consequence, the implementation of SE tools requires a large number of so-called Pseudo Measurements to overcome this observability problem. A probabilistic load model based on historical data or analysis of customer billing data is required for modeling the load. Therefore, modelling the loads as pseudo measurements is considered in the absence of measured load information [37].
- Virtual measurements: These are the zero power injections at the buses which have no loads and no generations.

Measurement noise (variance)

Having knowledge of noise characteristics is another important input to SE algorithm. It determines the accuracy of the measurements for accurate estimation of the system states. Measurement variance for telemetered measurements is obtained from the accuracy of the metering devices in the network. The virtual measurements are very accurate measurements therefore they have very low variances associated to them. While pseudo measurements are the measurements with high degree of uncertainty, therefore they have error components with high variances.

Measurement variance can be obtained from the equation (2.1). The standard deviation is used to provide the weight of each measurement as all the measurements are modelled assumed to have a normal distribution.

$$\sigma = \frac{\mu \times \%error}{3 \times 100} \tag{2.1}$$

As shown in Fig. 2.2, $\pm 3\sigma$ deviation covers around 99.73% area of Gaussian curve. Hence, for a measurement z given % of error about mean μ_z, the standard deviation of error can be obtained from equation (2.1).

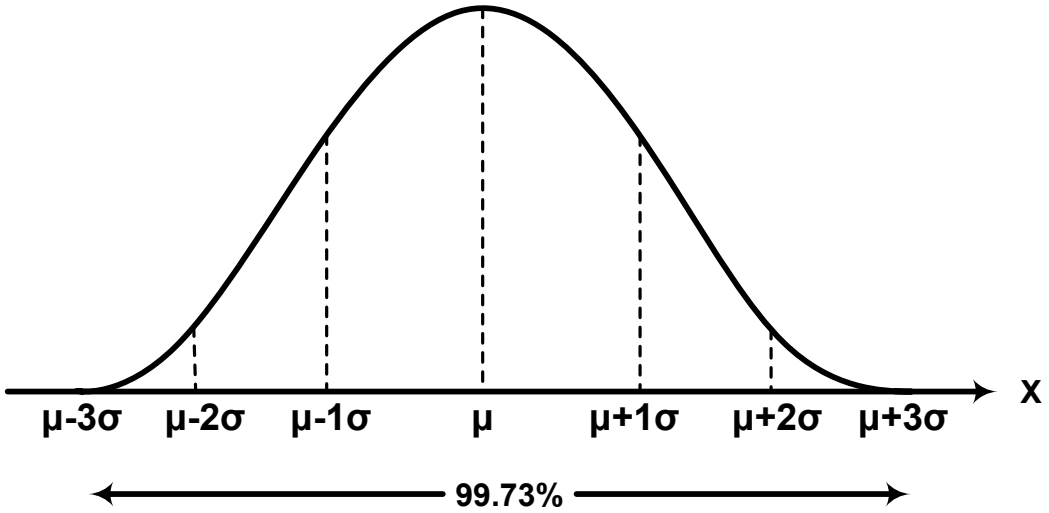


Fig. 2.2 Normal distribution curve

Network data

The modelling of various network components of DSSE is a challenging task. For instance, the presence of unsymmetrical-network components and unbalanced-load on unbalanced distribution system makes it essential to consider the exact model of the system components (three-phase model). It includes information about line resistance, reactance, tap setting connectivity information etc. [41].

The following provides information regarding three phase model of various components of the network such as distribution line, transformers and switches.

- Line model

– In the case of balanced three phase system, the line impedance has been calculated based on the assumptions of balanced three-phase currents and complete transposition of

conductors. However, the distribution overhead lines and underground cables can be three-phase, two-phase or single-phase and are most often non-transposed serving unbalanced loads. In addition, since the voltage drops due to the mutual coupling of the lines is playing important part in the analysis of the distribution network, it is important to compute the impedance of the overhead and underground line segment as accurate as possible. Therefore, it is necessary to retain the self and mutual impedance terms of the conductors and take into account the ground return path for the unbalanced currents [42]. A modified Carson's equation [42] is commonly applied to model the overhead lines and underground cables.

$$Z_{ii=} r_i + 0.095 + j0.121.\left(Ln\frac{1}{GMR_i} + 7.934\right)\ \ \Omega/mile \tag{2.2}$$

$$Z_{ij=} 0.095 + j0.121.\left(Ln\frac{1}{D_{ij}} + 7.934\right)\qquad \Omega/mile \tag{2.3}$$

Where

Z_{ii}: Self-impedance of conductor *i* in Ω/mile

Z_{ij}: Mutual impedance between conductors *i* and *j* in Ω/mile

r_i : Resistance of conductor *i* in Ω/mile

GMR_i: Geometric Mean Radius of conductor *i* in feet

D_{ij} : distance between conductors *i* and *j* in feet

While using the modified Carson's equations there is no need to make any assumptions, such as transposition of the lines. By assuming an untransposed line and including the actual phasing of the line and correct spacing between the conductors, the most accurate values of the phase impedances, self and mutual, are determined.

- While applying modified Carson's equations (2.2) and (2.3) to a three phase overhead or underground circuit which consists of *3* phases and *n* neutral conductors the resulting impedance matrix will be (*3*+*n*)×(*3*+*n*). For most applications, it is necessary to have the *3*×*3* phase impedance matrix. Therefore, the following Kron reduction (2.4) is applied in order to break the impedance matrix into the *3*×*3* phase frame matrix. In this approach,

all the lines will be modelled by *3×3* phase impedance matrix and for two phase and single phase lines the missing phases are modelled by setting the impedance element to zero [42].

$$[Z_{abc}] = [Z_{ij}] - [Z_{in}] \times [Z_{nn}]^{-1} \times [Z_{nj}] \quad (2.4)$$

Where

$[Z_{abc}]$: Phase impedance matrix after Kron reduction

$[Z_{nn}]$: Self-impedance matrix of *n* neutral conductors in Ω/mile

$[Z_{in}]$: Mutual impedance matrix between conductors *i* and *n* neutral conductors in Ω/mile

$[Z_{nj}]$: Mutual impedance matrix between *n* neutral conductors and conductors *j* in Ω/mile

- Transformer model

- The three phase transformer banks are commonly used in the distribution network and provide the final voltage transformation to the customer's load. The conventional transformer models based on a balanced three-phase assumption can no longer be used when system is unbalanced. Three phase transformers are modeled by an admittance matrix which depends on the connection type. The admittance matrix of a transformer is sub-divided into sub-matrices for both self and mutual admittances between the primary and secondary. In the analysis of the distribution feeder, it is required to model the various three phase transformer connections correctly. The comprehensive calculations of three phase transformers and their various connections can be found in reference [42].
- Besides stepping up/down of voltage, the other important network function offered by the transformer is voltage regulation through on-load tap changing mechanism (OLTC). Generally OLTC is equipped with high voltage winding as the current it has to handle is lower. In the context of state estimation it is important to study the applications of On-load tap-changers (OLTCs) for regulating voltage in power networks. OLTCs assist voltage regulation by changing the transformer ratio without interrupting load current. It changes the ratio of a transformer by adding or subtracting turns from either the primary or the secondary winding depending on the situation. Therefore transformer is fitted with taps winding which is connected to the OLTC. The tap changer control mechanism initiates when there is an unexpected or gradual change in power demand which can

affect the voltage at the transformer bus. The procedure of conventional OLTC mechanism can be described as follows: The conventional OLTC starts with comparison of the voltage measurement which has been obtained from the secondary side of transformer voltage, with the reference value of voltage. If the voltage deviation exceeds the predefined value of dead band a timer inside the control mechanism starts. If the difference doesn't return inside of the specified limit for certain period of time (commonly ±0.83% off the nominal voltage for dead band and 30 or 60 seconds for time delay), it will conduct a command to the mechanical system to perform a tap changing action. Fig. 2.3 and Fig. 2.4 shows the general OLTC control algorithm and OLTC tap positions figure. The ideal tap position is somewhere between two actual tap positions which leads to a voltage at reference value. Applying the one above the ideal position results in a voltage higher than reference value and vice versa. Thus the tap changer will keep moving between these two positions if there is not a wide enough dead band set in the controller to stop it [43], [44]. The numbers of taps are finite and vary. Some OLTC acts on 32 tap positions, some on 16 etc. The voltage adjustment or control is in step, which is of discrete value. When tap position is considered as control variable the voltage control is a discrete optimization problem which is complex to solve.

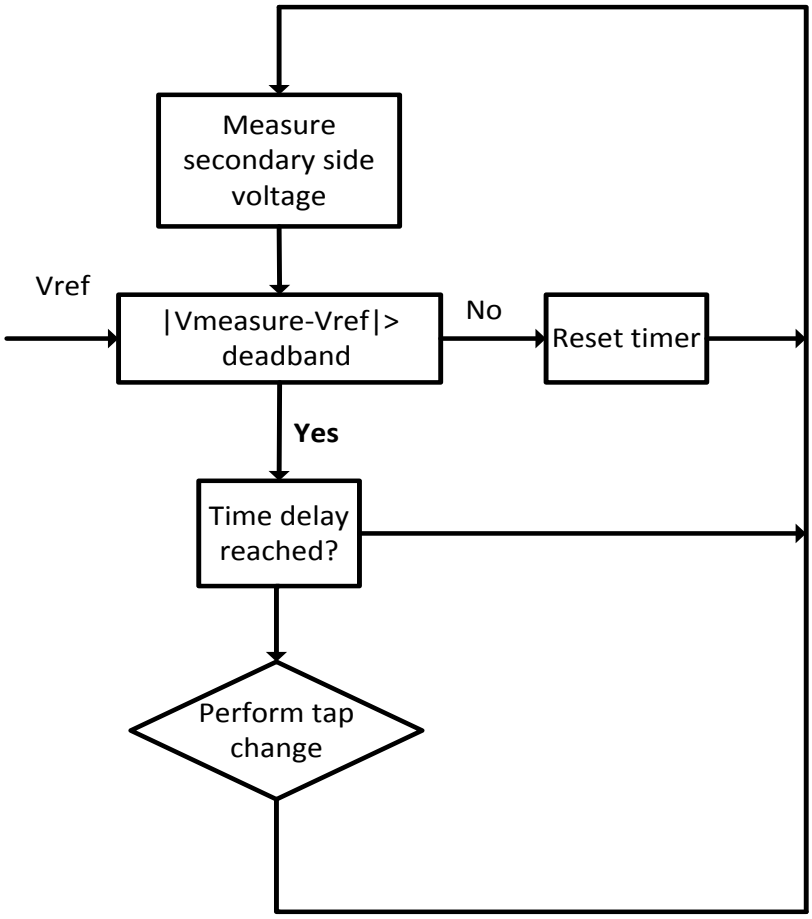


Fig. 2.3 Conventional OLTC control algorithm [43]

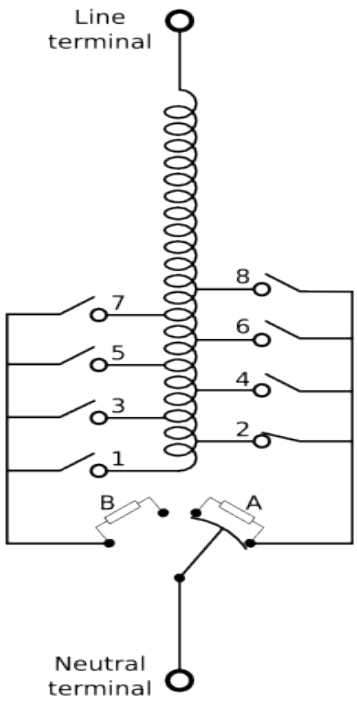


Fig. 2.4 On Line tap changer (OLTC) [45]

- Switch model

– Switches are modelled as branches with zero impedance when the switch is closed or as branches with zero admittance when it is open. The operational constraints imposed by the open or closed status of the switching branches will be as follows:

  – When the switch between bus *i* and bus *j* is closed for branch *i-j*, the voltages and angles for bus *i* and bus *j* for all the three phases are equal.

$$V_i - V_j = 0 \quad , \quad \delta_i - \delta_j = 0$$

  – When the switch is open between bus *i* and bus *j*, the active and reactive power flow through the switch will be zero

$$P_{ij} = 0 \ , \quad Q_{ij} = 0$$

These are to be included as equality constraints in the state estimation formulation.

- Load model

The loads on distribution network are generally unbalanced and are connected in a grounded wye configuration or an ungrounded delta configuration. It is also possible to have three-phase, two-phase, or single-phase loads with varying degree of unbalance. The loads are commonly indicated by complex power consumed per phase and supposed to be line-to-neutral for wye load and line-to-line for delta load [42].

In this study, loads are modelled as constant impedance, constant current and constant complex power or any combination of the three. Typically, the load values are given as nominal power delivered to the load and are converted into the appropriate constant model parameters. The general form of ZIP model is as follows [46]:

$$P_L = P_n \left(c_{1P} + c_{2P} \left(\frac{V}{V_n} \right) + c_{3P} \left(\frac{V}{V_n} \right)^2 \right) \tag{2.5}$$

$$Q_L = Q_n \left(c_{1Q} + c_{2Q} \left(\frac{V}{V_n} \right) + c_{3Q} \left(\frac{V}{V_n} \right)^2 \right) \tag{2.6}$$

The two-phase and single-phase loads are modelled by setting the values of the complex power to zero for the non-existent phases for both the wye and delta connected loads [42].

2.1.2 State estimator block

The purpose of the state estimation is to find the best estimate of the system states based on the available information about the system and measurements. The static state of an electric power system is defined as the vector of the voltage magnitudes and angles at all network buses. One way to achieve this is by application of maximum likelihood estimation (MLE), which has been explained in the following section.

Measurement model

Considering the vector $z = [z_1 z_2 \ldots\ldots\ z_m]^T$ as a set of given measurements where m is the number of measurements and vector $x = [V_1 \ldots V_n\ \delta_2 \ldots\ldots\ \delta_n]^T$ as the state vector containing voltage magnitudes and voltage angles, where n is the number of buses. The non-linear function relating the vector of measurements to the state vector x defined as:

$$z = h(x) + r \tag{2.7}$$

Where the vector $r \sim \mathrm{N}(0, R)$ is zero mean measurement noise vector with covariance matrix $R = Cov(r) = E[r.r^T] = diag(\sigma_1^2, \sigma_2^2, \ldots, \sigma_m^2)$. These errors are assumed to be independent of one another. In order to be able to solve the estimation problem, the number of measurements should be equal or more than the number of state variables. For instance having *n* numbers of buses in the network, the number of state variables would be $2n - 1$; n voltage magnitudes and n-1 voltage angles with one angle taken as a reference. Therefore, the number of measurements (m) required to obtain the value of states variable should be $m \geq (2n - 1)$. In distribution system number of actual measurements is less than the states, so it is not possible to have a solution of the states. The option is to add pseudo measurements in order to have unique solution. Certainly errors have been added to these pseudo measurements as the pseudo measurements are not as accurate as the actual measurement.

Measurement function:

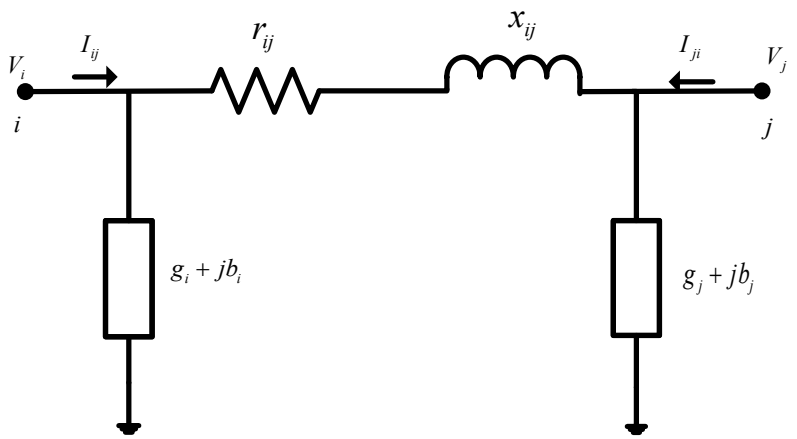


Fig. 2.5 Two-port π-model of a transmission line

The general two-port π-model for the network branches for a transmission system is shown in Fig. 2.5. This model has been used to relate the state vector to each type of measurements. The same model can be expanded to the three-phase distribution system such that each element of the π-model for network branches is a 3×3 matrix rather than single element.The most common type of measurements include the bus power injections, line power flows, bus voltage magnitude and magnitudes of current flows in the lines [47].

- Power injections

In three phase system $x = [V_i^k, \delta_i^k]$, where $V_i^k = [V_i^a \; V_i^b \; V_i^c \;]^T$ is the vector of three-phase voltage magnitude at bus *i*, $\delta_i^k = [\delta_i^a \; \delta_i^b \; \delta_i^c \;]^T$ denotes the phase angles of bus *i* except the reference bus.

Where

i=1:n *n* : Number of buses

k=1:3 *k* : phases that can be 1, 2 or 3

In three-phase model, the power injected at bus *i* for phase *k* can be written as:

$$P_i^k = V_i^k \sum_{l=1}^{3} \sum_{j=1}^{n} V_j^l [G_{ij}^{k,l} cos(\delta_i^k - \delta_j^l) + B_{ij}^{k,l} sin(\delta_i^k - \delta_j^l)] \quad (2.8)$$

$$Q_i^k = V_i^k \sum_{l=1}^{3} \sum_{j=1}^{n} V_j^l [G_{ij}^{k,l} sin(\delta_i^k - \delta_j^l) - B_{ij}^{k,l} cos(\delta_i^k - \delta_j^l)] \quad (2.9)$$

Where

P_i^k , Q_i^k: Active and reactive power injections of phase *k* in bus *i*.

G+jB : System admittance matrix,

n : Number of buses

l : Number of phases that can be 1, 2 or 3 phase.

- The power flow

The power flow from bus *i* to bus *j* for phase *k* can be written as follows:

$$P_{ij}^k = V_i^k \sum_{l=1}^{3} V_i^l [G_{ij}^{k,l} cos(\delta_i^k - \delta_j^l) + B_{ij}^{k,l} sin(\delta_i^k - \delta_j^l)] - V_i^k \sum_{l=1}^{3} V_j^l [G_{ij}^{k,l} cos(\delta_i^k - \delta_j^l) + B_{ij}^{k,l} sin(\delta_i^k - \delta_j^l)] \quad (2.10)$$

$$Q_{ij}^k = -V_i^k \sum_{l=1}^{3} V_i^l [G_{ij}^{k,l} sin(\delta_i^k - \delta_j^l) - B_{ij}^{k,l} cos(\delta_i^k - \delta_j^l)] - V_i^k \sum_{l=1}^{3} V_j^l [G_{ij}^{k,l} sin(\delta_i^k - \delta_j^l) - B_{ij}^{k,l} cos(\delta_i^k - \delta_j^l)] \quad (2.11)$$

Where

P_{ij}^k , Q_{ij}^k : Active and reactive power flow of phase *k* from bus i to bus *j*.

V_i^l : Voltage magnitude of phase *l* at bus *i*.

δ_i^l : Angle of phase *l* in bus *i*.

- The line current

The line current flow between bus *i* and bus *j* for a phase *k* is given by:

$$I_{ij}^k = \frac{\sqrt{(P_{ij}^k)^2 + (Q_{ij}^k)^2}}{V_i^k} \tag{2.12}$$

Measurement Jacobian

It is required to linearize the vector of measurement functions to apply the state estimator. Therefore the Jacobian matrix whose elements are the first order derivatives of the measurement functions with respect to the state variables should be obtained as follows:

$$H = \begin{bmatrix} \frac{\partial h_1(x)}{\partial \delta_1} \cdots & \frac{\partial h_1(x)}{\partial \delta_{n-1}} & \frac{\partial h_1(x)}{\partial V_1} \cdots & \frac{\partial h_1(x)}{\partial V_n} \\ \frac{\partial h_2(x)}{\partial \delta_1} \cdots & \frac{\partial h_2(x)}{\partial \delta_{n-1}} & \frac{\partial h_2(x)}{\partial V_1} \cdots & \frac{\partial h_2(x)}{\partial V_n} \\ \vdots & \vdots & \vdots & \vdots \\ \vdots & \vdots & \vdots & \vdots \\ \frac{\partial h_m(x)}{\partial \delta_1} \cdots & \frac{\partial h_m(x)}{\partial \delta_{n-1}} & \frac{\partial h_m(x)}{\partial V_1} \cdots & \frac{\partial h_m(x)}{\partial V_n} \end{bmatrix} \tag{2.13}$$

The organisation and evaluation of Jacobian elements corresponding to the real and reactive power injections, real and reactive power flows, the branch current flows and the voltage magnitude measurements are very routine but involves lengthy expressions and manipulation of expressions particularly for three phase system. So in order not to lose the flow of this chapter into lengthy mathematical details, they are given in details in Appendix C.

Maximum likelihood estimation

The state vector *x* is associated to the measurement vector *z* by the measurement model. The measurement vector is stochastic due to measurement noise and is known in advance. However there is no prior information about the state vector which is deterministic. Considering $f(z|x)$ as a joint probability density function (pdf) of *z* with the unknown *x* consequently computing $f(z|x)$ results in estimating *x* based on maximum likelihood

criterion. The Maximum Likelihood Estimation (MLE) is the method which has been extensively used in statistics. It has been applied in state estimation to define the state of the system. It begins by creating the likelihood function of the measurement vector. The likelihood function is simply the product of each of the probability density functions of each measurement. Let assume all the measurements have Gaussian probability distribution function (pdf). The joint pdf of these independent measurements can be expressed as the product of individual pdf's [39], [47].

$$f_m^z = f_{(z1)}\, f_{(z2)} \ldots\ldots\ldots\ldots f_{(zm)} \tag{2.14}$$

Where:

$$z = [z_1, z_2, \ldots \ldots z_m]^T$$

The function f_m^z is called the likelihood function for z. It is a measure of probability of observing the particular set of measurements in the vector z. The objective of the maximum likelihood estimation is to maximise the likelihood function by varying the assumed parameters of density function. In order to make the process of determining the optimum parameter value simpler, the function is exchanged by its logarithm. This can be done by maximizing the logarithm of the likelihood function $f_m(z)$ or minimizing the weighted sum of squares of the residuals [47]. Hence, it can be obtained by solving the following problem:

Maximize: $\log f_m(z)$

Or

$$min\, J(x) = \sum_{i=1}^{m} w_{ii}\, r_i^2 \tag{2.15}$$

Where x is the vector of state variables such as voltage magnitudes and angles and will be obtained by minimising the objective function of equation (2.15).

Subject to: $z_i = h_i(x) + r_i \qquad \mathrm{i} = 1, 2 \ldots \mathrm{m}$ (2.16)

Where,

x State variables such as voltage magnitudes and angles

m Number of measurements

w_{ii} Weighting factor of measurement variable *i*

z_i Measured value of i^{th} measurement, $z = [z_1^a z_1^b z_1^c \dots z_i^a z_i^b z_i^c \dots z_m^a z_m^b z_m^c]$.

h_i i^{th} measurement as a function of state *x*.

r_i i^{th} measurement error

The solution to this problem is known as the weighted least square (WLS) estimation of *x*.

2.2 Weighted Least Square (WLS) estimation

The weighted least square (WLS) technique is common type of state estimation. The basic idea is to improve the state variables by minimizing the sum of the residual squares. This is the well-known least squares (LS) method, which has become the foundation of classical statistics [47], [48]. Considering the objective function in equations (2.15), (2.16) the solution to the state estimation problem can be obtained by calculating the first and second derivatives of *J(x)* based on the Newton method. The following first order optimality condition must be satisfied at the minimum. To find the minimization of this objective function the derivative should be set at zero. This is shown in compact form as follows [47]:

$$g(x) = \frac{\partial J(x)}{\partial x} = -H^T(x)R^{-1}[z - h(x)] = 0 \tag{2.17}$$

Where $$H(x) = [\frac{\partial h(x)}{\partial x}] \tag{2.18}$$

This matrix, H(x), is called the measurement Jacobian matrix. Ignoring the higher order terms of the Taylor series expansion of the derivative of the objective functions yields an iterative solution known as the Gauss-Newton method [47].

$$x^{k+1} = x^k + [\, H^T(x^k)R^{-1}H(x^k)]^{-1}[\, H^T(x^k)R^{-1}(z - h(x^k))] \tag{2.19}$$

Since, the measurement Jacobian, *H(x)* is simply the derivative of the measurement function with respect to the state vector, By knowing the error covariance matrix *R*, and the measurement function, *h(x),* it is possible to iteratively solve this optimization.

For the first iteration of the optimization the measurement function and measurement

Jacobian should be calculated at flat voltage profile where all of the voltage magnitudes are 1.0 per unit and all of the voltage angles are 0 degrees. Consecutively, the next iteration of the state vector can be calculated again and again until a desired tolerance is reached.

2.3 Robust state estimation

The robust estimation was initially introduced by Huber [49]. Later Mili et.al [50] applied this theory in concept of power system state estimation. The estimator is called robust if the estimated states are unaffected by large deviations in measured data. The robust estimator is remaining neutral regardless of the existence of bad data. The M-estimators are class of robust estimators used in power system and are based on the maximum likelihood concept. Some types of these estimators have been explained in appendix D.

Although the bad data rejection properties of the robust estimators are very attractive, they could suffer from the possible existence of local minima. Other disadvantages of these estimators are their slow convergence or occasionally divergence, numerically unobservable situation due to the rejection of several measurements particularly in the case of poor local redundancy, high risk of wrong identification and partial rejection of bad data, except for QC.

2.4 Bad data detection

Detection of measurements error and eliminating them is important task for state estimator. Bad data may occur due to faulty or wrong standardizations of the measuring equipment and telecommunication standard which considerably weakens the performance of the state estimator. State estimator is capable of filtering some of these errors if these errors are obvious and there is acceptable redundancy in the number of measurements. However, not all types of bad data are recognizable. Therefore, more advanced method is required to detect and eliminate them. Various methods of bad data detection and elimination could be used based on the type of applied state estimator. In WLS method, bad data detection is done by processing the properties of measurement residuals after the state estimation procedure [47]. However in this thesis the bad data detection has not been investigated due to the broad size of this topic.

2.5 Mathematical modelling for three-phase state estimation

The solution to DSSE problem is formulated as a minimization of the following objective function subject to satisfying several equality and inequality constraints. The goal is to obtain the bus voltage magnitudes, angles and tap positions that minimizes weighted square of the difference between the measured quantity and the estimated quantity which are functions of estimated states. It is expressed as:

$$min\, J(x) = \sum_{i=1}^{m} w_{ii}\, r_i^2 \tag{2.20}$$

Subject to:

$$z_i = h_i(x) + r_i \tag{2.21}$$

$$c(x) = 0 \qquad \text{Equality constraint} \tag{2.22}$$

$$g_{min} \le g(x) \le g_{max} \qquad \text{Inequality constraints} \tag{2.23}$$

Where,

$\boldsymbol{x}$ State variables such as voltage magnitudes and angles.

$\boldsymbol{m}$ Number of measurements.

$\boldsymbol{w_{ii}}$ Weighting factor of measurement variable *i*, $z = [z_1^a z_1^b z_1^c \dots z_i^a z_i^b z_i^c \dots z_m^a z_m^b z_m^c]$.

$\boldsymbol{z_i}$ Measured value of i^{th} measurement

$\boldsymbol{h_i}$ i^{th} measurement as a function of state *x*.

$\boldsymbol{r_i}$ i^{th} measurement error

2.5.1 Equality constraints c(x):

The equality constraints are the set of equation corresponding to virtual measurements.

$$0 = P_{Gi}^k - P_{Di}^k - \sum_{l=1}^{3}\sum_{j=1}^{n} V_i^k V_j^l \left[G_{ij}^{k,l}\, cos\left(\delta_i^k - \delta_j^l\right) + B_{ij}^{k,l}\, sin\left(\delta_i^k - \delta_j^l\right)\right] \tag{2.24}$$

$$0 = Q_{Gi}^k - Q_{Di}^k - \sum_{l=1}^{3}\sum_{j=1}^{n} V_i^k V_j^l \left[G_{ij}^{k,l}\, sin\left(\delta_i^k - \delta_j^l\right) - B_{ij}^{k,l}\, cos\left(\delta_i^k - \delta_j^l\right)\right] \tag{2.25}$$

Where P_{Gi}^k and Q_{Gi}^k are the real and reactive power injected at bus *i* respectively, the load demand at the same bus is represented by P_{Di}^k and Q_{Di}^k. Indices *n* is number of buses and *l* is the number of phases which can be 1, 2 or 3 phase.

2.5.2 Inequality constraints

These are the set of constraints of continuous and discrete variables that represent the system operational and security limits, such as setting upper and lower limits for control variables. These are as follows:

- **Bus voltage** - Voltage magnitudes at each bus in the network:

$$V_{min,i}^k \leq V_i^k \leq V_{max,i}^k$$

- **Bus angle -** The bus angle at each bus in the network:

$$-\delta_{\min i}^k \leq \delta_i^k \leq \delta_{\max i}^k$$

2.6 Case studies

The WLS method has been applied on standard IEEE-13 and IEEE 123 bus distribution system. The topologies of the two test systems are shown in Fig. 2.6 and Fig. 2.7. Some of the features of the two systems are listed here:

2.6.1 The standard IEEE-13 bus test feeder

The IEEE-13 bus distribution test system is shown in Fig. 2.6. This feeder is small however it has remarkable features. It represents a typical distribution network with voltage magnitude measurements only at the substation, with more branch current measurements than power flow measurements, and all loads are considered as pseudo measurements. Some of its features are listed as follows:

• It is short and rather high loaded for a 4.16 kV feeder.

• One substation voltage regulator consisting of three single phase units connected in wye configuration.

• It includes both overhead and underground lines with a various phasing.

• It has one transformer: grounded wye-grounded wye.

• It has unbalanced spot and distributed loads.

This small feeder will provide a good test to analyse the most common features of distribution network. The details of the network data and loadings are given in Appendix A.

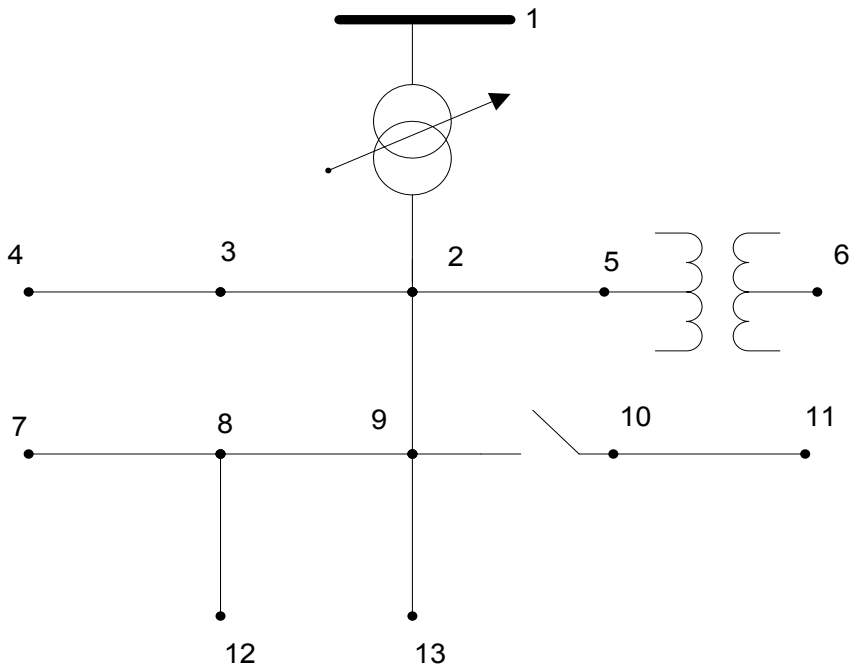


Fig. 2.6 IEEE-13 bus distribution system

2.6.2 The standard IEEE-123 bus test feeder

The 123 bus distribution test system is shown in Fig. 2.7. The IEEE-123 node is the most comprehensive feeder that operates at a nominal voltage of 4.16 kV and is characterized by:

1. Overhead and underground line segments with various phasing.

2. Unbalanced loading with all combinations of load types (PQ, constant I, constant Z)

3. All loads are “spot loads” located at a node

4. Four step-type voltage regulators

6. Switching to provide alternate paths of power-flow

The network data and loadings are given in Appendix B.

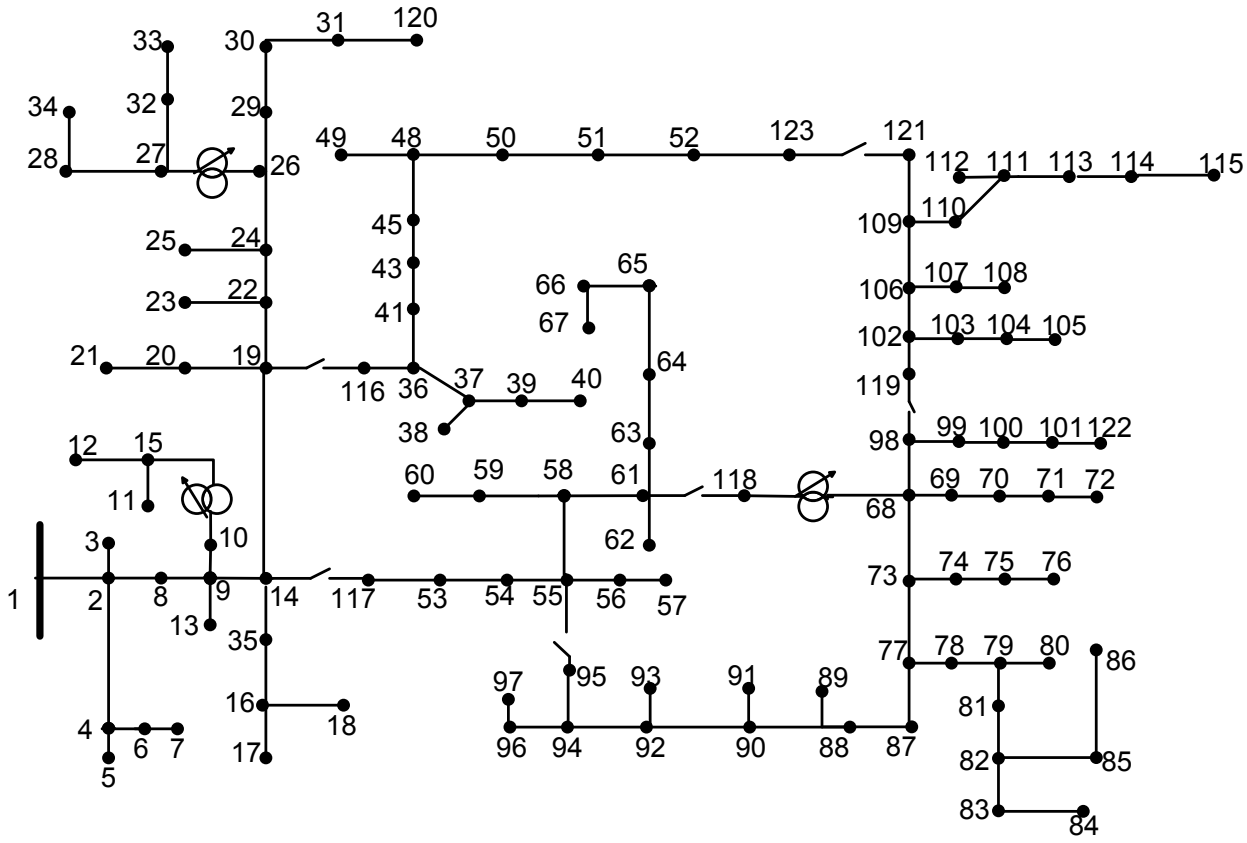


Fig. 2.7 IEEE-123 bus distribution system

The proposed modified WLS approach was implemented in MATLAB by Intel(R)Xeon(R) processor @2.40 GHz with 12.0 GB of RAM and has been tested on IEEE-13 bus and IEEE-123 bus test systems to validate the proposed algorithm. The network parameters and load data are obtained from [51] and [52]. The topologies of the test systems are shown in Fig. 2.6 and Fig. 2.7. The systems consist of both overhead lines and underground cables. The overhead lines and underground cables have been modelled with modified Carson's equations as has been described in section (2.1.1). There are both three-phase and single-phase loads consequently, the system is unbalanced. The three-phase loads are either star or delta connected. The loads are either constant current or constant impedance or constant power and have been modelled in ZIP-model as it has been described in section (2.1.1). The

distribution feeder is either three-phase or three-phase with grounded neutral or single or two-phase laterals. Therefore, the impedance of each overhead line or underground cable is represented as either a 3x3 or a 4x4 matrix compared to a single element in single phase representation. However, the 4x4 matrix for three-phase lines with grounded neutral is converted to 3x3 matrix by Kron's reduction [42]. The tap changers are assumed to have fixed taps. Measurements were generated using three-phase power flow program with addition of normally distributed noise component to generate noisy measurements. The error of true measurement was assumed 3% while the error in pseudo measurement (load data) was considered 20%. For 13-bus model test system the switch between buses 9 and 10 is considered to be closed. In 123-bus model test system the switches between buses 14 and 117, 61 and 118, 19 and 116, 98 and 119 are considered closed and the switches between buses 123 and 121 and 55 and 95 are considered open.

2.7 Results and discussions

Table 2.1 shows the real and estimated vector of voltages and Table 2.2 shows the real and estimated vector of angles at different phases of the IEEE-13 bus model distribution network. In Table 2.1, the value of voltage has been taken as 1.0 where there is no phase available for the given bus. Also, in Table 2.2, the dashes show that there is no phase available for the given bus. The obtained results are found to be very satisfactory within the allowable error range. Also, the percentage errors of the voltage magnitudes shown in Table 2.1 are found to be satisfactory. Fig. 2.8, Fig. 2.9, Fig. 2.10 show the real and estimated vector of voltages and Fig. 2.11, Fig. 2.12, Fig. 2.13 show the real and estimated vector of angles for the IEEE-123 bus model distribution network. In Fig. 2.8, Fig. 2.9 and Fig. 2.10 the value of voltages have been taken as 1.0 where there are no phases available for the given buses on the graphs. The obtained results are found to be very satisfactory within the allowable error range. Fig. 2.14 to Fig. 2.19 demonstrate the real and estimated value of voltages and angles for different phases in the network considering different switch status for 123 bus test system. Assuming that the switches between buses 123-121, 14 and 117, 61 and 118, 98 and 119 are considered closed and the switches between19-116 and 55-95 are open.

Table 2.1 True and estimated voltages for IEEE-13 bus distribution system by WLS

Bus Num	True V_a	Estimated V_a	% error phase a	True V_b	Estimated V_b	% error phase b	True V_c	Estimated V_c	% error phase c
1	1	0.999	0.100	1.000	1.003	0.300	1	1.001	0.100
2	1	1	0.000	0.989	0.987	0.202	1.006	1.006	0.000
3	1	1	0.000	0.989	0.987	0.202	1.006	1.007	0.099
4	0.994	0.994	0.000	0.992	0.991	0.101	1.005	1.007	0.199
5	0.993	0.991	0.201	0.992	0.994	0.202	1.005	1.006	0.100
6	0.998	0.994	0.401	0.998	1	0.200	1.011	1.010	0.099
7	1	1	0.000	1	1	0.000	1.007	1.006	0.099
8	0.989	0.988	0.101	1	1	0.000	1.008	1.007	0.099
9	0.989	0.988	0.101	0.994	0.994	0.000	1.009	1.007	0.198
10	0.989	0.988	0.101	0.994	0.994	0.000	1.009	1.007	0.198
11	0.988	0.990	0.202	0.994	0.995	0.101	1.008	1.004	0.397
12	0.987	0.987	0.000	1	1	0.000	1	1	0.000
13	0.989	0.992	0.303	0.994	0.996	0.201	1.009	1.005	0.396

Table 2.2 The true and estimated angle for IEEE-13 bus distribution system by WLS

Bus Number	**True δ phase a**	**Estimate δ phase a**	**True δ phase b**	**Estimate δ phase b**	**True δ phase c**	**Estimate δ phase c**
1	0	0	-120	-120	120	120
2	-	-	-119.566	-119.567	119.357	119.610
3	-	-	-119.618	-119.620	119.423	119.624
4	-0.241	-0.286	-119.684	-119.689	119.549	119.662
5	-0.264	-0.308	-119.701	-119.705	119.547	119.656
6	-0.498	-0.542	-119.866	-119.869	119.386	119.471
7	-	-	-	-	119.392	119.471
8	-0.649	-0.661	-	-	119.414	119.495
9	-0.631	-0.643	-119.249	-119.268	119.423	119.504
10	-0.631	-0.643	-119.249	-119.268	119.423	119.504
11	-0.673	-0.663	-119.259	-119.260	119.452	119.523
12	-0.624	-0.636	-	-	-	-
13	-0.632	-0.644	-119.248	-119.267	119.423	119.504

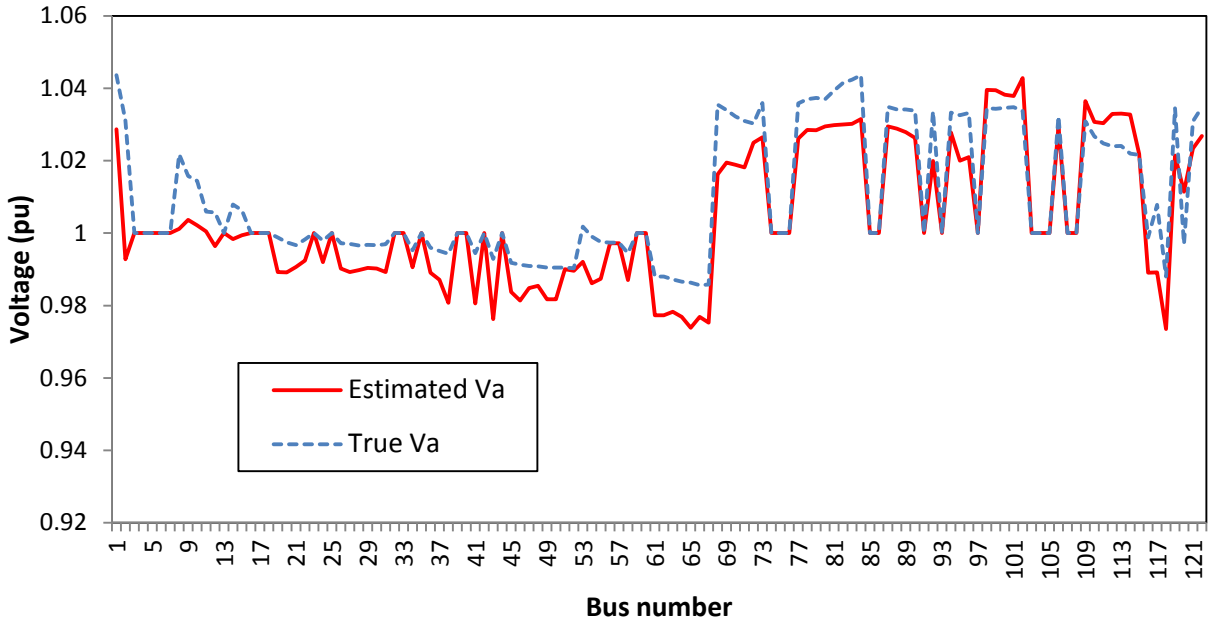


Fig. 2.8 True and estimated voltage for IEEE-123 bus system at phase a by WLS

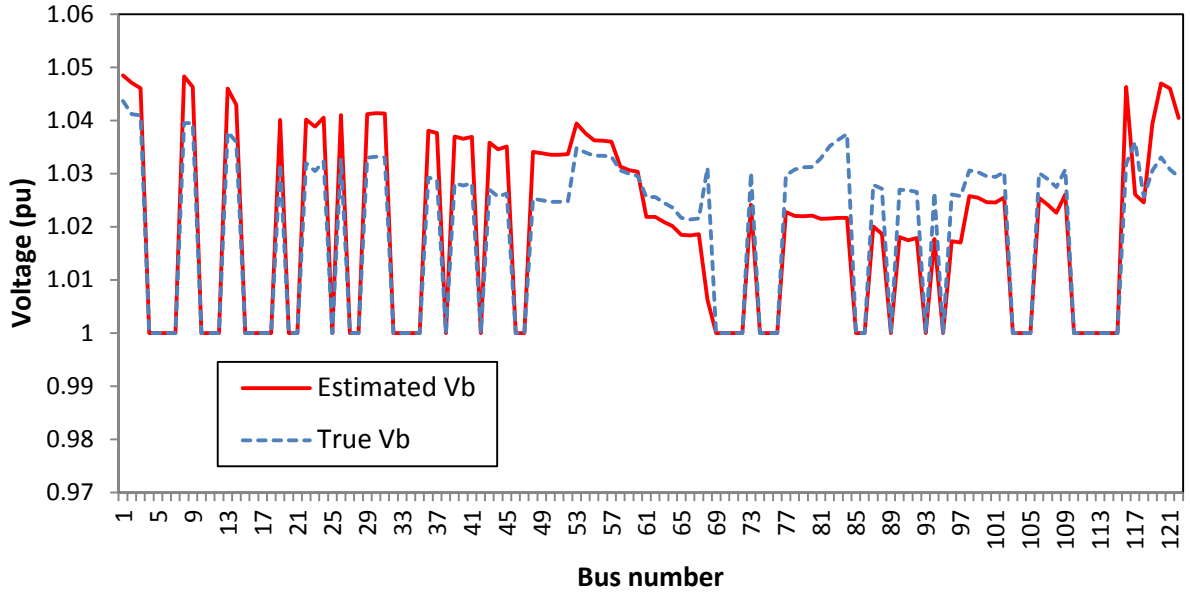


Fig. 2.9 True and estimated voltage for IEEE-123 bus system at phase b by WLS

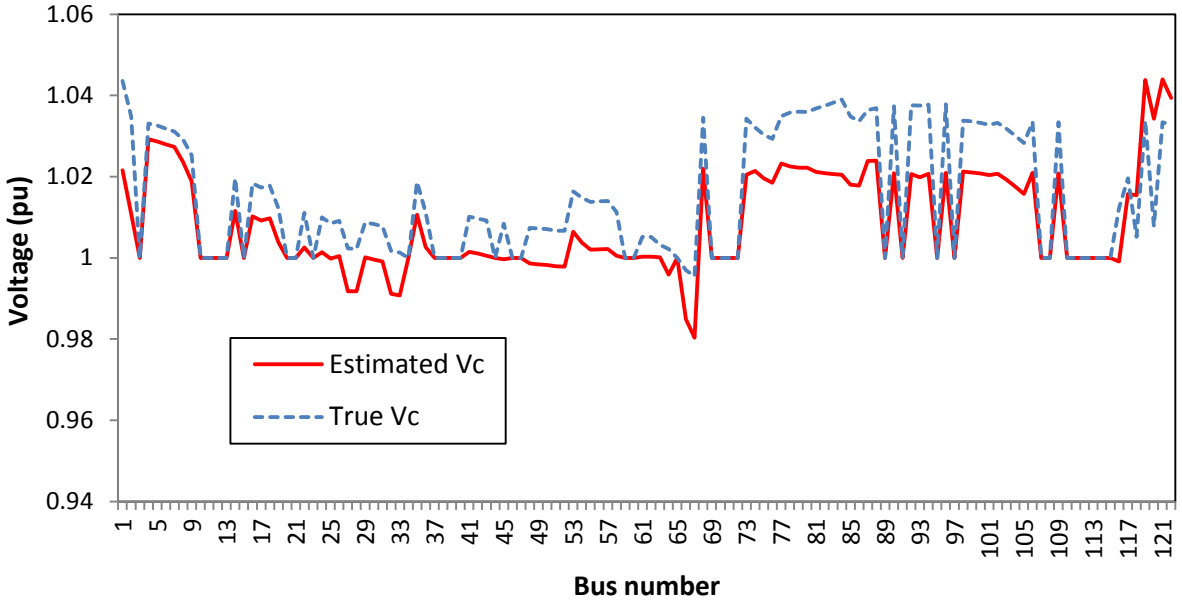


Fig. 2.10 True and estimated voltage for IEEE-123 bus system at phase c by WLS

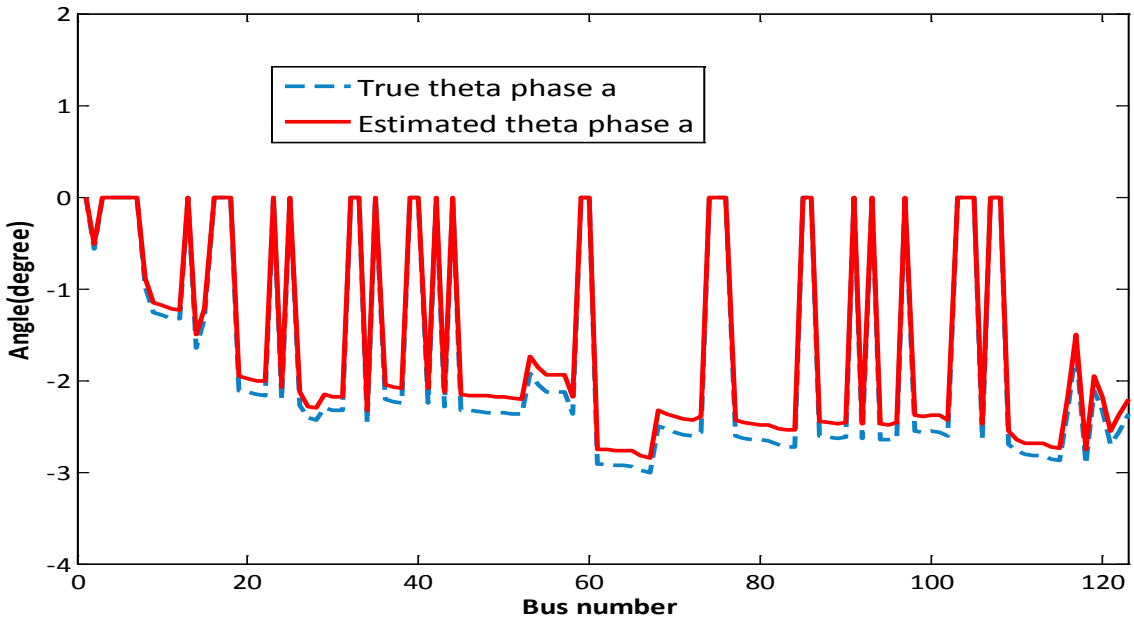


Fig. 2.11 True and estimated angles for IEEE-123 bus system at phase a by WLS

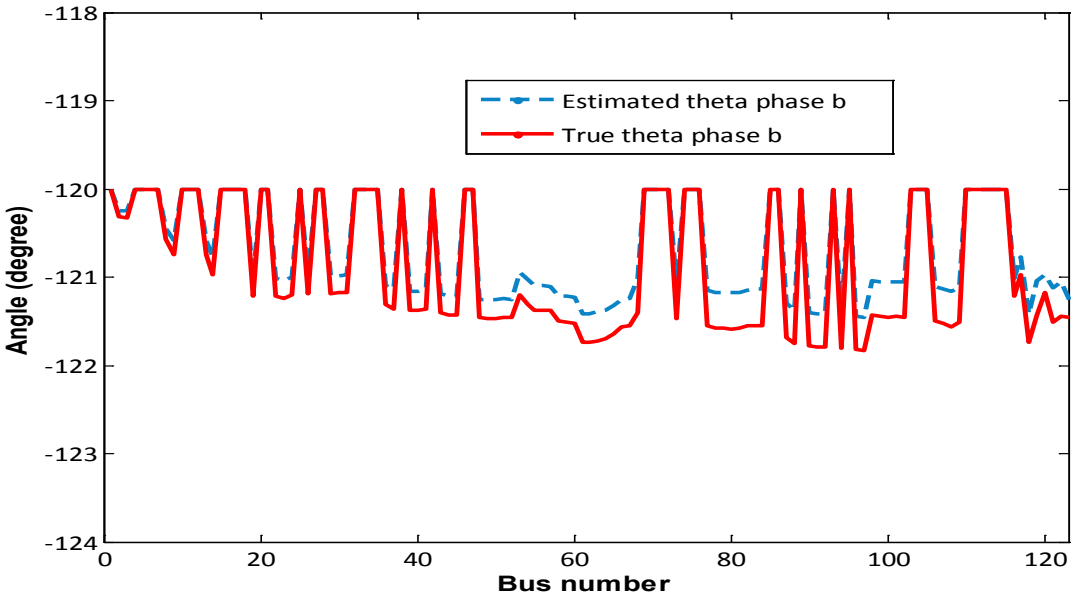


Fig. 2.12 True and estimated angles for IEEE-123 bus system at phase b by WLS

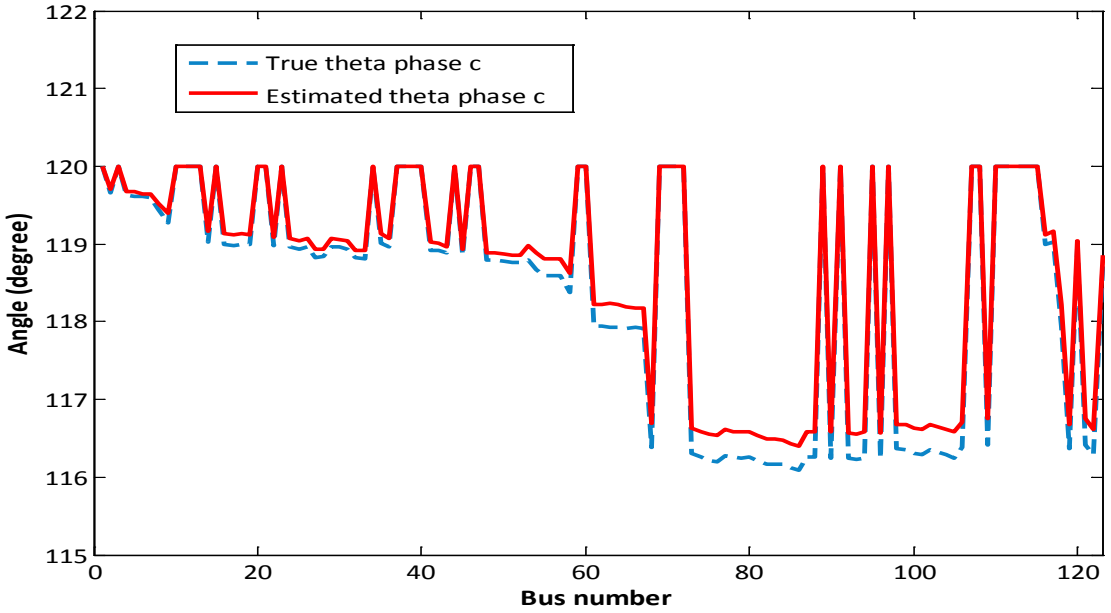


Fig. 2.13 True and estimated angles for IEEE-123 bus system at phase c by WLS

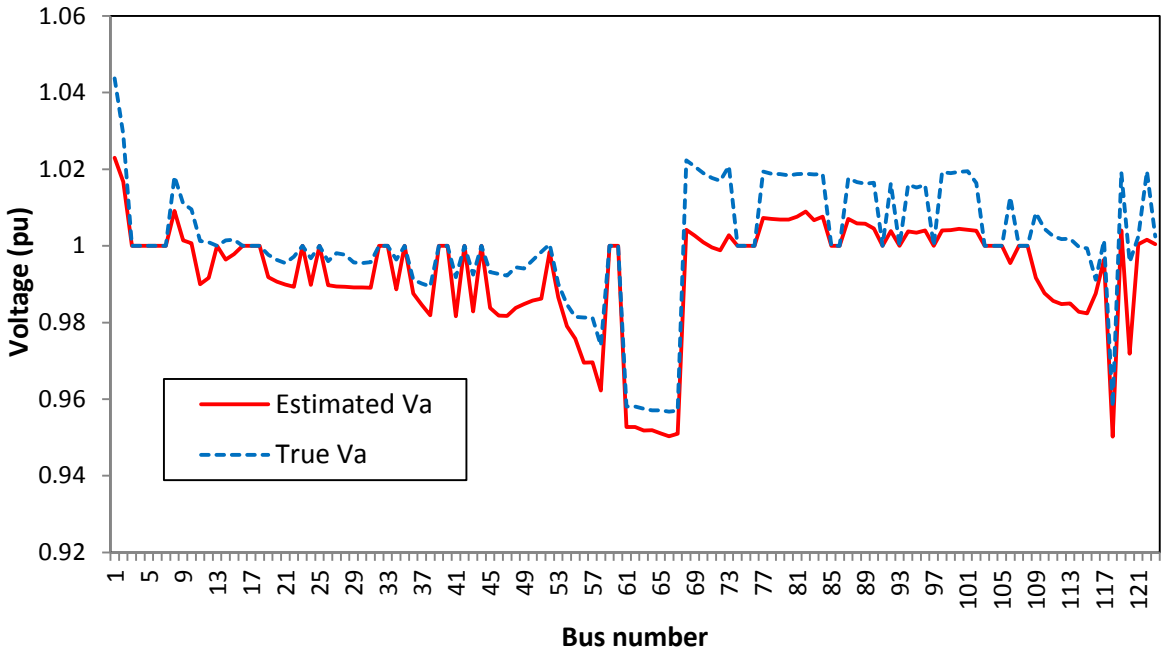


Fig. 2.14 True and estimated voltage for IEEE-123 bus system at phase a by WLS for different switch status

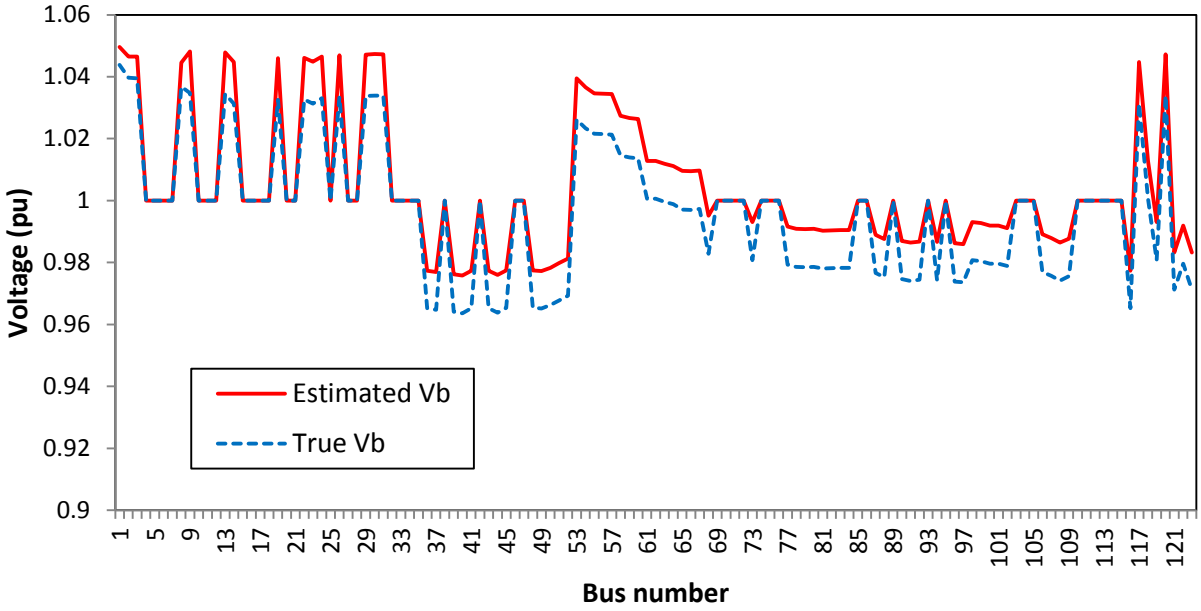


Fig. 2.15 True and estimated voltage for IEEE-123 bus system at phase b by WLS for different switch status

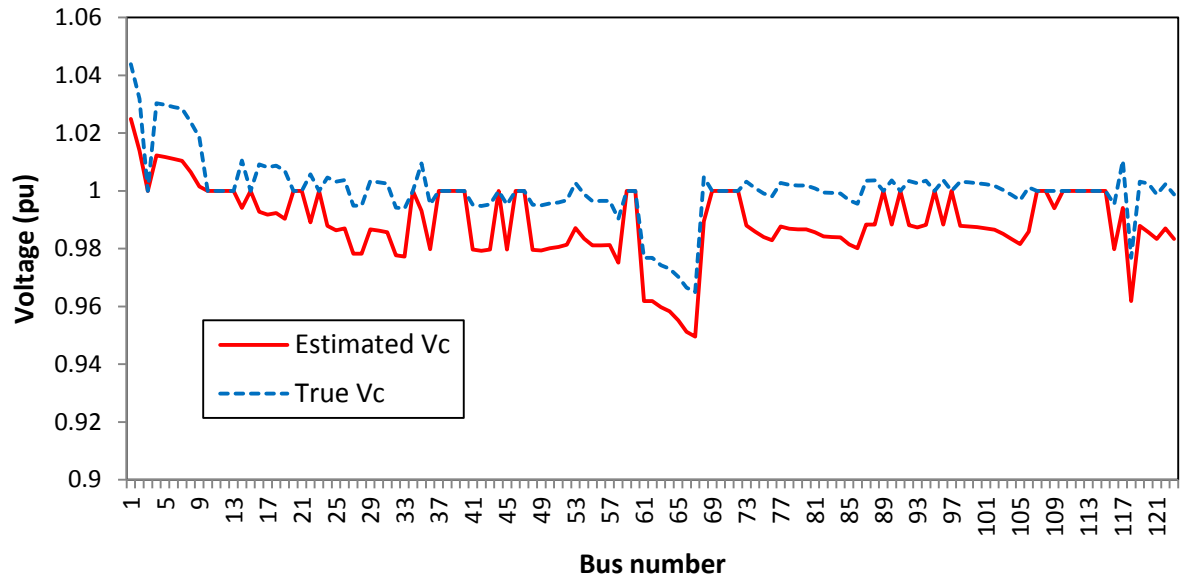


Fig. 2.16 True and estimated voltage for IEEE-123 bus system at phase c by WLS for different switch status

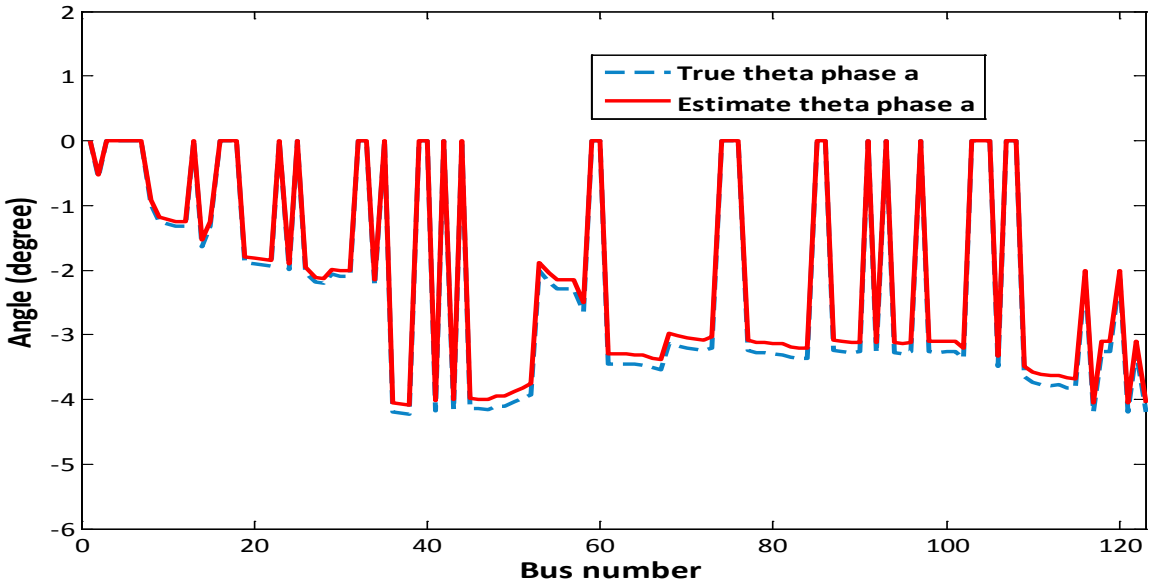


Fig. 2.17 True and estimated angles for IEEE-123 bus system at phase a by WLS for different switch status

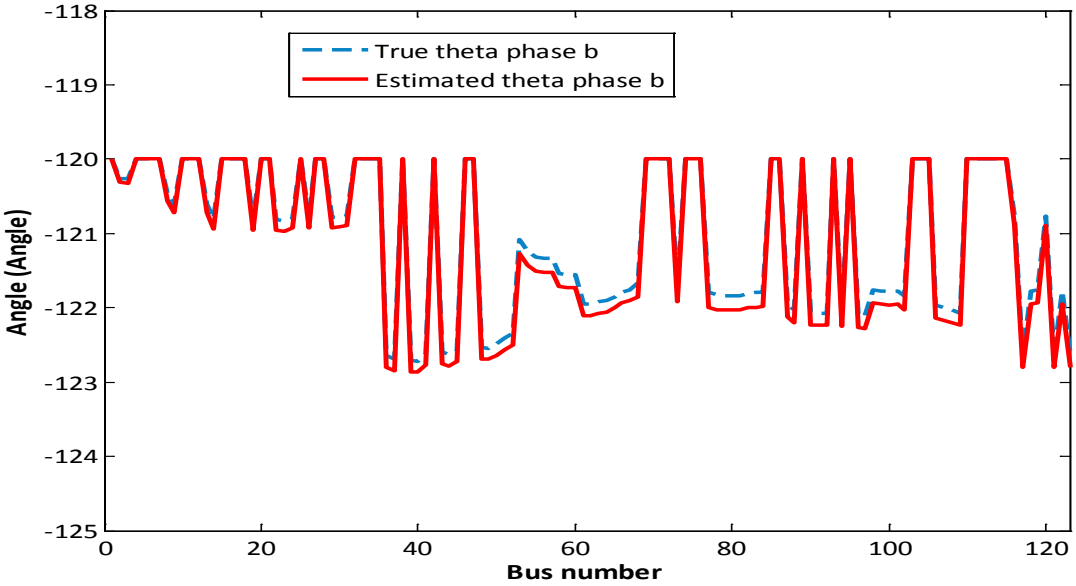


Fig. 2.18 True and estimated angles for IEEE-123 bus system at phase b by WLS for different switch status

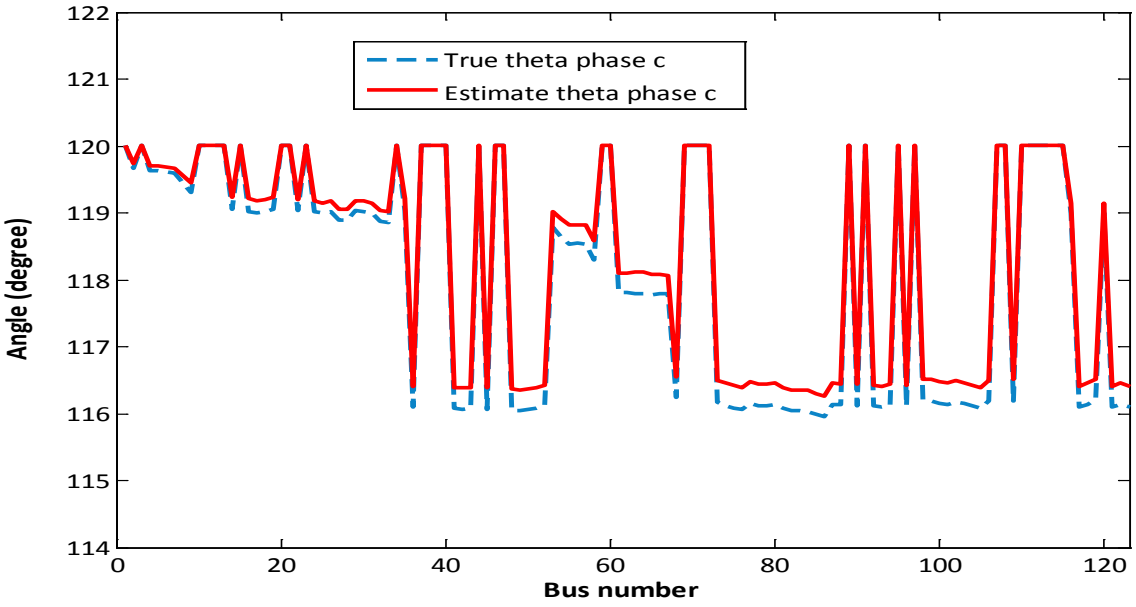


Fig. 2.19 True and estimated angles for IEEE-123 bus system at phase c by WLS for different switch status

2.8 Conclusions

This chapter presented an overview of state estimation in distribution network. Various methods of robust estimation and their strengths and weaknesses have been discussed briefly. The mathematical modelling of the three-phase state estimator alongside the three phase model of various components of the distribution network such as distribution lines, transformers, loads and switches have been described in details. Finally, the WLS estimator method has been applied to estimate the state of the system in IEEE-13 bus and IEEE-123 bus distribution networks. The results shown are satisfactory for the studied networks. This also validates the understanding of WLS and its application to power distribution system from the first principle.

However, the assumption of fixed taps in this study is likely to reduce the effectiveness of state estimation process and the accuracy of the estimated values of voltage magnitudes. The reactive power through transformer will differ considerably from their actual values when a tap measurement is in error or is not available but the tap changing control is in action. In the following chapter, in order to improve the estimate accuracy and to prevent potential observability problems, transformer tap setting has been added as a new state variable in state estimation algorithm and any available information on the tap setting value has been converted to a regular measurement, to be used in the estimation process. The peculiarity of tap as state variable is that it is discrete in nature making state estimation a mixed integer optimization problem. That is difficult to solve by WLS or other conventional techniques. The main focus of the research is thus developing three-phase state estimation techniques that will handle discrete variables. The next two chapters will concentrate on two methods: Hybrid particle swarm optimization (HPSO) and Ordinal Optimization (OO).

Chapter 3

Three phase state estimation by Particle Swarm Optimization

Distribution networks in many countries are experiencing the problem of rapid voltage fluctuation because of the real power infeed from the distributed generations (DGs). The output from DGs being not very predictable (solar and wind), the voltage variation in the network is very severe. So the voltage control is as important as feeder flow control. On load tap changing transformer (OLTC) in the primary substation (typically 33/11kv) is also subjected to rapid control actions because of the randomly varying DG injection. It is very important to include the tap positions as an estimated variable so that network control can be performed more effectively.

There have not been many literatures in tap observability detection. The authors in [21] proposed a robust algorithm based on Givens rotation [54] the gain matrix to obtain the state and tap position under erroneous zero injection. The method is demonstrated to work well in Brazilian system models of varying complexity. The authors in [22] used node voltages, angles and tap position as state variables under the assumption that the taps are continuous. However, in practice OLTC has discrete tap positions so inaccurate estimate produces inaccurate computed values of other network quantities such as feeder flows, losses etc. So,

the incorporation of the discrete tap variables in distribution network state estimation (DSSE) is very much required for effective network control.

DSSE is commonly formulated as a weighted least square (WLS) problem [47]. However, transformer tap positions make the problem a mixed integer nonlinear one. So, the solution of the problem through normal equation framework is not possible as the objective function is not differentiable [23].

Authors in references [24] and [25] have assumed continuous taps instead of discrete and have incorporated rounding technique or sensitivity method to address the complexity of discrete values.

However, this assumption reduces the accuracy of the DSSE and the solution does not represent the actual network taps positions. Therefore, the estimation of transformer tap positions has to be obtained from the solution of the mixed integer non-linear optimization problem containing continuous and discrete values [26], [27].

There have been plethora of interests in the application of artificial intelligence such as neural networks (NN), genetic algorithms (GA), honey bee mating optimization (HBMO), and particle swarm optimization (PSO) in recent years. To overcome the computational difficulty of such complex optimization problem, these algorithms have been successfully applied to wide range of optimization problem where they can handle mixed integer variables of the objective functions as they do not need the function to be continuous and differentiable [28].

PSO appears to be a very effective technique compared to GA and other evolutionary algorithms as it is simple in concept and implementation. It has limited number of parameters in comparison to other heuristic optimization methods. It can be easily applied to diverse issues where it can produce satisfactory solutions and stable convergence characteristics [29].

However, PSO has weak form of selection that increases the amount of time to get to the effective area in the solution space.

A hybrid form of PSO (HPSO) is used to overcome this situation [54]. HPSO combine the feature from PSO and GA. HPSO has been applied in balanced state estimation problem [30]. HPSO uses a selection method which is based on the evolution from generation to generation.

Reference [30] considered a balanced three phase distribution network model without considering unbalanced nature of the system and discrete tap as state variables.

This chapter proposes a full three phase state estimator including unbalanced load, network model and the discrete taps as additional estimated variables based on HPSO optimization technique in order to estimate the discrete value of the transformer taps. The contribution of this chapter lies in handling the complexity of the unbalanced system and correctly computing the discrete values of the tap. The performance of the proposed method has been tested on IEEE 13-bus and 123-bus unbalanced test system models and the results are presented.

I have also made several modifications of traditional PSO and HPSO techniques to obtain solutions faster. This chapter is organized as follows: In Section 3.1 the PSO solution method is described. Section 3.2 provides an overview of HPSO. Section 3.3 presents the HPSO approach in the context of three phase unbalanced state estimation for distribution network model. Section 3.4 demonstrates the results and discussions of the state estimation for IEEE-13 bus and IEEE-123 bus model networks. Section 3.5 summarised and concludes the research content and outcome described throughout the chapter.

3.1 Particle Swarm Optimization (PSO)

The PSO is a population based optimization method first proposed by Kennedy & Eberhart [55], which is used to search the solution space of a given problem to find the candidate solution which can maximize or minimize a particular objective function. Some of the attractive features of the PSO include the ease of application and the fact that no gradient information is required which allows the PSO to be used on functions where the gradient is either unavailable or computationally expensive to obtain. It can generate high quality solutions and has stable convergence characteristic so can be used to solve a wide array of different optimisation problems. It uses a number of particles that constitute a swarm. Each particle traverses the search space looking for the global minimum (or maximum). During flight, each particle adjusts its position according to its own experience, and the experience of neighbouring particles, making use of the best position encountered by itself *(pbest)* and its neighbours *(gbest)*. Let X and *Vel* represent a particle position and its corresponding velocity in a search space, respectively. The best previous position of a particle is recorded and represented as *pbest*. The index of the best particle among all the particles in the group is

represented as *gbest*. The modified velocity and position of each particle can be calculated as shown in the following formulas [56]:

$$Vel_{ij} = W \times {Vel_{ij}}^{0} + C_1 \times R_1 \times (X_{pbest} - {X_{ij}}^{0}) + C_2 \times R_2 \times (X_{gbest} - {X_{ij}}^{0}) \quad (3.1)$$

$$X_{ij} = {X_{ij}}^{0} + Vel_{ij} \quad (3.2)$$

i i^{th} particle

j Dimension of velocity associated with particle *i*

Where Vel_{ij} and X_{ij} are respectively the velocity and position of the particle at iteration j, W is the weighting function, C_1 *and* C_2 are the weighting factors and R_1 and R_2 are random numbers between 0 and 1. In equation (3.1) X_{pbest} is the $pbest$ of particle and X_{gbest} is the $gbest$ of the group.

3.1.1 Selection of parameters for PSO and simulation condition

The selection of key parameters to set up PSO such as *W,* C_1, C_2 and Vel_{max} is an important task as these parameters govern the rate of convergence.

Weighting function (W):

W is a weighting factor which is related to the velocity of the particle during the previous iteration. It controls the amount of the previous velocity that the particle takes in the next iteration. This value is equal to 1.0 for the original PSO. The concept of velocity will be lost if this value is set to zero. Shi and Eberhart [57] investigated the effect of W in the range (0.0, 1.4). The faster convergence is obtained by setting this value between (0.8, 1.2). However, setting of inertia weight that decreased from 0.9 to 0.4 has generated satisfactory results [56].

The weighting function is obtained as:

$$W = \left[\left(W_{ini} - \frac{(W_{ini} - W_{fin}) \times iter}{iter_{max}}\right)\right] \quad (3.3)$$

Where W_{ini} and W_{fin} are the initial and final weight respectively, $iter_{max}$ is the maximum iteration number and $iter$ is the current iteration number.

Acceleration coefficients (C_1 *and* C_2):

C_1 and C_2 affect the maximum step size of a particle in a single iteration. C_1 regulates the maximum step size of a particle in the direction of $pbest$ while C_2 regulates the maximum step size in the direction of the $gbest$ [56] as shown in equation (3.1).

The particle velocity is limited by Vel_{max} to minimize the possibility of the particle escaping the search space. The search space is defined by the bounds X_{min}, X_{max} for the vector of state variables comprising of:

$$V_{min} \leq V \leq V_{max}$$

$$\delta_{min} \leq \delta \leq \delta_{max}$$

$$t_{min} \leq t \leq t_{max}$$

Therefore the vector of Vel_{max} is typically set to the following for each vector of state variables:

$$Vel_{max} = K \times (X_{max} - X_{min}) \quad (3.4)$$

Where $0.1 \leq K \leq 1.0$

Initially, PSO has been performed several times with different values of the key parameters of $W, C_1, C_2 and\ Vel_{max}$ to achieve the satisfactory results.

3.1.2 Improving the speed of convergence

In my PhD research I have made appropriate modification to update the position of the particle by changing the direction when reaching the search space boundary in order to improve the speed of convergence. The direction of the particle is thus modified in such a way that it keeps the particle inside its range when the velocity takes the particle out of its boundary $[X_{min}, X_{max}]$. So the new position of the particle will be updated based on the following equation instead of (3.2).

$$X_{ij} = X_{ij}{}^{0} - Vel_{ij} \quad (3.5)$$

The optimal solution be close to the boundary the α factor helps to reach the solution faster.

$$X_{ij} = X_{ij}{}^{0} - \alpha Vel_{ij} \tag{3.6}$$

Where, α is an optimally chosen number between 0 and 1. I have discussed about a suitable value of alpha later in the discussion section.

3.1.3 General algorithm for PSO

1. Generate initial population of particles with random velocities and positions. In this study, these particles are bus voltage magnitudes and angles and transformer tap positions.

2. These initial particles must be feasible candidate solutions that satisfy the practical operation constraints. Set upper and lower limits for these particles (V, δ, t).

3. For each particle of the population, calculate the error with the help of equation (2.16) in Chapter 2.

4. Obtain value of each particle in the population using the evaluation function (fitness function) and the penalty function. The value of fitness function is obtained as follows:

$$FF(x) = \frac{1}{(1+J(X)+Penalty(X))} \tag{3.7}$$

Where *J(x)* comes from equation (2.15) and *Penalty(x)* as follows:

$$Penalty\ (x) = \rho \sum_{i}^{N} (x_i - x_0)^2 \tag{3.8}$$

Should there be a violation of equality and/or inequality constraints at each iteration, the quadratic penalty function takes care of it by adding a large value to the objective function.

The shape of the proposed penalty function is displayed in Fig. 3.10. A quadratic penalty function very effectively moves the decision variables closer to the limit while giving less preference to the decision variables which are not so close to limit violation.

N = number of penalised control variables.

$\boldsymbol{\rho}$= scalar quadratic penalty weight.

x_i= control variable current value (pu).

x_0 = control variable penalty offset (pu).

5. Compare each particle's value with its *pbest.* The best evaluation value among the *pbest* is denoted as *gbest.*

6. Update the time counter $t = t + 1$.

7. Update the inertia weight w given by equation (3.3).

8. Modify the velocity *Vel* of each particle according to equation (3.1).

9. Modify the position of each particle according to (3.2) and (3.6). If a particle violates its position limits in any dimension, set its position at the proper limit according to (3.6).

10. Each particle is evaluated according to its updated position. If the value of each particle is better than the previous *pbest*, the current value is set to be *pbest*. If the best *pbest* is better than *gbest*, this value is set to be *gbest.*

11. If the maximum of a variation of the state variable Δx is smaller than 0.001 and the iteration has reached maximum number of iteration specified go to step ≠12. Otherwise go to step ≠6 until the end criteria are satisfied.

12. The particle that generates the latest *gbest* is the optimal value.

Fig. 3.1 illustrates the general PSO algorithm.

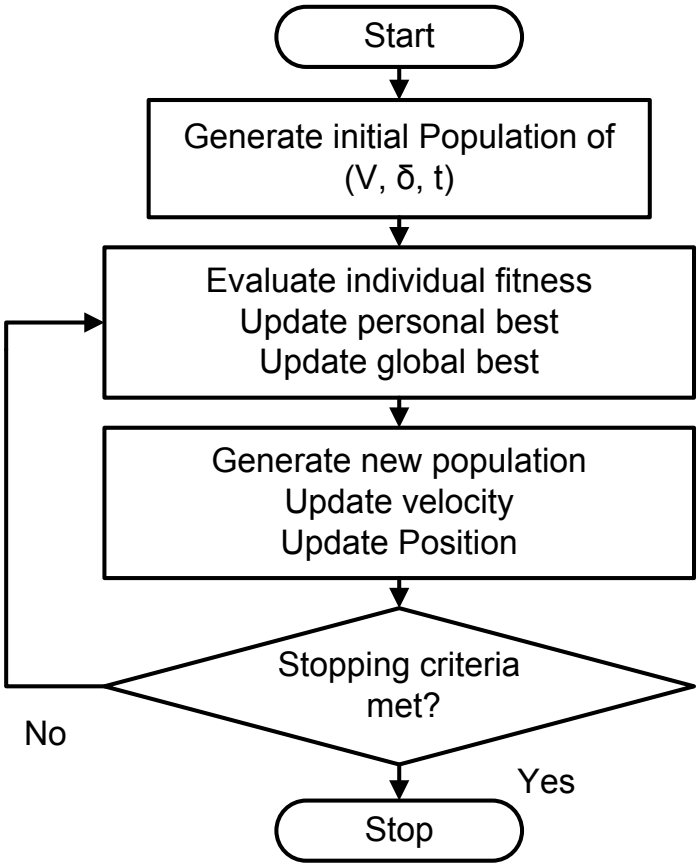


Fig. 3.1 General algorithm for PSO

3.2 Hybrid Particle Swarm Optimization (HPSO)

The PSO algorithm has a weak selection process which very much depends on *pbest* and *gbest*, therefore, the searching area is limited by *pbest* and *gbest.* This leads to increase in the amount of time that it takes to get to the effective area in the solution space. The hybrid particle swarm optimization (HPSO) method has been introduced based on tournament selection method of genetic algorithm (GA), in order to improve the weakness of PSO method in this area. The introduction of the tournament selection mechanism in PSO algorithm, the effect of *pbest* and *gbest* is gradually eliminated by the selection which can result in the wider search area. The purpose of the selection in evolutionary algorithm is to influence the execution of the algorithm on a specific region of search space; usually one that delivered promising solutions in the recent past. Particle positions with low values are replaced by those with high values using the tournament selection method [54]. Therefore, the number of highly evaluated particles is increased while the number of lowly evaluated particles is reduced at

each iteration. It should be mentioned that although, the particle position is substituted by another particle position, the information related to each particle is reserved. Therefore, the intensive search in a current effective area and dependence on the past high evaluation position are realized [54].

3.3 Distribution state estimation by HPSO

This section presents the application of the HPSO algorithm for solving the DSSE problem. The set of tasks involve:

3.3.1 Network configuration and network data

The presence of unsymmetrical-network components and unbalanced-load on unbalanced distribution system makes it essential to consider the exact model of the system components (three-phase model). It includes the information about line resistance, reactance, tap setting connectivity information etc. This information regarding three phase model of various components of the network such as line, transformers and switches has been discussed and modelled in details in Chapter 2.

3.3.2 Power flow calculation

Three-phase power flow program suitable for distribution system has been set up with network information and load data to generate measurement data as an input to the state estimator. The normally distributed noise component has been added to these measurements to produce input for state estimator. Usually 1% to 3% error is associated with true measurements while the error for pseudo measurements (load data) is considered to vary between 20% and 50%.

3.3.3 State estimation based on HPSO algorithm

The following steps have been taken to estimate the state by HPSO estimator.

3.3.1.1. Set up a set of HPSOs parameters such as number of particles *N*, weighting function *W*, acceleration coefficients C_1 and C_2 and maximum number of iterations.

3.3.1.2. Generate an initial population of state variables (V, δ and t) with random velocities and positions in the solution space.

3.3.1.3. Set upper and lower limits for state variables (V, δ and t).

3.3.1.4. For each state variable if the variable is within the set limits go to the following step. Otherwise, that variable is infeasible.

3.3.1.5. The state has been calculated based on the minimization between measurements and calculated value based on HPSO algorithm.

Fig. 3.2 illustrates the distribution system state estimation using HPSO algorithm.

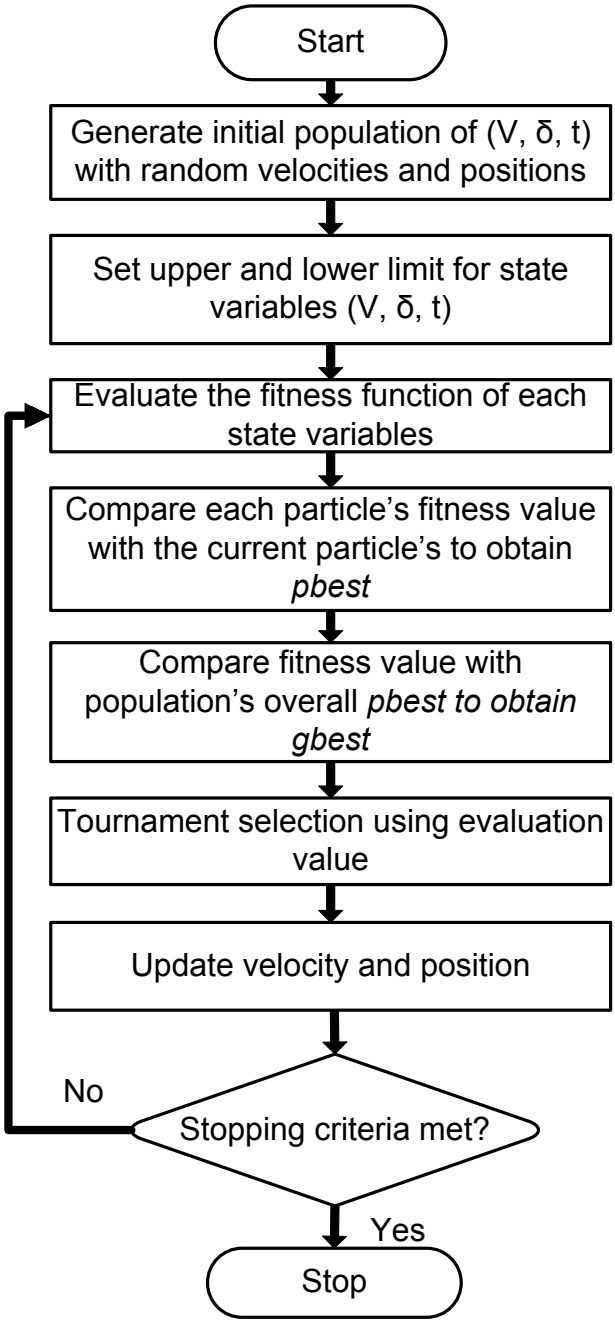


Fig. 3.2 Setting up of HPSO

3.4 Results and discussions

3.4.1 Case studies

The proposed modified PSO and HPSO approach were implemented in MATLAB by Intel(R)Xeon(R) processor @2.40 GHz with 12.0 GB of RAM and has been tested on IEEE-13 bus and IEEE-123 bus test systems to validate the proposed algorithms. The network parameters and load data are obtained from [51] and [52]. The topologies of the test systems are shown in Fig. 2.6 Chapter 2 and Fig. 3.9. The systems consist of both overhead lines and underground cables. The overhead lines and underground cables have been modelled with modified Carson's equations [42]. There are both three-phase and single-phase loads. The three-phase loads are either star or delta connected. The loads in the system have been modelled in ZIP-model.

Measurements were generated using three-phase power flow program with addition of normally distributed noise component to generate noisy measurements. The error of true measurement was assumed 3% while the error in pseudo measurement (load data) was considered 20%.

Several trials are performed for appropriate parameter value selection. Appropriate combination of W_{ini}, W_{fin}, C_1, C_2 have been applied. The following parameters have been chosen for both PSO and HPSO estimators; W_{ini}=0.9, W_{fin}=0.4, C_1=C_2=2.05. The values are very close to those recommended by other authors in [30] and [56].

In order to choose the best value for alpha, the HPSO algorithm was run for different values of alpha between 0 and 1 in step of 0.1 in order to obtain the value with the least convergence time. It is found that α=0.2 produces the best convergence speed for theses example systems. The number of particles and the number of iterations are 200 and 1000 respectively. The lower and upper limits of control variables corresponding to the coding on the PSO and HPSO are set in such a way that the inequality constraints of the control variables are satisfied as listed in (3.9) to (3-11). The shape of the proposed penalty function is displayed in Fig. 3.10.

$$0.95pu < V_i^a, V_i^b, V_i^c < 1.05\ pu \tag{3.9}$$

$$-30° < \delta_i^a, \delta_i^b, \delta_i^c < +30° \tag{3.10}$$

$$0.9 < t_i^a, t_i^b, t_i^c < 1.1 \tag{3.11}$$

The tap ratio of transformer is specified in the range of 0.9 to 1.1 in steps of 0.00625. The zero injections, voltages and angles across the closed switch and voltage at the regulator bus have been taken as equality constraints in the state estimation formulation. A weighted quadratic penalty function is added to the objective function to take care of each of these equality constraints. The switch between bus 9 and bus 10 is assumed to be closed for 13 bus test system. The power flow results have been used as initial guess for both PSO and HPSO estimator in order to achieve a fast solution. The Fig. 3.3, Fig. 3.4 and Fig. 3.5 show the real and estimated vector of voltages for PSO method and Fig. 3.6, Fig. 3.7 and Fig. 3.8 show the real and estimated vector of voltages for HPSO method at different phases of the IEEE-13 bus model distribution network. There are 5 switches in the 123 bus system. The switch between buses 121 and 123 is assumed to be open while other switches are assumed to be closed for this network. Fig. 3.11, Fig. 3.12 and Fig. 3.13 show the real and estimated vector of voltages of the IEEE-123 bus model distribution network for HPSO algorithm. In Fig. 3.3 to Fig. 3.8 and Fig. 3.11 to Fig. 3.16 the value of voltage has been taken as 1.0 where there is no phase available for the given bus on the graphs. The obtained results are found to be very satisfactory within the allowable error range. The main advantage of the PSO and HPSO based methods are in correct estimation of the transformer taps as it is shown in Table 3.1 for 13 bus test system and Table 3.2 for 123 bus system, which are the most important findings from this research.

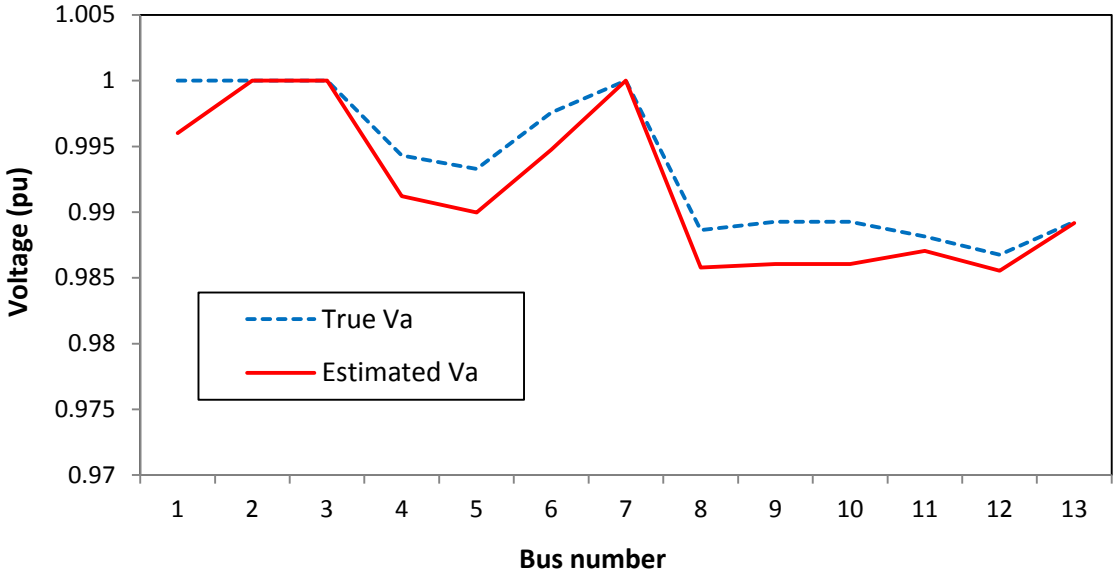


Fig. 3.3 True and estimated voltage for IEEE-13 bus system at phase a by PSO

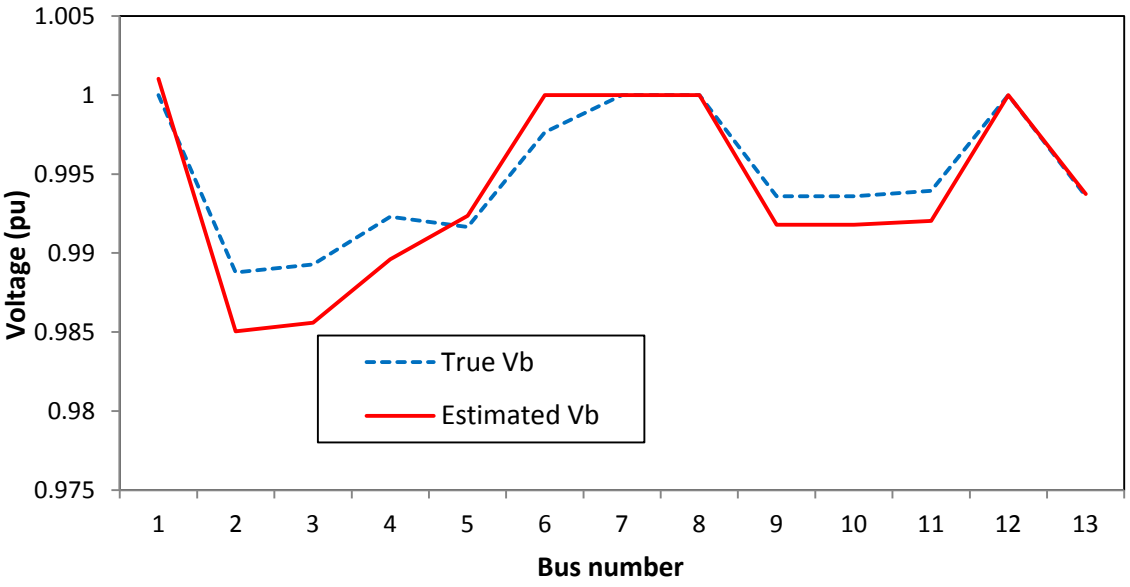


Fig. 3.4 True and estimated voltage for IEEE-13 bus system at phase b by PSO

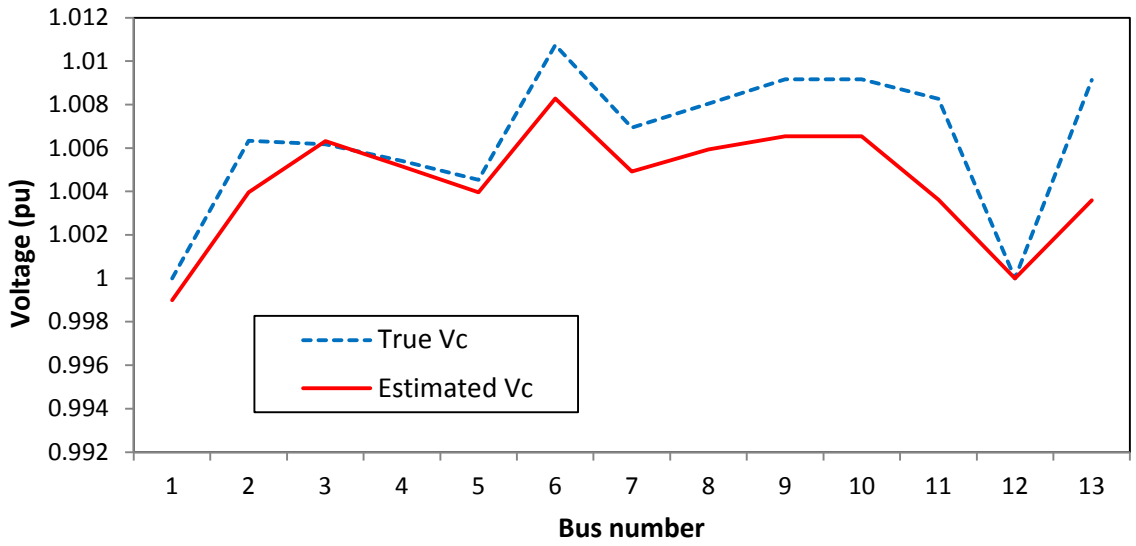


Fig. 3.5 True and estimated voltage for IEEE-13 bus system at phase c by PSO

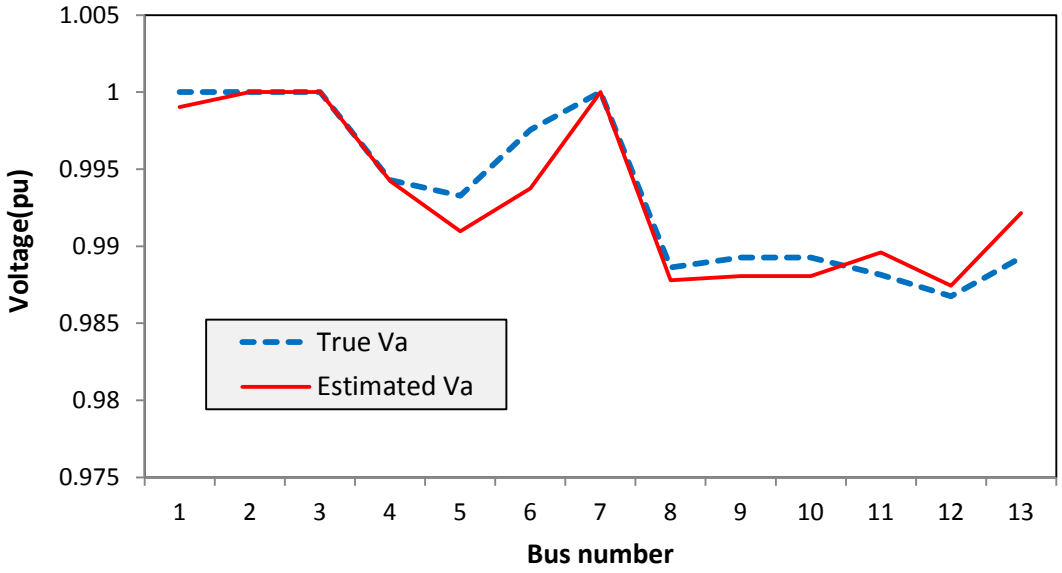


Fig. 3.6 True and estimated voltage for IEEE-13 bus system at phase a by HPSO

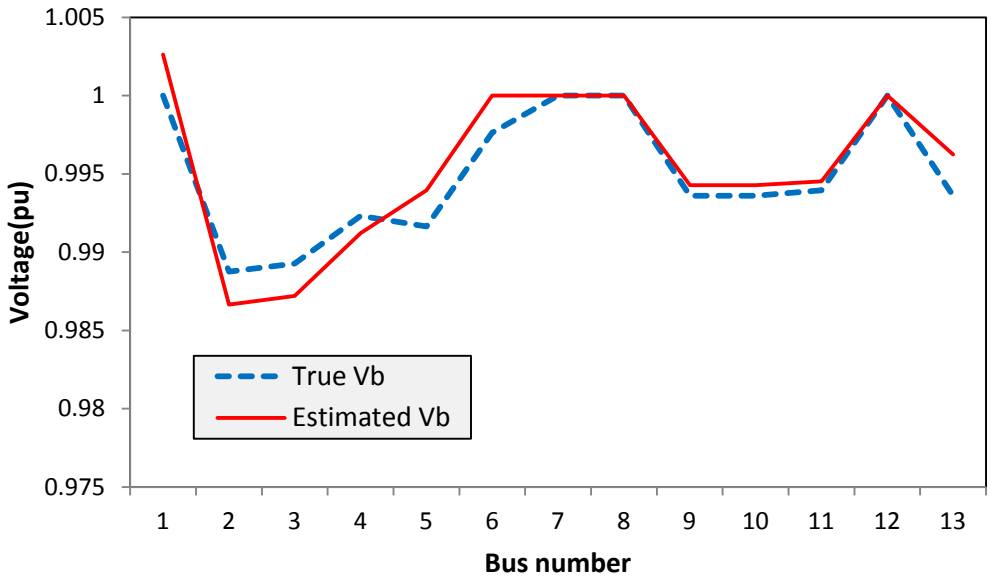


Fig. 3.7 True and estimated voltage for IEEE-13 bus system at phase b by HPSO

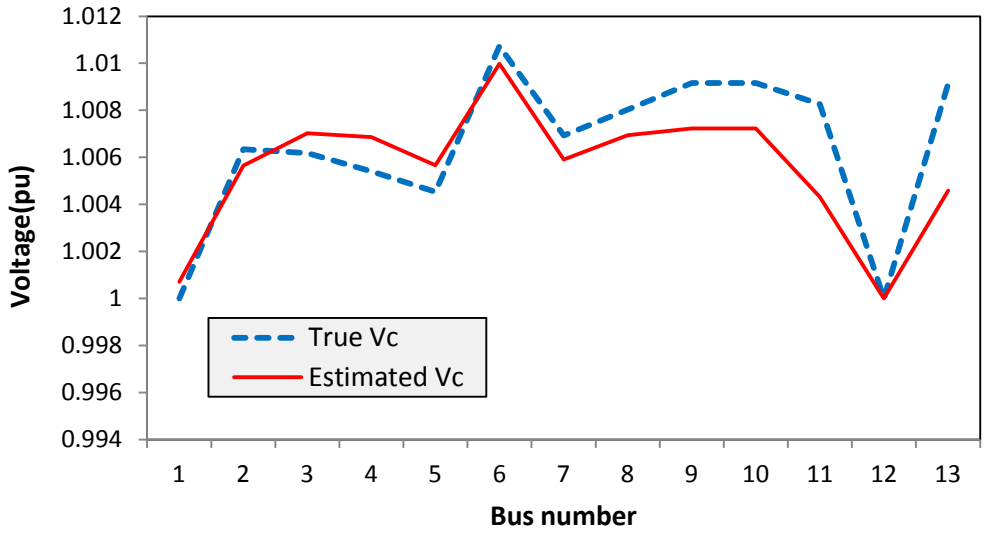


Fig. 3.8 True and estimated voltage for IEEE-13 bus system at phase c by HPSO

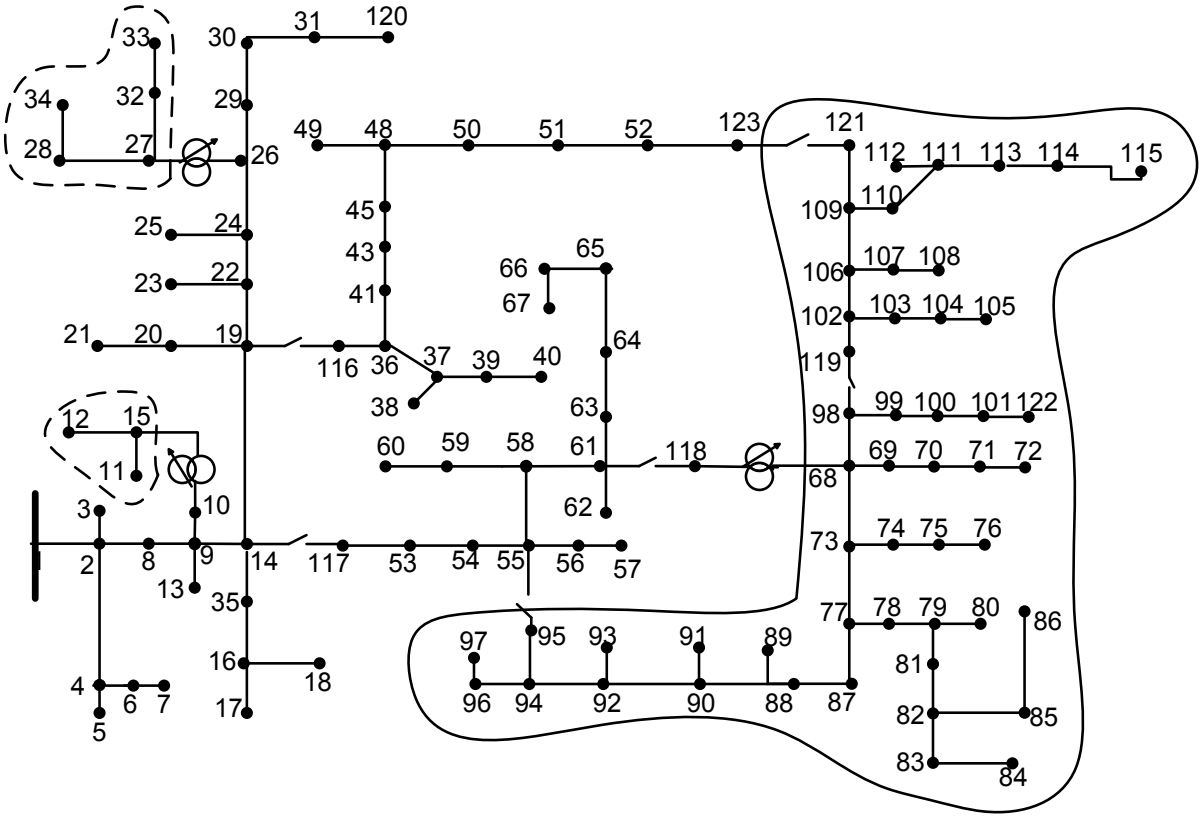


Fig. 3.9 IEEE-123 bus distribution system

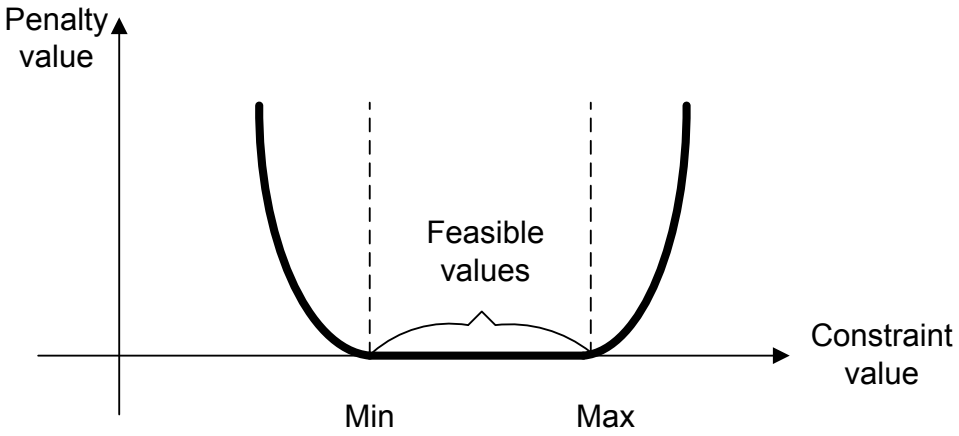


Fig. 3.10 Proposed penalty function

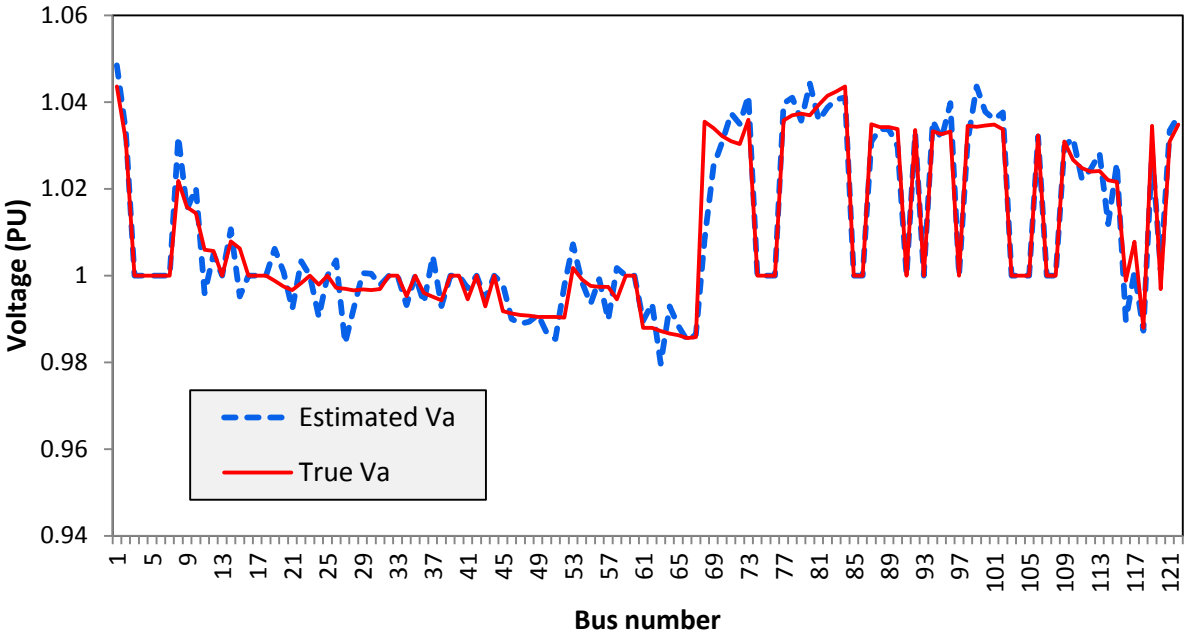


Fig. 3.11 True and estimated voltage for IEEE-123 bus system at phase a by HPSO

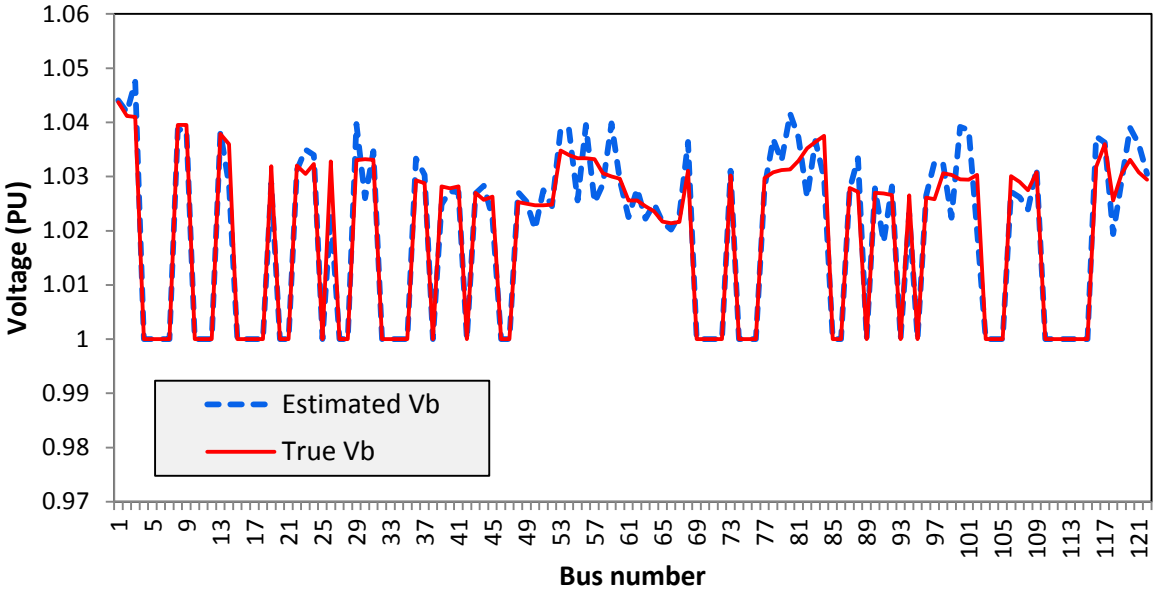


Fig. 3.12 True and estimated voltage for IEEE-123 bus system at phase a by HPSO

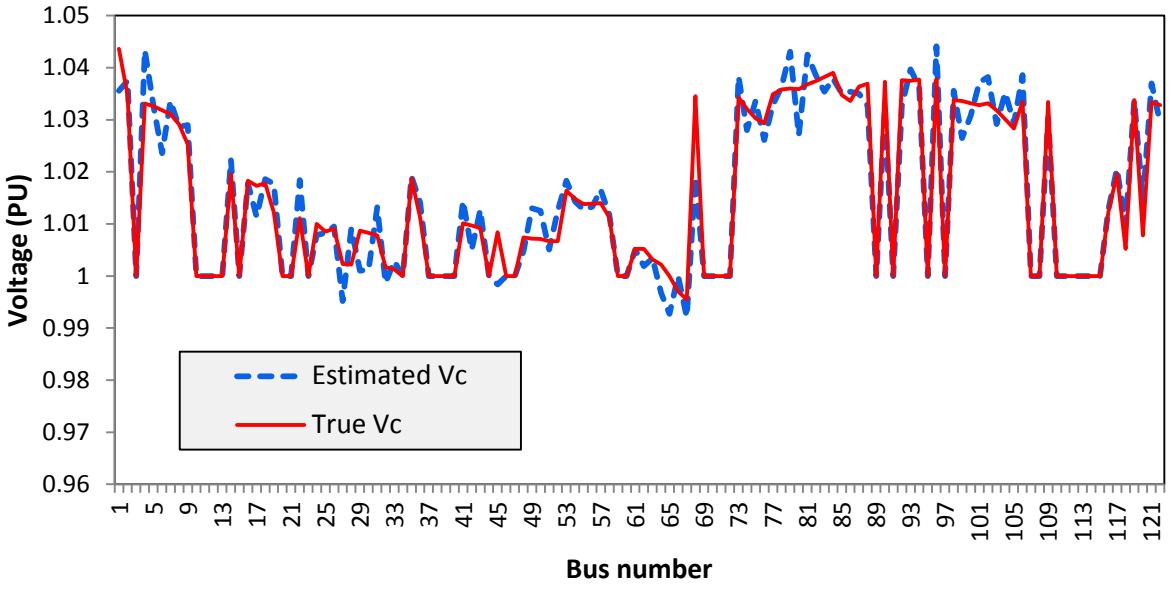


Fig. 3.13 True and estimated voltage for IEEE-123 bus system at phase c by HPSO

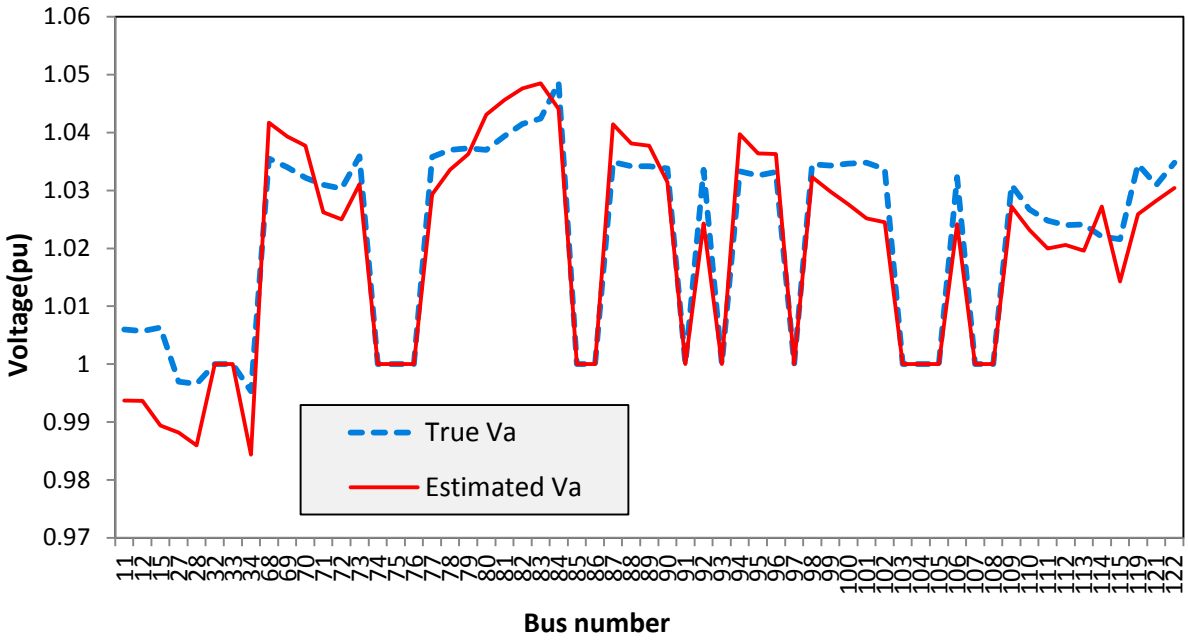


Fig. 3.14 True and estimated voltage for reduced model of 123 bus system at phase a by HPSO

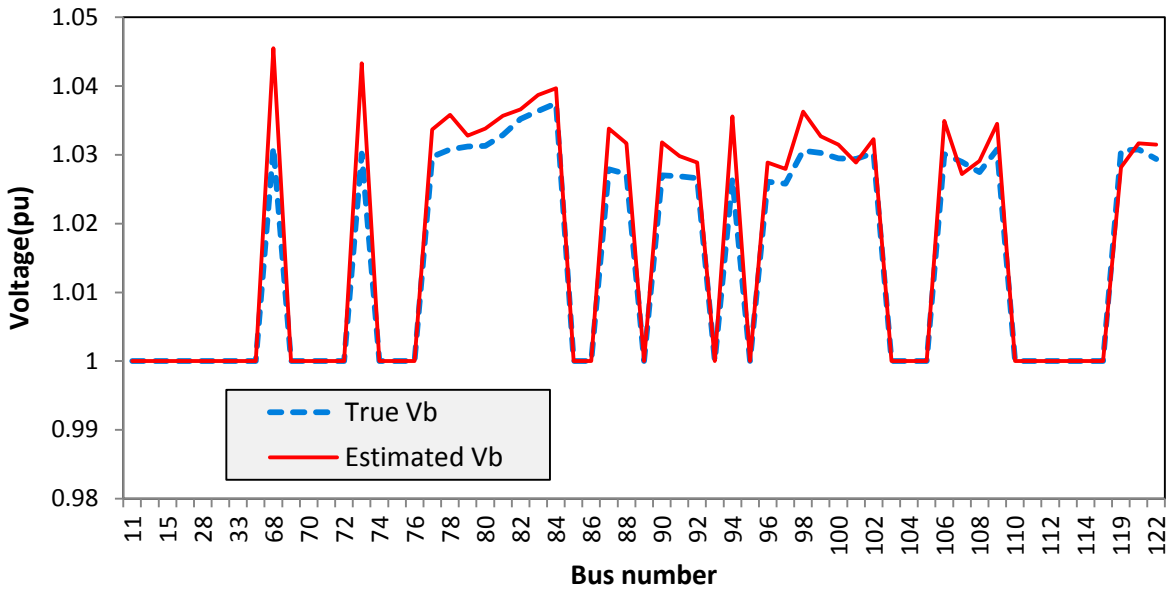


Fig. 3.15 True and estimated voltage for reduced model of 123 bus system at phase b by HPSO

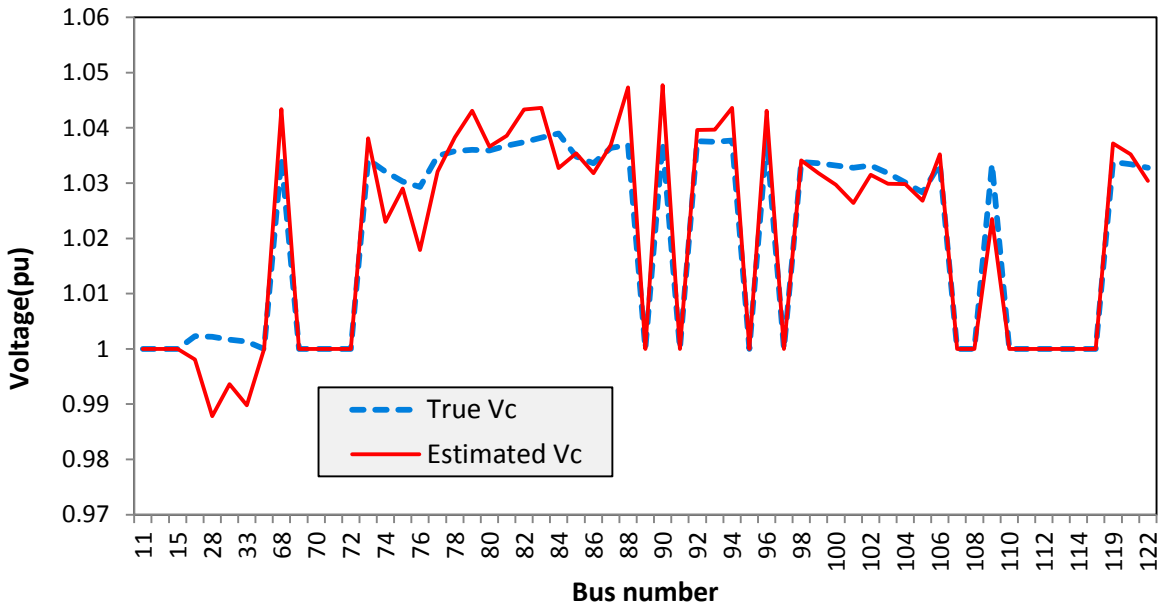


Fig. 3.16 True and estimated voltage for reduced model of 123 bus system at phase c by HPSO

Table 3.1 The true and estimated tap position for 13 bus system at bus 6

Phase	a	b	c
True Tap position	2	2	1
Estimated tap position PSO	2	2	1
Estimated tap position HPSO	2	2	1

Table 3.2 True and estimated tap position for 123 bus system

State variable	**True value**	**WLS**	**HPSO**
T15-Phase a	-1	-1	-1
T27-Phase a	0	0	0
T27- Phase c	-1	-1	-1
T68-Phase a	8	7	8
T68-Phase b	1	1	1
T68-Phase c	5	4	5

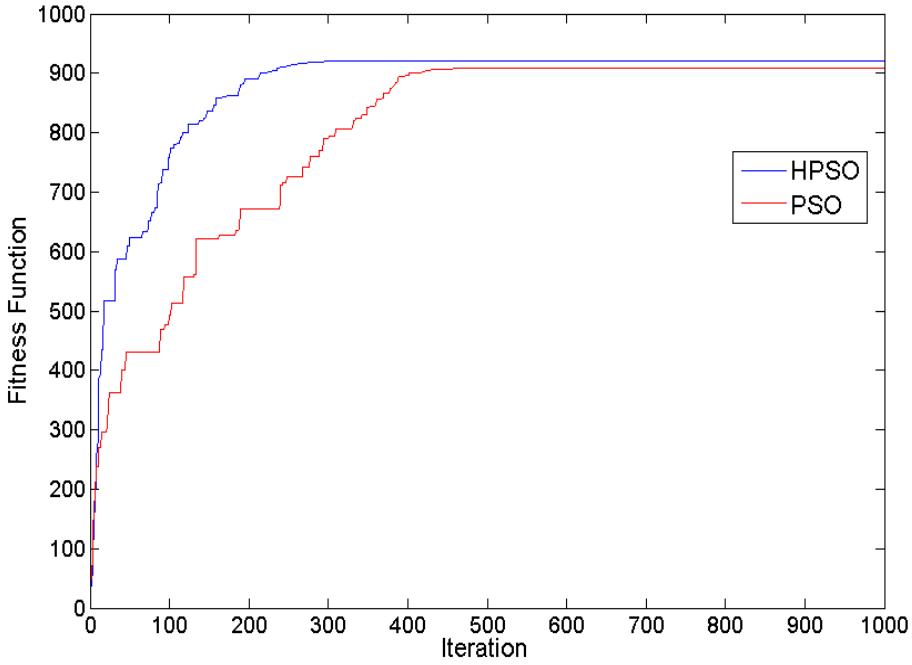


Fig. 3.17 Convergence characteristic of HPSO and PSO

3.4.2 Discussions

In this chapter, PSO and HPSO algorithms have been applied to obtain tap position estimates. Both methods have been tested on IEEE-13 and IEEE-123 bus test systems. PSO takes on an average of 6-7 hours to obtain the solution on 13-bus test system. I have modified the particle position update equation for improving the speed of convergence as given in equation (3.6). Therefore, the execution time reduced to 2−3 hours. HPSO on the other hand takes 18−20 minutes to converge for 13-bus test system. The convergence characteristic of HPSO and improved PSO with correction are shown in Fig. 3.17 for 13-bus test system. As can be seen from convergence characteristic, HPSO method is much faster than PSO method.

In the ideal smart grid environment in principle the state estimator in distribution system should be running in real time. There are several practical limitations to realize this in practice. Even the data from modern smart meters are communicated to distribution SCADA every few hours. The most automated distribution network in the UK does not transmit data more than twice a day. The telecommunication infrastructure in most automated distribution network is such that it is not possible to transmit half hourly measured and stored smart meter

data more than twice a day to the control centre. The authors in [58] have documented in details the standard and practice of data transmission from smart meters in various countries across the world. Given this situation, one obvious question arises: is there any possibility for real time state estimation in power distribution system in the forcible future? The frequency of tap operation is also another practical consideration. Considering the operating life of transformer, after 3000 operations, it requires maintenance and after 30000 operations the transformer tap changing mechanism should be replaced with a new one. In that case changing the tap position every few seconds will damagingly result in shortening the transformer operating life. So it is convincing that unlike transmission system the state estimation in distribution system will not run every 2-5 seconds.

Also, the HPSO method with correction for improving the speed has been applied to IEEE 123 bus test system model. It takes on an average of 4 hours to obtain the solution. However, by identifying and considering only those buses where voltage and angles are affected significantly by changing the tap changer position the execution time has reduced to 90 minutes as a result of the reduction in the number of state variables. Those buses have been enclosed through a dashed line in Fig. 3.9 and the results are shown in Fig. 3.14, Fig. 3.15 and Fig. 3.16. One way to improve the speed of convergence of HPSO is to parallelize the algorithm. In the context of computation in power transmission, it has been explored to obtain improvement in speed of computation. The authors in [59] have achieved 4.8 times faster than normal PSO for transmission system state estimation. Because of the similarity of the structure of the equations and between the inter relationship between variables it is possible to achieve similar results based on the application of parallel PSO for the given network in this study. This is not pursued further because of the lack of access to parallel computing cluster. The comparison of the results of tap estimation from WLS and HPSO reveals that estimation of the continuous values of tap changer may result in an inaccurate tap position since it is based on the rounding technique while HPSO provides the exact position of transformer taps by estimating the discrete values of transformer tap positions. So HPSO output provides more accurate voltage and angle estimates thus helps in obtaining better estimate of line and transformer loading and losses. The impact of correct tap position on losses evaluation is very significant. This needs further calculations, comparison and discussions. Chapter 5 will deal with this.

3.5 Conclusions

The technique proposed in this chapter has addressed the transformer taps estimation in the context of distribution system state estimation (DSSE). It has, for the first time, applied HPSO method to estimate transformer tap positions without any assumption and also in unbalanced three phase distribution system. The simulation results on IEEE 13-bus and IEEE 123-bus standard system models showed that the HPSO method has generated reliable estimate for transformer taps with discrete variables in distribution network while minimizing the objective function. It is also demonstrated that it performs better when compared to PSO. This study also contributes to novel strategies to expedite solution from PSO and HPSO. This research has introduced novel strategy to expedite the HPSO solution by changing direction of the position of the particle near the limits. This is one of the contributions of this chapter. The solution from HPSO is accurate and is very useful for computation of various quantities accurately used in the operational planning time scale i.e. voltage and var control (VVC). HPSO based tap optimization research described in this chapter is recently published in IEEE Transactions on Smart Grid [34].

Like all the methods based on heuristic search, the HPSO method takes longer time (tens of minutes) to converge in a reasonably sized network model. This apparently weakens the case for HPSO for DSSE in real time. It is important to note that state estimation in distribution SCADA is not done in real time. Since the life expectancy of the tap changing mechanism is influenced by the number of operations of the taps, it is also not allowed to have frequent tap operation when rapid changes of loads and generation take place. HPSO can be applied for network computation used for operational planning purposes such as hour ahead contingency analysis and reactive power control scheduling. The HPSO based solution in this way is very attractive to operate the network with higher efficiency even though the calculation is not done in real time. This has been the motivation of the research described in the following chapter, exploring another type of the mixed integer non-linear (MINLP) optimization solver such as Ordinal optimization which is more suitable for real time SE in distribution network.

Chapter 4

Distribution state estimation by Ordinal Optimization

Chapter 3 has applied the Hybrid Particle Swarm Optimization (HPSO) method in an unbalanced three phase distribution network model. It has included discrete tap as an additional state variables. However, like all other methods based on heuristic algorithm, the HPSO method takes unacceptably longer solution time (tens of minutes to hours) for a reasonably sized network model. This apparently weakens the case for application of heuristic methods in controlling smart power distribution grid of the future in operational time scale.

In a pursuit to find faster solution, this chapter proposes an ordinal optimization (OO) based algorithm for more accurate estimation of states in power distribution system with continuous and discrete variables. The proposed algorithm has a high probability of finding a good enough solution according to the OO theory and can handle vast amount of computationally complex problems in short period of time without compromising the quality of the solution noticeably. The benefits of the approach in terms of accurate estimation of on-load tap changers (OLTC) tap positions and shorter computation time are illustrated through simulations involving 129 bus unbalanced distribution network model (extended model of

IEEE-123 bus distribution network). This proposed methodology provides more accurate results when compared with conventional weighted least square (WLS) algorithm that ignores the discrete nature of the tap positions in the solution process. The results prove the suitability of the proposed algorithm in smart power distribution grid of the future.

References [26] and [33] considered ordinal optimization (OO) and mixed-integer quadratic programming on a balanced three-phase network model without considering the unbalanced nature of the distribution system.

This chapter studies a full three phase state estimator including unbalanced load network model and the discrete taps as additional estimated variables based on OO optimization technique in order to estimate the discrete value of the transformer taps.

The purpose of application of OO theory in DSSE problem is to limit the searching space to the good subset of search space through limited sampling [32]. This will reduce the solution time. The method helps to find a good enough solution with high probability instead of the best in solving problems with the huge search space. This is the case in finding the optimal solution for DSSE problem with continuous and discrete variables combined. The performance of the proposed method has been tested on 129 bus distribution network. The results are very encouraging for its potential application in real time operation.

Following this introduction, the rest of this chapter is organized in the following manner. Section 4.1 provides mathematic formulation of the three phase state estimation problems with continuous and discrete variables. In Section 4.2 a general overview of OO solution method is described. Section 4.3 presents the OO approach in the context of three phase unbalanced state estimation for distribution network model. Section 4.4 provides the results, performance comparison with other techniques, discussions on the value of the contribution for the distribution network operators. Section 4.5 summarizes and concludes the chapter.

4.1 Mathematic formulation of the three phase state estimation problems with continuous and discrete variables

The solution to SE problem with continuous and discrete variables is formulated as a minimization of the following objective function subject to satisfying several equality and inequality constraints. The goal is to obtain the bus voltage magnitudes, angles and tap

positions that minimizes weighted square of the difference between the measured quantity and the estimated quantity which are functions of estimated states. It is expressed as:

$$min\, J(x) = \sum_{i=1}^{m} w_{ii}\, r_i^2 \tag{4.1}$$

Subject to:

$$z_i = h_i(x_c, x_d) + r_i \qquad i = 1, 2 \ldots m \tag{4.2}$$

$$c(x_c x_{,d}) = 0 \tag{4.3}$$

$$g_{min} < g(x_c, x_d) < g_{max} \tag{4.4}$$

Where,

$\boldsymbol{x_c}$: Continuous state variables (voltage magnitudes and angles).

$\boldsymbol{x_d}$: Discrete state variables (transformer taps positions).

$\boldsymbol{z_i}$: Measured value of i^{th} measurement.

$\boldsymbol{m}$ Number of measurements

$\boldsymbol{h_i}(x_c, x_d)$: i^{th} measurement as a function of the state vector variables (continuous or discrete).

$\boldsymbol{w_{ii}}$ Weighting factor of measurement variable *i*,

$\boldsymbol{r_i}$: i^{th} measurement error.

Where in three phase system $x_c = [\delta_2^{abc} \ldots \delta_i^{abc} \ldots V_1^{abc} \ldots V_i^{abc} \ldots]^T$ is the concatenation vector of three-phase voltage angles and magnitude at all buses, where $\delta_i^{abc} = [\delta_i^a\ \delta_i^b\ \delta_i^c\ ]^T$ denotes the continuous vector of phase angles of all buses except the reference bus, $V_i^{abc} = [V_i^a V_i^b V_i^c]^T$ denotes the vector of voltage magnitudes and $x_d = [\ldots t_i^{abc} \ldots]^T$ where $t_i^{abc} = [t_i^a\ t_i^b\ t_i^c\ ]^T$ is the discrete vector of all the taps.

The equality constraints $c(x_c, x_d)=0$ are the set of equation corresponding to virtual measurements. The virtual measurements are zero injection busses such as transformer, substation busbars with no local generation and demands etc. The details are in references

[34] and [41].

The inequality constraints ($g_{min} < g(x_c, x_d) < g_{max}$) are the set of continuous and discrete constraints that represent the system operational and security limits, such as setting upper and lower limits for decision/control variables such as voltage, angle and tap positions.

Real measurements $h_i(x_c, x_d)$: are real and reactive powers, bus voltages and branch currents. All the relevant expressions in three phase format are detailed in Chapter 2.

4.2 Ordinal Optimization

Ordinal optimization is a method to obtain an approximate solution to the problem of minimising or maximising an objective function over a large set of designs. The main idea behind OO is to reduce the search space to the good enough subset by limited sampling. Ordinal optimisation is based on two concepts stating that the optimisation of complex problems can be made much easier by order comparison and goal softening [32], [60].

1. Order comparison: It is easier to find order than value. For instance finding whether A is bigger than B is much easier than finding the exact value of A and B.

2. Goal softening: For many practical problems, it makes the problem easier and it is sufficient to find good enough solution with high probability instead of getting the best.

4.2.1 Application of OO to complex optimisation problems

The procedure for the practical application of OO to complex optimization problems is as follows [61]:

Step 1. Uniformly sample N designs from θ to form θ^N.

Step 2. Estimate the performance of the designs in θ^N using a crude and computationally fast model.

Step 3. Reducing the size of search space to good enough subset, *G*, by sampling a small number of alternatives (top-*g*). In such a way that the reduced search space contain at least one solution inside the top $n\%$ with the probability level of *P*.

Step 4. Evaluation of the objective function value for each sampled alternatives using an approximate but computationally efficient model.

Step 5. The estimated top-s designs from an approximate model are compared via an exact model to form the selected subset, *S*.

Step 6. OO theory ensures that *S* contains at least *k* truly good enough designs from among the true top-*g* samples.

Where

θ = search space of optimisation variables

θ^N= set of *N* chosen designs

N = number of designs uniformly chosen from θ

G = good enough subset, usually the true top-g designs in θ^N, which is a subset of the search space in which the members fulfil some of the design standards that are set out by the designer

S = selected subset, usually the estimated top-s designs in θ^N, which is a subset of search space in which the members are selected by using certain evaluation methods

$G \cap S$ = set of truly good enough designs in *S*

k = alignment level which is the degree of matching between *G* and *S*

P = alignment probability = $Pr[|G \cap S| \geq k]$, the probability that there are actually *k* truly good enough designs in *S*.

Fig. 4.1 demonstrates general OO algorithm.

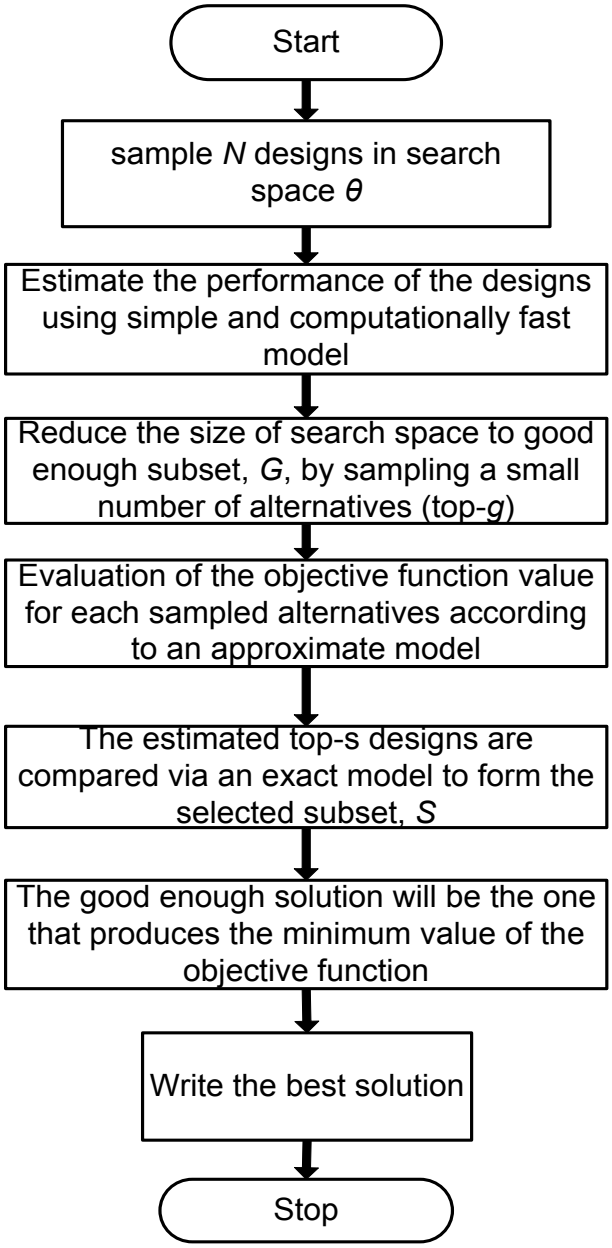


Fig. 4.1 General flow chart of OO

4.3 Distribution system state estimation by Ordinal Optimization

The OO has been applied for the placement of meters in power distribution planning [62].

To our understanding it has not been applied to estimate the states in unbalanced power networks with discrete variables such as OLTC and switched capacitor. This section describes the various steps i have devised to adopt the application of OO method in three-phase state estimation for distribution system in order to obtain the accurate estimate of

transformer tap positions. The steps are as follows:

4.3.1 Network configuration & network data

The first step is modelling of various network components of distribution system such as lines, transformers, switches and load model for DSSE. This is owing to the presence of unsymmetrical-network components and unbalanced-load in distribution systems. Therefore, it is required to consider the exact model of the system components (three-phase model). It includes the information about the line resistance, reactance, tap setting connectivity information etc. The comprehensive three phase model of the various components of the network such as the distribution line, transformers, switches and load model can be found in references [42] and [46].

4.3.2 Select N designs in search space

N designs in the search space θ are chosen as follows. For instance the size of search space with *m* discrete numbers of transformer tap positions which can change between the steps of -16 and 16 would be 32^m. This is a large search space. In order to reduce the size of search space the conventional method of WLS state estimation should be applied while setting all the discrete values of the network as continuous variables [26]. Since all the variables are continuous the problem alters to the convex problem and the standard solution for WLS estimator can obtain the optimal solution for each state variables. The mathematical formulation of the state estimation with only continuous values can be written as follows:

Where *x* is a concatenation of x_c and x_{cd}.

$$x = [x_c \; x_{cd}]^T \tag{4.5}$$

And x_{cd} denotes the continuous tap ratios.

$$min\, J(x) = \frac{1}{2}\sum_{i=1}^{m}[(Z_i - h_i(x)]{R_{ii}}^{-1}[(Z_i - h_i(x)] \tag{4.6}$$

Subject to:

$$c(x_c \; x_{cd}) = 0 \tag{4.7}$$

$$g_{min} < g(x_c, x_{cd}) < g_{max} \tag{4.8}$$

This problem is solved with the previous method of non-linear programming algorithm such as efficient dual-type method to obtain the estimated values of states variables. The corresponding continuous values of the discrete variables now will be set to either the nearest lower bound integer or upper bound integer value of that component. After estimating the continuous values of transformer tap positions and setting them to the nearest lower bound or upper bound integer values the size of *N* design will be obtained $N = 2^m$.

$$\overline{x_{cdJ}} = \left(\overline{x_{cJ}} \text{ or } \underline{x_{cj}}\right) \tag{4.9}$$

Where

$\overline{x_{cdJ}}$**:** is the j^{th} discrete value of discrete variable x_{cd}.

However, the number of these 2^m samples is still larger than the representative set *N*, which is ≅ 1000 found by uniform selection. Therefore, the weighted minimum norm deviations given by $\left\|\frac{\hat{x_{cdj}}-\bar{x_{cdj}}}{\hat{x_{cdj}}}\right\|$ of each transformer tap are compared, where $\hat{x_{cd}}$ is the solution of (4.6)-(4.8). If this weighted minimum norm deviation is less than pre-assigned positive value *val*, then that discrete variable x_{dj} is fixed at either $\overline{x_{cJ}}$ or $\underline{x_{cj}}$, whichever is smaller. By this way, some *K* components are fixed such that $2^{m-K} = N;\ m - K = 10$.

4.3.3 Evaluate and order *N* designs

In order to evaluate the *N* samples of designs an approximate but computationally efficient model is applied. At this step the sensitivity analysis of the discrete variables with respect to the objective function is applied [26], [63]. The first derivative of the objective function with respect to discrete variables for transformer taps has been calculated. Therefore, the value of the sensitivity function for different combinations of transformer tap positions in the system will be obtained. The following shows the equations relating to obtaining the sensitivity values for transformer tap positions.

$$J(x_c, x_d) = \frac{1}{2}\sum_{i=1}^{m}[(Z_i - h_i(x_c, x_d)]{R_{ii}}^{-1}[(Z_i - h_i(x_c, x_d)] \tag{4.10}$$

$$\frac{\partial J}{\partial T_j} = -\sum_{i=1}^{m}[(Z_i - h_i(x_c, x_d)].{R_{ii}}^{-1}.\frac{\partial h_i(x_c, x_d)}{\partial T_j} \tag{4.11}$$

Where

$J(x_c, x_d)$: is the objective function

$\frac{\partial J}{\partial T_j}$: is the first derivative of objective function with respect to transformer taps

Consequently, the sensitivity function is specified by

$$\sum_{j=1}^{Ntrans-k} T_j . \frac{\partial J}{\partial T_j} = -\sum_{j=1}^{Ntrans-k} \left\{ T_j . \left[\sum_{i=1}^{m} [(Z_i - h_i(x_c, x_d)] . R_{ii}^{-1} . \frac{\partial h_i(x_c, x_d)}{\partial T_j} \right] \right\} \quad (4.12)$$

T_j: j^{th} component of discrete value of transformer tap value

4.3.4 Select the best subset

At this stage the absolute value of the sensitivity function evaluated for the 2^{10} tap combinations will be organised in ascending order to identify the top-*s* samples set in the $N \cong 1000$ designs. The size of the top-s sample set, called the selected subset, depends on the number of alignments k; the size of the good enough subset, g_d; the noise characteristic of modelling error; the shape of the ordered performance curve (OPC); and the size of the representative set and alignment probability. The size of *s* is determined by the formula given in [61].

$$s = e^{\alpha_0} k^{\gamma} {g_d}^{\beta_0} + \vartheta \quad (4.13)$$

Where, k is the alignment level, $g_d$is the number of good enough designs, ϑ is the noise factor and $\alpha_0, \beta_0, \gamma$, are coefficients whose values depend on the OPC curve and noise characteristics. The values for this case are given in the next section. The top-s samples with smallest absolute sensitivity function values will construct the selected subset [63].

4.3.5 Good enough solution

Each sample of selected subset S will be evaluated using the standard WLS SE method. Therefore, the value of the objective function for each sample will be obtained. The good enough solution will be the one (i.e. alignment level k=1) that produces the minimum value of the objective function [26].

4.4 Results and discussions

4.4.1 Case study

The proposed OO approach was implemented in MATLAB and has been tested on 129 bus distribution network (extended model of IEEE-123 bus distribution network) to validate the proposed algorithms. It is required to have at least 10 tap changers for OO to be effective. So, two additional transformers have been installed between nodes 26, 125 with 3 additional phases and one between 62, 119 with 2 additional phases. The system now consists of 129 buses and 123 lines and 11 transformer tap changers.

The network parameters and load data are obtained from [51] and [52]. The topology of the system is shown in Fig. 4.2. The system is configured and modelled based on the assumption of unbalanced three phase system. There are both three-phase and single-phase loads.

Measurements were generated using three-phase power flow program with addition of normally distributed noise component to generate noisy measurement. The error of true measurement was assumed 3% while the error in pseudo measurement (load data) was considered to be 20%.

We take the representative set of N=1000 designs samples, with alignment probability of P=0.95. It is assumed that the good enough subset consists of the top 5% of the representative set and the number of alignments to be 1 as mentioned in Section (4.3). Taking into account the noise of modelling error to be very large and the worst OPC which has a lot of bad designs, according to equation (4.13), the coefficients are given as α_0= 8.2995, g_d=50, k=1, γ= 1.3777, β_0, = −1.4986, ϑ= 8. The value of s is chosen to be equal to 20.

The lower and upper limit of control variables correspond to the coding on the OO is set in such a way that the inequality constraints of the control variables are satisfied.

$$0.95pu < V_i^a, V_i^b, V_i^c < 1.05\ pu$$

$$-30° < \delta_i^a, \delta_i^b, \delta_i^c < +30°$$

$$0.9 < t_i^a, t_i^b, t_i^c < 1.1$$

The transformer tap ratios are specified in the range of 0.9 to 1.1 in steps of 0.00625.

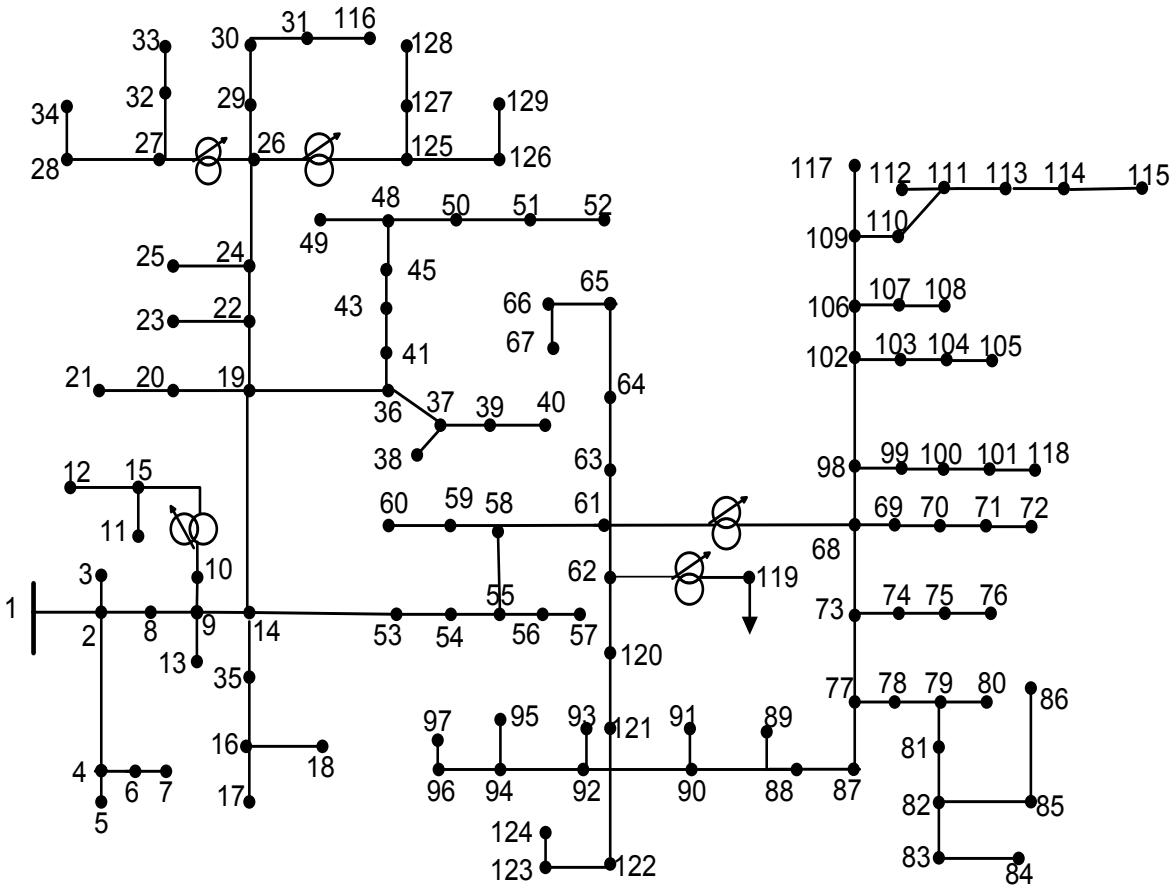


Fig. 4.2 129 bus distribution system (extended model of IEEE-123 bus distribution network)

4.4.2 Results and comparisons

The detailed results of the OO selected subset for the 129 bus test system are shown on Table 4.1. Fig. 4.3, Fig. 4.4 and Fig. 4.5 show the real and estimated vector of voltages for the 129 bus model distribution network. In Fig. 4.3, Fig. 4.4 and Fig. 4.5 the value of voltage has been taken as 1.0 where there is no phase available for the given bus on the graphs. The obtained results are found to be satisfactory within the tolerable error range. The discrete values of transformer tap positions by OO are presented in Table 4.2 and it has been compared with the results obtained through WLS rounding technique. The comparison of the results of tap estimation from OO and WLS reveals that estimation of the continuous values

of tap changers result in an inaccurate tap position while OO provides the exact position of transformer taps by estimating the discrete values of transformer tap positions. So, OO output provides more accurate voltage and angle estimates and thus helps in obtaining better estimate of line and transformer loading and losses. This is very useful for optimum scheduling of voltage and var control resources.

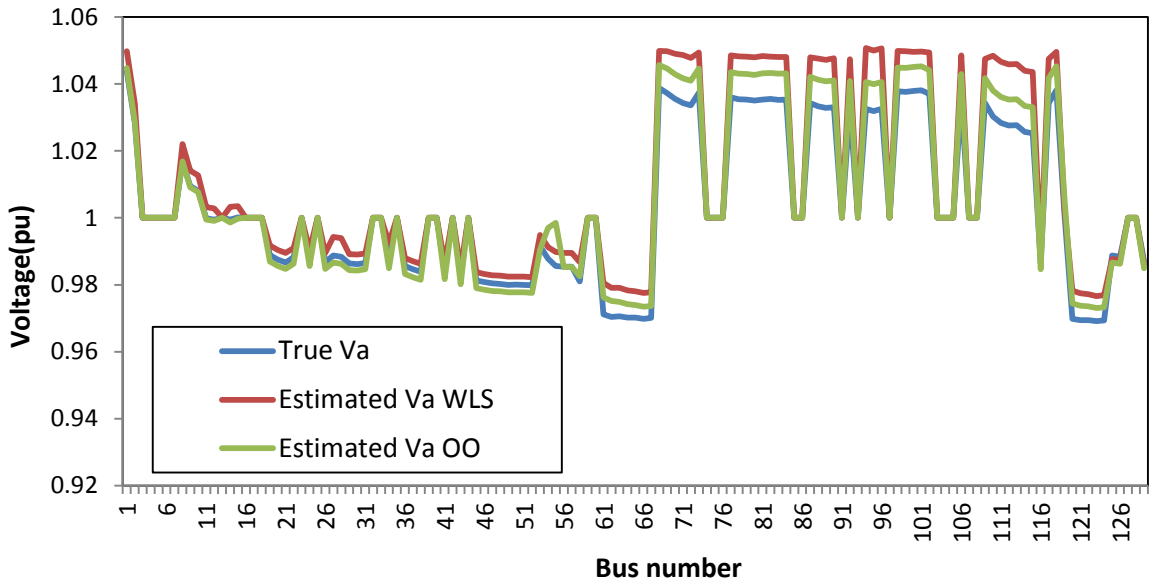


Fig. 4.3True and estimated voltage with WLS &OO for phase a for 129 bus system (extended model of IEEE-123 bus distribution network)

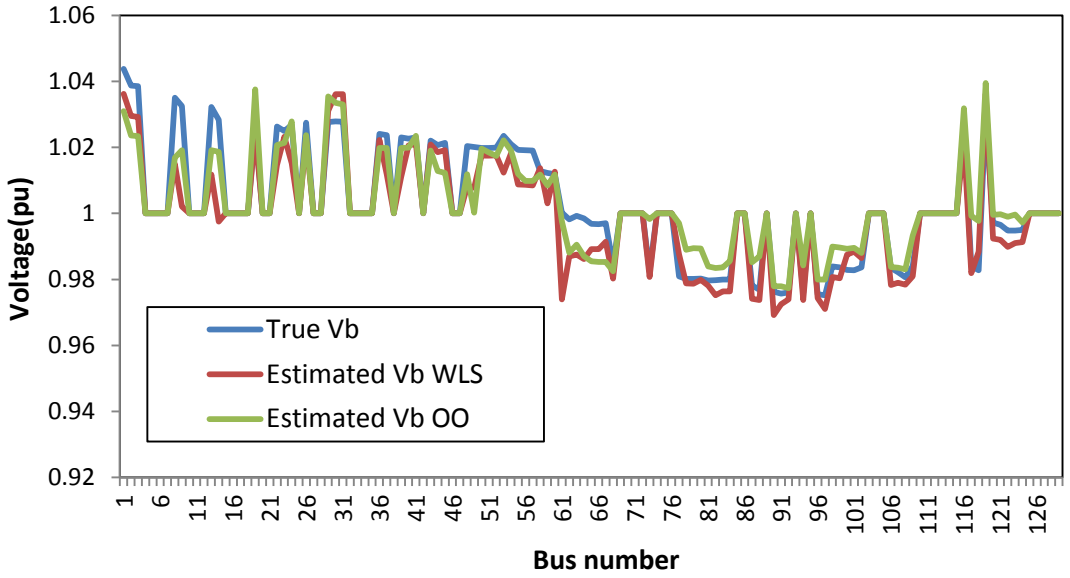


Fig. 4.4 True and estimated voltage with WLS &OO for phase b for 129 bus system (extended model of IEEE-123 bus distribution network)

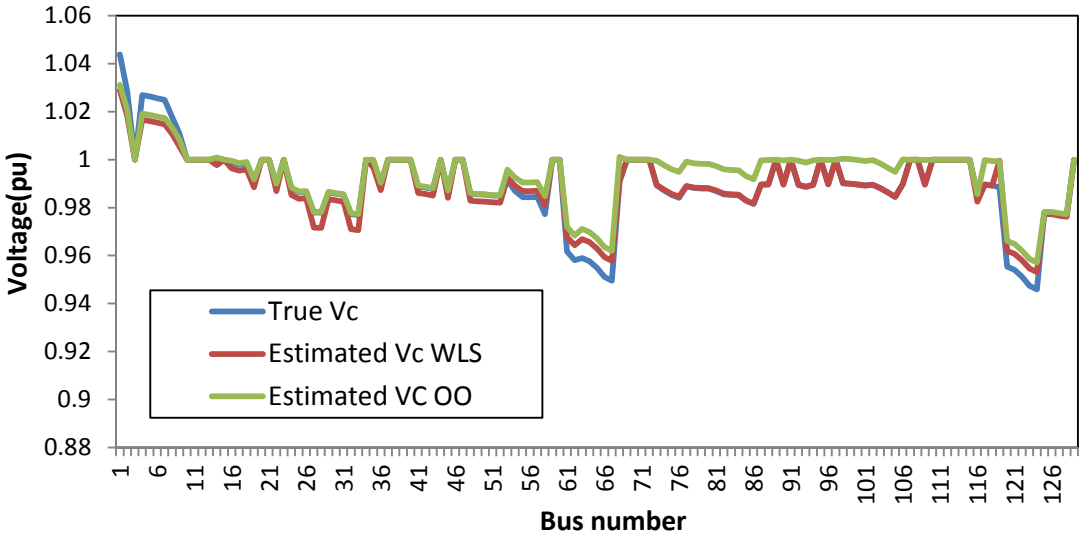


Fig. 4.5 True and estimated voltage with WLS &OO for phase c for 129 bus system (extended model of IEEE-123 bus distribution network)

Table 4.1 Value of the objective function and its sensitivity to tap position for 129 bus system (extended model of IEEE-123 bus distribution network)

Number	**Sensitivity Value**	**NN Number**	**Value of Objective Function**
1	9.09234E+13	642	2.73E+06
2	9.09259E+13	674	2.80E+06
3	9.09268E+13	658	2.37E+06
4	9.09269E+13	706	3.37E+06
5	9.09293E+13	690	2.42E+06
6	9.09294E+13	738	3.45E+06
7	9.09303E+13	722	2.85E+06
8	9.09328E+13	754	2.92E+06
9	9.09331E+13	130	2.72E+06
10	9.09356E+13	162	2.79E+06
11	**9.09365E+13**	**146**	**2.37E+06**
12	9.09366E+13	194	3.37E+06
13	9.09389E+13	178	2.42E+06
14	9.09391E+13	226	3.45E+06
15	9.094E+13	210	2.85E+06
16	9.09424E+13	242	2.92E+06
17	9.11063E+13	646	3.12E+06
18	9.11088E+13	678	3.20E+06
19	9.11097E+13	662	2.74E+06
20	9.11098E+13	710	3.78E+06

Table 4.2 True and estimated tap position for 129 bus system (extended model of IEEE-123 bus distribution network) by OO &WLS

Transformers	**Phase**	**True**	**OO**	**WLS**
T10-15	Phase a	1	1	1
T26-27	Phase a	0	0	0
T26-27	Phase c	1	1	1
T61-68	Phase a	-8	-8	-8
T61-68	Phase b	-1	-1	-1
T61-68	Phase c	-5	-5	-5
T62-119	Phase a	-5	-5	-4
T62-119	Phase b	-5	-5	-5
T62-119	Phase c	-5	-5	-4
T26-125	Phase a	0	0	0
T26-125	Phase c	1	1	1

Table 4.3 Speed of solution in HPSO and OO for 129 bus system (extended model of IEEE-123 bus distribution network)

HPSO	260 mins
OO	10 mins

The accurate solution of OLTC positions has been attempted in recently published research [34] for 123 bus network model by a custom designed Hybrid Particle Swarm Optimization (HPSO). The same method is applied to this extended network model. The results obtained from HPSO in respect of tap position matches with that obtained by OO. The solution times are displayed in Table 4.3. It is clearly seen that the OO is faster. It is important to have state estimation solved in seconds not in minutes. That way WLS is the best but at the cost of

accuracy of the solution. One way to deal with this is to run WLS as main algorithm and in every few hours OO can run to obtain the correct tap positions. Even after massive deployment of smart meters in the system – the data transmission to the control centre is very slow- maximum at the rate of every few hours. In this context OO method will be very effective for operational planning such as contingency analysis rather than requiring it to drive real time network control.

4.5 Conclusions

This chapter discussed transformer taps estimation with continuous and discrete variables in the context of three phase distribution state estimation (SE). The OO technique has been applied to estimate the transformer tap position for the first time in unbalanced three phase distribution network model. The simulation results on 129 bus system showed that the OO method can generate a reliable estimate for transformer taps with discrete variables in distribution network in short period of time. It is also demonstrated that OO is much faster than other accurate methods such HPSO.

Chapter 5

State estimation for accurately computing losses in distribution network

The operation and control of distribution network is very significant activity in electricity supply system as it is the main link between the bulk power and consumers. Because the distribution network carries larger currents, losses are more. In a well ran power network total losses are 6-8% of the total energy produced. About 80% of total losses are incurred at the distribution voltage level. In the UK about 6% of electricity generated is lost in the distribution network each year. The cost of the losses is around £1bn [64]. This is paid by the customers through their electricity bills. While losses occur throughout every voltage level within the electricity distribution network, they are highest at lower voltage levels, such as 33kV (Extra high voltage, (EHV)), 11kV (high voltage, (HV)) and 415V (low voltage (LV)). Obtaining accurate losses figures in the network helps in developing tools to reduce them and in setting much fairer electricity tariff. So, accurate losses estimation and its subsequent reduction will decrease the energy bills for the customers.

5.1 Breakdown of losses in the UK distribution network model

The Fig. 5.1 shows the breakdown of Losses in the UK electricity distribution network. As it is shown the highest proportion of distribution losses comes from transformers (31%) and low voltage circuits (42%). The most effective approach to loss minimization is to run the network at rated voltage level. The accurate estimation of losses clearly helps to develop tools to develop and place control to minimize them.

5.2 Loss estimation and minimization-proposed strategy

One way to reduce losses and improve the voltage profile is by applying transformer tap control. At transmission level SCADA routinely deploys state estimator in real time to compute transmission losses and effect network voltage control. This can be applied at distribution level as well.

The proposed HPSO and OO algorithms in Chapter 3 and Chapter 4 have shown to be capable of accurately estimating the network bus voltage magnitudes and angles and discrete tap values. This is due to the fact that the estimated value of taps positions based on these methods are representative of actual taps positions of the system as these algorithms can handle discrete nature of taps. Therefore the calculated losses based on these methods are more accurate in comparison with the conventional estimation method of WLS which is based on assumption of continuous taps values. Given the customer has to bear the cost of the losses HPSO and OO based estimated voltage and angles and tap positions when used to calculate operational losses for pricing, they will result in more fairer value.

Considering two-port π-model of Fig. 2.5, the equations for calculating the losses in the network are as follow.

$$\text{Total losses} = \sum_{l=1}^{L} S_l \tag{5.1}$$

$$S_l = S_{ij} + S_{ji} \tag{5.2}$$

$$S_{ij} = V_i \times I_{ij}^* \tag{5.3}$$

$$S_{ji} = V_j \times I_{ji}^* \tag{5.4}$$

Where

L: Total number of lines in the network

S_{ij}: Power flow from bus *i* to bus *j*

S_{ji}: Power flow from bus j to bus i

$I_{ij}^{*}\ and\ I_{ji}^{*}$: Conjugated value of current from bus i to bus j and vice versa

S_l: The value of loss in line l

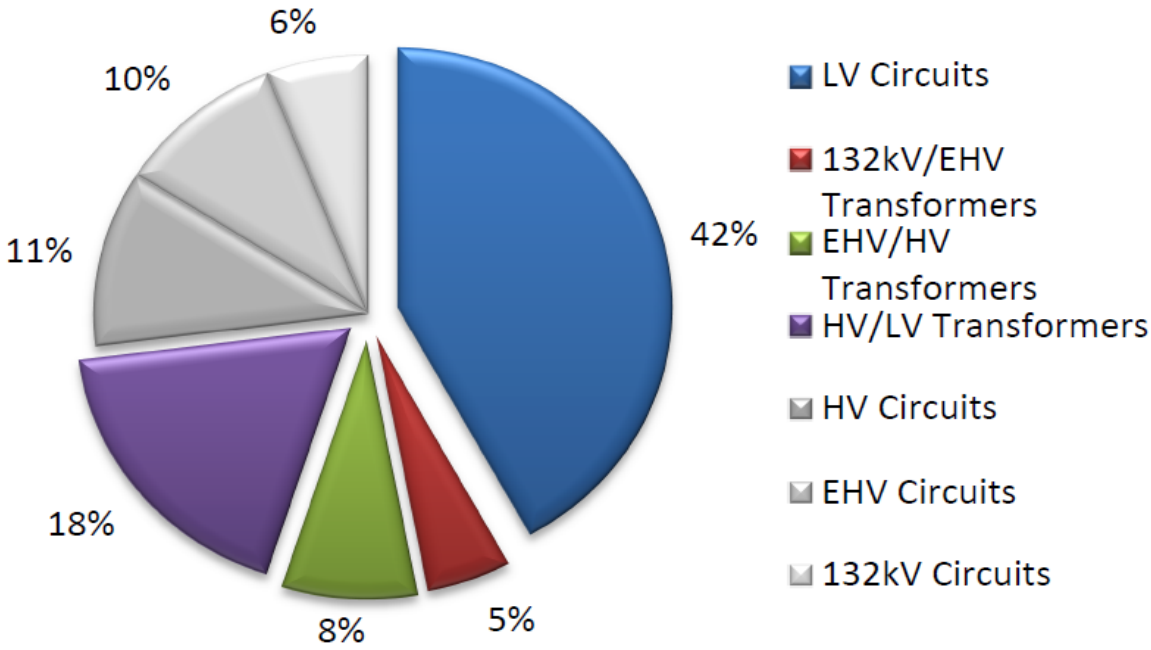


Fig. 5.1 Breakdown of distribution network losses [64]

5.3 Case studies and discussions

This section studies the estimation of losses for two different model networks of IEEE-123 test bus system and 129 bus test system. The study involves application of HPSO and OO method to compute the losses respectively.

5.3.1 Estimation of losses by HPSO for IEEE-123 bus test system

The proposed HPSO method of Chapter 3 has been applied on standard IEEE-123 bus unbalanced test system model and the estimated value of states (voltage magnitudes and angles and discrete tap values) have been used to obtain the value of losses for this network. The 123 bus test system topologies, data and estimated value states are the same as it has been discussed in chapter 3, section 3.4.1. The power losses in the lines for 123 node system

have been computed based on the value of estimated states and the results have been compared with the most common method of state estimation WLS. Fig. 5.2 and Fig. 5.3 present the estimated value of losses by both HPSO and WLS techniques. As it is shown in Fig. 5.2 and Fig. 5.3 the real power losses obtained by WLS are 53.60, 10.64, 36.97 KW for three phases and total is 101.21 KW. The respective values obtained by HPSO method are 50.63, 10.1, and 34.98 KW and total is 95.71 KW. The difference in total computed losses by the two methods are 5.5 KW. The corresponding values for the total reactive power losses obtained by WLS are 108.01, 40.91, 55 KVAr and by HPSO method are 102.67, 38.89 and 52.29 KVAr. The difference in total computed losses by the two methods are 10.54 KVAr. The total capacity of the system is 3855.257 KVA or 3620.498 KW. Such differences in losses by both methods are considerable for the system whose total capacity is 3855.257 KVA.

It is clearly seen that HPSO based technique provides more accurate loss figures. This is due to the fact that the estimation of the continuous values of tap changer by WLS method may result in an inaccurate tap position since it is based on the rounding technique while HPSO provides the exact position of transformer taps by estimating the discrete values of transformer tap positions. So HPSO output provides more accurate voltage and angle estimates thus helps in obtaining better estimate of line and transformer loading and losses. This is very useful in dynamic price setting for efficient electricity market operation and also for optimum scheduling of voltage and var control resources. This clearly justifies value of the HPSO based state estimation. Compared to WLS based approach the computed network losses are noticeably different which is very useful outcome of this proposed methodology. One network operator (Scottish and Southern Energy) in the UK has already found this approach useful for network loss calculation in their 33/11 kV network.

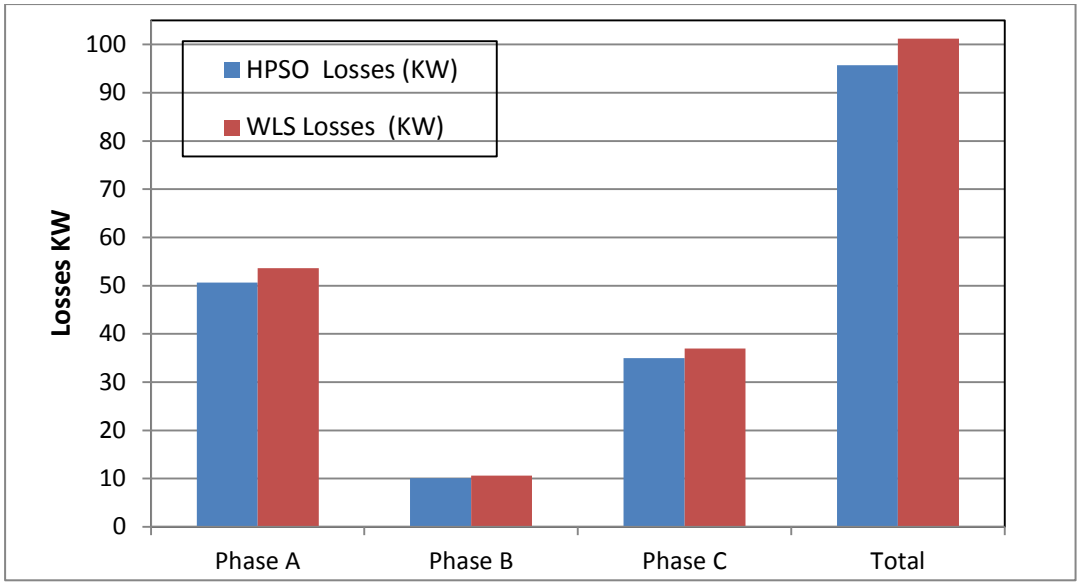


Fig. 5.2 KW losses for HPSO and WLS for 123 bus system

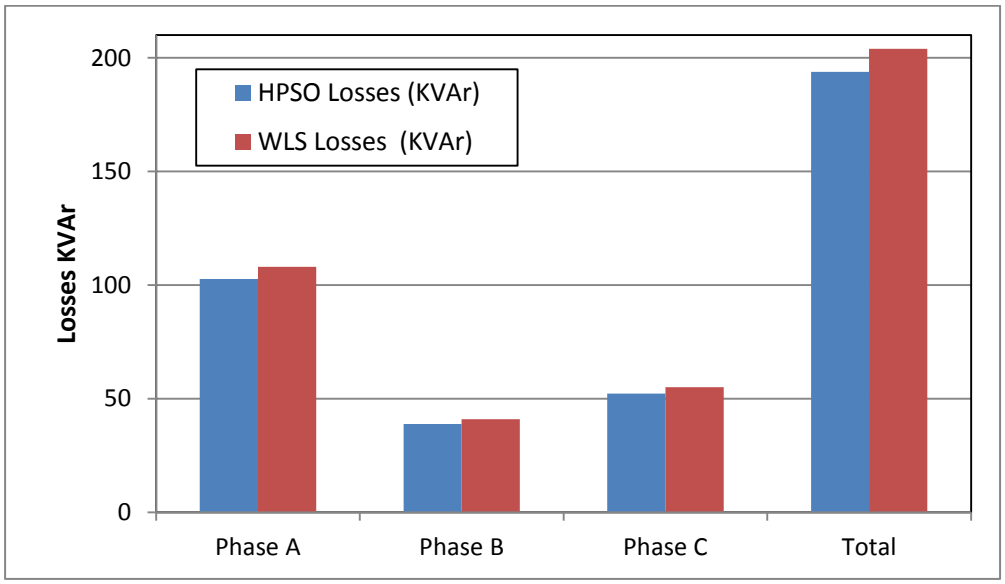


Fig. 5.3 KVAr losses for HPSO and WLS for 123 bus system

5.3.2 Estimation of losses by OO for 129 bus test system

The 129 bus distribution test system which has been applied in Chapter 4 with the same topology and data has been used for this study. The estimated values of voltage magnitudes and angles and tap positions for this system are obtained from Chapter 4, section 4.4.2 and have been used to calculate the losses for the network. The power losses in the lines for 129 node system have been computed and the results compared with WLS estimation method and

are shown in Fig. 5.4 and Fig. 5.5. The real power losses obtained by WLS are 73.83, 17.16, 36.83 KW for three phases and total is 127.82 KW. The respective values obtained by OO method are 67.17, 13.16, and 31.2 KW. The difference in total computed losses by the two methods are 16.3 KW. The corresponding values for the total reactive power losses obtained by WLS are 117.5, 54.1, 67.67 KVAr and by OO method are 111.5, 48.16 and 62.3 KVAr. The difference in total computed losses by the two methods are 17.2 KVAr. The total capacity of the system is 4878.625 KVA or 4187 KW. Such differences in losses by both methods are appreciable for the system whose total capacity is 4878.625 KVA.

It is evident that OO based technique provides more accurate loss figures. As it is obvious that the customer has to pay the cost of the losses, OO based estimated voltage and angles and tap positions when used to calculate operational losses for pricing, they will result in more reasonable price. Since the annual cost of the losses is about £1bn pounds in the UK, the accurate estimation of losses clearly helps to develop tools to develop and place control to minimize them.

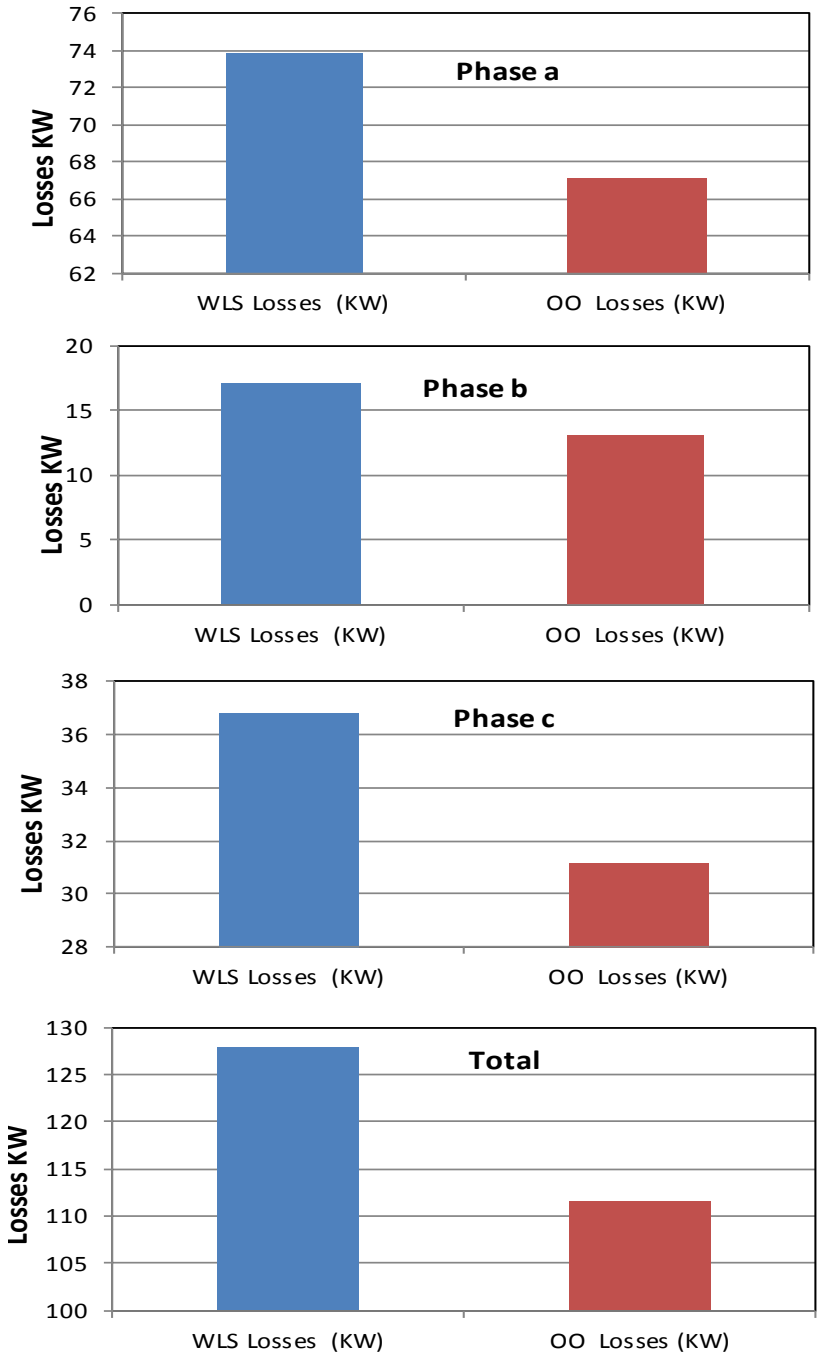


Fig. 5.4 KW losses for OO and WLS for 129 bus system (extended model of IEEE-123 bus system)

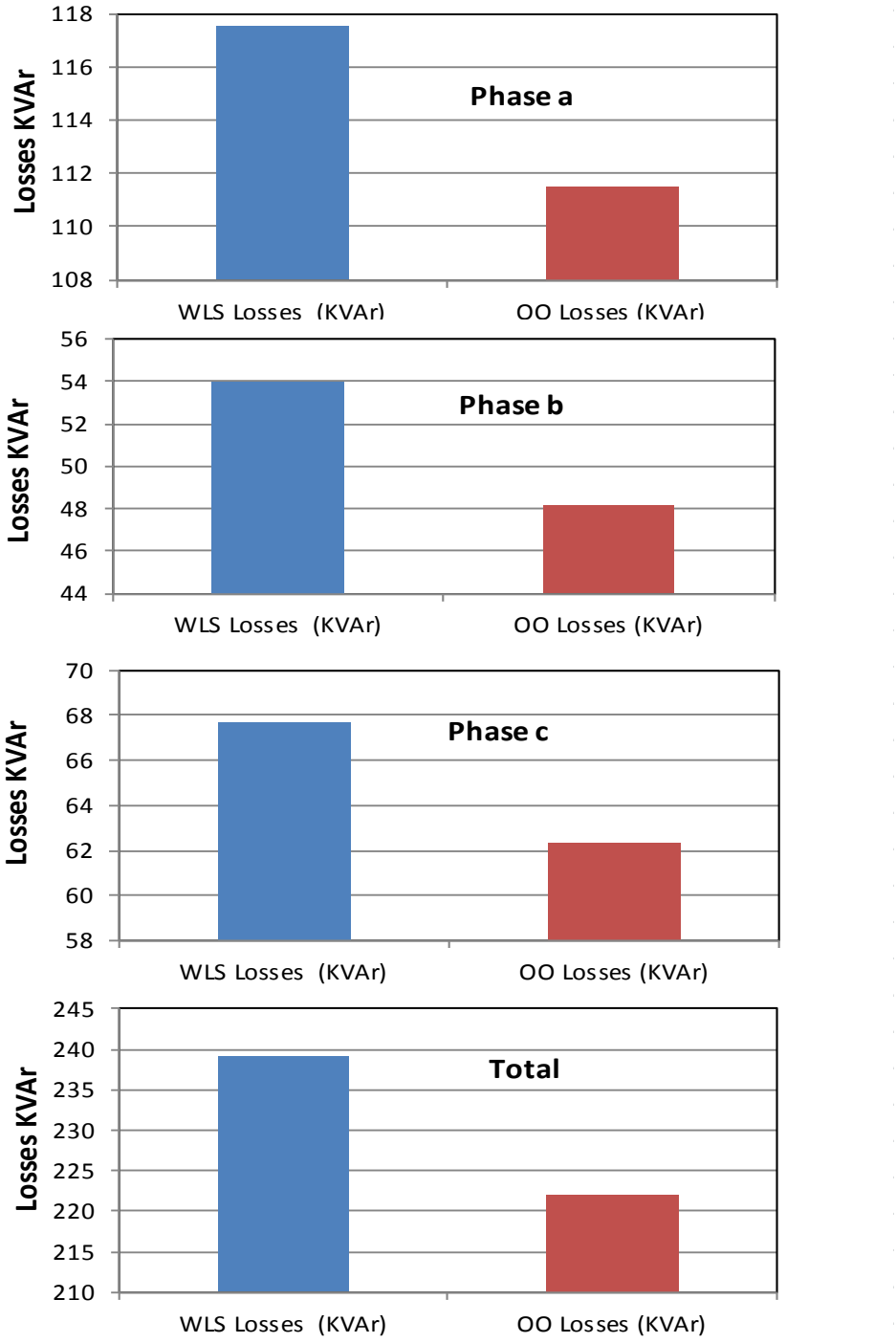


Fig. 5.5 KVAr losses for OO and WLS for 129 bus system (extended model of IEEE-123 bus system)

5.4 Conclusions

This chapter studied the loss estimation in distribution network based on various methods of state estimation which have been studied in the previous chapters of this research such as WLS, HPSO and OO. The losses have been calculated for IEEE-123 bus system based on WLS and HPSO methods and the obtained results based on both methods have been compared. Likewise, the values of losses have been obtained for 129 bus test system based on WLS and OO methods and the results have been compared to realize which method can provide more accurate estimate of losses.

The obtained results for operational losses from HPSO on IEEE-123 bus system and OO on 129 bus system revealed that the estimated losses from HPSO and OO methods are much accurate than WLS method. In that sense these methods are better than WLS method as they provide higher accuracy. Such lower losses will help lowering the overall cost of electricity. In a distribution network such as that of UK where about 6% of electricity generated is lost, accurate estimation of that has huge technical and commercial benefits. These techniques definitely will help realize those benefits.

Chapter 6

Conclusions and future work

6.1 Summary of thesis contributions

This chapter recapitulates the research contribution and technical insight gathered from this PhD project. The research had built upon the knowledge of the operational philosophy of distribution networks and the associated need and importance of Distribution System State Estimation (DSSE). It focussed on the appropriate algorithms to obtain more accurately estimated states estimated.

Increasing requirement for the automation in distribution system has demanded new DSSE techniques to be developed. However, any alterations in existing methods or introduction of new techniques require meeting some performance criteria. These criteria have been discussed in this thesis to find the potential application in evaluating the suitability of the DSSE techniques.

The initial attainment of this study was to detect an appropriate estimator for unbalanced distribution system which could handle discrete value of transformer tap position. The application of WLS for distribution network is commonly based on the assumptions of either fixed taps or continuity of transformer tap positions value. However, the assumption of fixed or continuous taps could reduce the effectiveness of state estimation process and the accuracy

of the estimated values of voltage magnitudes. Moreover, the reactive power through transformer will vary significantly from their actual values when a tap measurement is in error or is not available but the tap changing control is in action.

This posed the challenge on applying the WLS on DSSE problem. Since the discrete nature of the tap positions makes state estimation problem a mixed integer optimization problem. This is difficult to be solved by WLS or other conventional techniques. This problem was addressed through the hybrid particle swarm optimization method in Chapter 3. The problem was formulated as a three phase state estimation problem including unbalanced load, network model and the discrete transformer taps as a new state variable in order to improve the estimate accuracy and to prevent potential observability problems. The solution to this problem was obtained by application of HPSO algorithm. The achievement of this method was the more accurate estimation of voltage magnitudes and angles and transformer tap positions. The contribution of this chapter lies in handling the complexity of the unbalanced system and correctly computing the discrete values of the tap. The efficacy of the approach was demonstrated on the IEEE-13 bus and IEEE-123 bus distribution network model. However, due to unacceptably longer solution time the application of this method is not suitable for real time control and operation of future smart power distribution network. The application of the proposed HPSO based estimation technique however, is very useful for various distribution system applications such as distribution network planning and loss calculations and more accurate customer billing and also day ahead operational planning.

In a search to finding faster solution, an ordinal optimization (OO) based algorithm has been proposed in Chapter 4. The proposed algorithm has an extremely high probability of finding a good enough solution according to the OO theory and has been demonstrated to handle vast amount of computationally complex problems in short period of time without compromising the quality of the solution noticeably. The OO method has been applied to estimate the transformer tap position for the first time in unbalanced three phase distribution network model. The simulation results on 129 bus unbalanced distribution network model proved the benefits of OO method in generating a reliable estimate of transformer tap positions with discrete variables in short period of time in distribution network. It is also demonstrated that OO is much faster than other accurate methods such as HPSO. This proposed methodology provides more accurate result when compared with conventional weighted least square (WLS) algorithm that ignores the discrete nature of the tap positions in

the solution process. The results prove the suitability of the proposed algorithm in operating and controlling smart power distribution grid of the future.

Another significant achievement of this thesis is in the accurate estimation of losses in the distribution network through proposed methods of HPSO an OO which has been explored in Chapter 3 and Chapter 4. The obtained results for operational losses from HPSO on 123 bus system and OO on129 bus system have been demonstrated in Chapter 6. The results indicated that the estimated losses from HPSO and OO methods are much accurate than WLS method. In that sense these methods are better than WLS method as they provide higher accuracy. The contribution of this chapter lies in accurate estimation of losses which help lowering the overall cost of electricity. This aspect of the work has received attention of one UK distribution network operator.

6.2 Future work

Although the main issues associated with the distribution system state estimation have been addressed in this thesis, future work will focus on the following aspects of the problem.

- The application of proposed algorithms HPSO and OO on the real UK distribution network in order to obtain more accurate value of the losses in their network is our immediate future work. One network operator (Scottish and Southern Energy) in the UK has already found these approaches useful for network loss calculation in their 33/11 kV network and has commissioned a project to evaluate losses in their model networks. Compared to WLS based approach the computed network losses are noticeably different which is very useful outcome of these developed methodologies.

- No gross error is assumed in tap measurement, the tap position measured can be corrupted while being telemetered. A further work continues for bad tap error detection in a large practical power distribution network model.

- Another approach for modelling the loads as pseudo measurements could be achieved by the inclusion of the load correlations in state estimation algorithm. As the real measurements in distribution networks are available mainly at the main

substation, alternative method for modelling the loads as pseudo measurements should be pursued to create the correlation between real measurements and loads.

- The future extension of the work would consider decentralised estimation for sate estimation in unbalanced distribution network. At the distribution networks the network configuration changes frequently due to regular interruptions, maintenances, closure of normal open points and addition of customers, etc. The decentralised estimation could take care of topology changes which happen regularly at distribution level more effectively.

References

[1] K.Li, “State estimation for power distribution system and measurement impacts,” *Power Systems, IEEE Transactions on*, vol. 11, pp. 911–916, May 1996.

[2] T. H. Chen, M. S. Chen, T. Inoue, P. Kotas, and E. Chebli, “Three-phase cogenerator and transformer models for distribution system analysis,”*Power Delivery, IEEE Transactions on*, vol. 6, pp. 1671–1681, Oct 1991.

[3] I. Roytelman and S. Shahidehpour, “State estimation for electric power distribution systems in quasi real-time conditions,” *Power Delivery,IEEE Transactions on*, vol. 8, pp. 2009–2015, Oct 1993.

[4] A. Sakis Meliopoulos and F. Zhang, “Multiphase power flow and state estimation for power distribution systems,” *Power Systems, IEEE Transactions on*, vol. 11, pp. 939–946, May 1996.

[5] C. Lu, J. Teng, and W. H. Liu, “Distribution system state estimation,”*Power Systems, IEEE Transactions on*, vol. 10, pp. 229–240, Feb 1995.

[6] M. Baran and A. Kelley, “State estimation for real-time monitoring of distribution systems,” *IEEE Transactions on Power Systems*, vol. 9, pp. 1601–1609, Aug 1994.

[7] W. M. Lin and J. H. Teng, “Distribution Fast Decoupled State Estimation by Measurement Pairing,” *IEE Proceedings on Generation Transmission and Distribution*, vol. 143, no. 1, pp. 43-48, Jan. 1996.

[8] H. Wang and N. Schulz, “A revised branch current-based distribution system state estimation algorithm and meter placement impact,” *Power Systems, IEEE Transactions on*, vol. 19, pp. 207–213, Feb 2004.

[9] C. Hansen and A. Debs, “Power system state estimation using threephase models,” *Power Systems, IEEE Transactions on*, vol. 10, pp. 818–824, May 1995.

[10] A. Rankovi, B. M. Maksimovi, and A. T. Sari, "A three-phase state estimation in active distribution networks," *International Journal of Electrical Power Energy Systems*, vol. 54, no. 0, pp. 154 – 162, 2014.

[11] C. Muscas, S. Sulis, A. Angioni, F. Ponci, and A. Monti, "Impact of different uncertainty sources on a three-phase state estimator for distribution networks," *Instrumentation and Measurement, IEEE Transactions on*, vol. 63, pp. 2200–2209, Sept 2014.

[12] P. P. Barbeiro, H. Teixeira, J. Krstulovic, J. Pereira, and F. Soares,"Exploiting autoencoders for three-phase state estimation in unbalanced distributions grids," *Electric Power Systems Research*, vol. 123, no. 0,pp. 108 – 118, 2015.

[13] A. Meliopoulos, B. Fardanesh, and S. Zelingher, "Power system state estimation: modeling error effects and impact on system operation," in *System Sciences, 2001. Proceedings of the 34th Annual Hawaii International Conference on*, pp. 682–690, Jan 2001.

[14] S. Zhong and A. Abur, "Effects of nontransposed lines and unbalanced loads on state estimation," in *Power Engineering Society Winter Meeting, 2002. IEEE*, vol. 2, pp. 975–979, 2002.

[15] D. Haughton and G. Heydt, "A linear state estimation formulation for smart distribution systems," *Power Systems, IEEE Transactions on*, vol. 28, pp. 1187–1195, May 2013.

[16] D. Thukaram, J. Jerome, and C. Surapong, "A robust three-phase state estimation algorithm for distribution networks," *Electric Power Systems Research*, vol. 55, no. 3, pp. 191 – 200, 2000.

[17] M. F. M. Jnior, M. A. Almeida, M. C. Cruz, R. V. Monteiro, and A. B. Oliveira, "A three-phase algorithm for state estimation in power distribution feeders based on the powers summation load flow method," *Electric Power Systems Research*, vol. 123, no. 0, pp. 76 – 84, 2015.

[18] I. Dzafic, D. Ablakovic, and S. Henselmeyer, "Real-time three-phase state estimation for radial distribution networks," in *Power and Energy Society General Meeting, 2012 IEEE*, pp. 1–6, July 2012.

[19] A. K. Ghosh, D. L. Lubkeman, M.J. Downey, and R. H. Jones, "Distribution Circuit State Estimation Using a Probabilistic Approach," *IEEE Transactions on Power Systems*, vol. 12, no. 1, pp. 45-51, Feb. 1997.

[20] M. K. Celik and W. -H. E. Liu, "A Practical Distribution State Estimation Algorithm," *IEEE PES General Meeting*, vol. 1, pp. 442-447, 1999.

[21] R. Pires, L. Mili, and F. Lemos, "Constrained robust estimation of power system state variables and transformer tap positions under erroneous zero-injections," *IEEE Trans. Power Syst*., vol. 29, no. 3, pp. 1144–1152, May 2014.

[22] M. Shiroie and S. Hosseini, "Observability and estimation of transformer tap setting with minimal pmu placement," in *IEEE Power and Energy Society General Meeting – Conv. and Delivery of Elec. Energy in the 21st Century 2008*, pp. 1–4, July 2008.

[23] Y. Fukuyama, "State estimation and optimal setting of voltage regulator in distribution systems," *in IEEE Power Eng. Society Winter Meeting 2001*, vol. 2, pp. 930–935, 2001.

[24] P.A. Teixeira, S. R. Brammer, W. L. Rutz, W. C. Merritt and J. L. Salmonsen, "State estimation of voltage and phase-shift transformer tap settings," Power *Industry Computer Appl. Conf*., pp. 416–422, May 1991.

[25] G.N. Korres, P.J. Katsikas and G.C. Contaxis, "Transformer tap setting observability in state estimation," *IEEE Trans. Power Syst*., vol. 19, no. 2, pp. 699–706, May 2004

[26] H. Maalouf, R. A. Jabr and M. Awad, "Mixed-integer quadratic programming based rounding technique for power system state estimation with discrete and continuous variables," *Electric Power Components and Systems,* vol. 41, no. 5, pp. 555–567, 2013.

[27] M. Liu, S.K. Tso and Y. Cheng, "An extended nonlinear primal-dual interior-point algorithm for reactive-power optimization of large-scale power systems with discrete control variables," *IEEE Trans. Power Syst.,* vol. 17, no.4, pp. 982–991, Nov 2002.

[28] A. Arefi, M.R. Haghifam and S.H. Fathi, "Distribution harmonic state estimation based on a modified pso considering parameters uncertainty," *IEEE Trondheim PowerTech 2011*, pp. 1–7, Jun. 2011.

[29] K. Lee and J. Park, “Application of particle swarm optimization to economic dispatch problem: Advantages and disadvantages,” *in 2006 IEEE PES Power Systems Conference and Exposition (PSCE ’06)*, pp. 188–192, Oct 2006.

[30] S. Naka, T. Genji, T. Yura and Y. Fukuyama, “A hybrid particle swarm optimization for distribution state estimation,” *IEEE Trans. Power Syst,* vol. 18, no. 1, pp. 60– 68, Feb 2003.

[31] S. Wang et al., “An improved branch current-based three-phase state estimation algorithm for distribution systems with DGs,” *in 2012 IEEE Innovative Smart Grid Technologies - Asia (ISGT Asia),* pp. 1–6, May 2012.

[32] M. M. Deng and Y.C. Ho, "Iterative ordinal optimization and its applications," *Proc. of the 36th IEEE Conf. on Decision and Control 1997*, vol. 4, pp. 3562-3567, Dec. 1997.

[33] S. S. Lin and S. C. Horng, "Algorithm for a class of constrained weight least square problems and applications," *IET Gener., Trans. & Distr*., vol.2, no.4, pp.576-587, Jul. 2008.

[34] S. Nanchian, A. Majumdar, B. Pal, "Three-Phase State Estimation Using Hybrid Particle Swarm Optimization," in *Smart Grid, IEEE Transactions on* , vol.PP, no.99, pp.1-1

[35] F. C. Schweppe and J. Wildes, "Power System Static-State Estimation, Part I: Exact Model," *IEEE Transactions on Power Apparatus and Systems*, vol. PAS-89, pp. 120-125, 1970.

[36] F. Bignucolo, R. Caldon. (2008, July). *State estimation of radial distribution Networks* [Online]. Available: www.pscc- central.org/uploads/tx_ethpublications/pscc2008_470.pdf

[37] Hoffman, Roy, S. Lefebvre, and J. Prevost. "Distribution state estimation: A fundamental requirement for the smart grid." *Proc. DistribuTECH* (2010).

[38] F. C. Schweppe, D. B. Rom, "Power System Static-State Estimation, Part II: Approximate Model,” *IEEE Transactions on Power Apparatus and Systems*, vol. PAS-89, pp. 125-130, 1970.

[39] R. Singh, “state estimation in Power Distribution Network Operation,” Ph.D. dissertation, Dept. Elect. Eng., Imperial College, London, April 2009.

[40] R. Singh, B. C. Pal, R. A. Jabr, "Choice of estimator for distribution system state estimation," in *Generation, Transmission & Distribution, IET* , vol.3, no.7, pp.666-678, July 2009.

[41] A.R. Ghasemi, R. Ebrahimi, A. Babaee and M. Hoseynpoor, "A Modified Newton-Raphson Algorithm of Three-Phase Power Flow Analysis in Unsymmetrical Distribution Networks with Distributed Generation," *J. Basic Appl. Sci. Res.*, vol. 9, no. 3, pp. 36–46, Sep. 2013

[42] W. H Keresting, *Distribution system modeling and analysis*. New York: CRC Press, 2002.

[43] F. Le, B. C. Pal, B. Cory, "Voltage regulation for primary level power networks by virtual voltage coordinated control," in *Power Engineering Society General Meeting, IEEE* , vol., no., pp.6, 2006.

[44] F. Le, "Voltage Stability Monitoring and Enhancement in Electrical Power Systems using Transformer Tap Changers", Ph.D. dissertation, Dept. Elect. Eng., Imperial College, London, November 2007.

[45] Wikipedia. [Online]. Available: https://en.wikipedia.org/wiki/Tap_changer

[46] K. Wang, H. Huang and C. Zang, "Research on Time-Sharing ZIP Load Modeling Based on Linear BP Network," in *Intelligent Human-Machine Systems and Cybernetics (IHMSC), 2013 5th International Conference on* , vol.1, no., pp.37-41, 26-27 Aug. 2013.

[47] A. Abur, and A. Gomez Exposito, *Power system state estimation, theory and implementation*. CRC Press, 2004.

[48] Monticelli, Alcir, *State estimation in electric power systems, a generalized approach*. Vol.507, Springer Science & Business Media, 1999.

[49] Huber, J. Peter, "Robust estimation of a location parameter." *The Annals of Mathematical Statistics* 35, no. 1 (1964): 73-101.

[50] L. Mili, M. G. Cheniae, P. J. Rousseeuw, "Robust state estimation of electric power systems," in *Circuits and Systems I: Fundamental Theory and Applications, IEEE Transactions on* , vol.41, no.5, pp.349-358, May 1994

[51] W. H. Kersting, "Radial distribution test feeders," in *Power Engineering Society Winter Meeting, 2001. IEEE* , vol.2, no., pp.908-912 vol.2, 2001.

[52] W. H. Kersting, "Radial distribution test feeders, " in *Power Systems, IEEE Transactions on* , vol.6, no.3, pp.975-985, Aug 1991

[53] G. H. Golub, C. F. Van Loan, *Matrix computations*, 1996, *Johns Hopkins University,* Press, Baltimore, MD, USA (1996): 374-426

[54] P. Angeline, "Using selection to improve particle swarm optimization," in *1998 IEEE International Conference on Evolutionary Computation Proceedings. IEEE World Congress on Computational Intelligence*, pp. 84–89, May 1998.

[55] J. Kennedy and R. Eberhart, "Particle swarm optimization," in *1995 IEEE International Conference on Neural Networks Proceedings*, vol. 4, pp. 1942–1948, Nov 1995.

[56] F. van den Bergh, "An analysis of particle swarm optimizers," Ph.D. dissertation, Dept. Elect. Eng., University of Pretoria, South Africa, Nov 2001.

[57] Y. Shi and R. Eberhart, "A modified particle swarm optimizer," in *1998 IEEE International Conference on Evolutionary Computation Proceedings, IEEE World Congress on Computational Intelligence*, pp. 69–73, May 1998.

[58] K. Samarakoon, J. Wu, J. Ekanayake, and N. Jenkins, "Use of delayed smart meter measurements for distribution state estimation," in *Power and Energy Society General Meeting, 2011 IEEE*, pp. 1–6, July 2011.

[59] H. M. Jeong, H. S. Lee, and J. H. Park, "Application of parallel particle swarm optimization on power system state estimation," in *Transmission Distribution Conference Exposition: Asia and Pacific, 2009*, pp. 1–4, Oct 2009.

[60] E. Atmaca, "An ordinal optimization based method for power distribution system control," *Elect. Power Syst. Res.*, vol. 78, no. 4, pp. 694–702, Apr. 2008.

[61] T. E. Lau and Y. C. Ho, "Universal alignment probabilities and subset selection for ordinal optimization," *Journal of Optimization Theory and Applications*, vol. 93, no. 3, pp. 455–489, 1997.

[62] R. Singh, B.C. Pal, R.A. Jabr, R.B. Vinter, "Meter Placement for Distribution System State Estimation: An Ordinal Optimization Approach," *IEEE Trans. Power Syst.,* vol. 26, no. 4, pp. 2328-2335, Nov. 2011.

[63] S. S. Lin, C. H. Lin and S. C. Horng, "An efficient algorithm for QCDP and implementation," *IEEE Trans. Power Syst.,* vol. 25, no. 1, pp. 234–242, Feb. 2010.

[64] Ofgem. (2014). *LCN Fund (Low Carbon Networks).* [Online]. Available: https://www.ofgem.gov.uk/sites/default/files/docs/2014/11/low_carbon_networks_fund_submission_from_ssepd_-_final_0.pdf

Appendix A: IEEE-13 bus test feeder

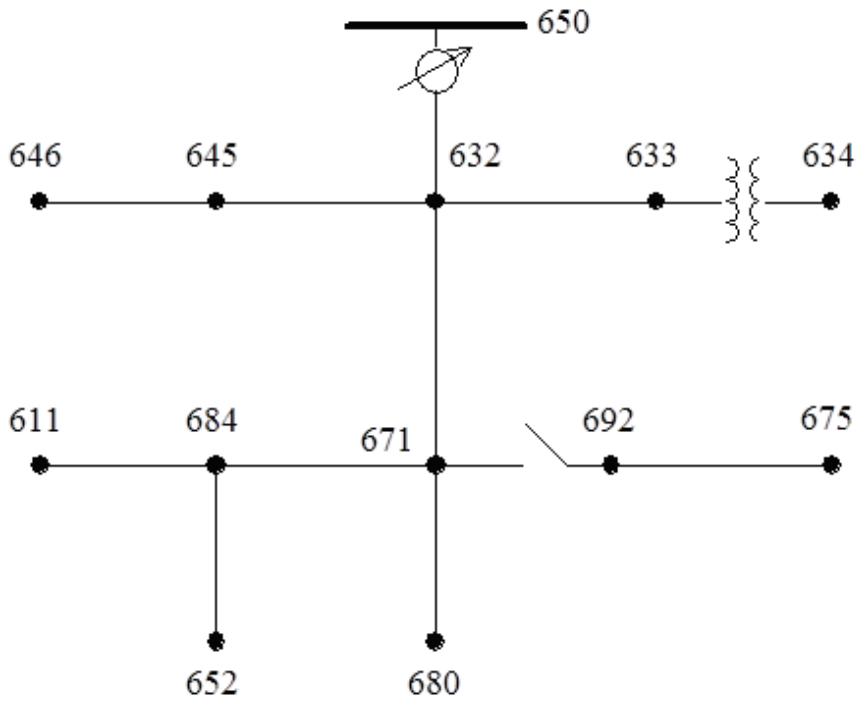


Fig. A.1 IEEE 13 bus test system

Table A.1 Overhead line configuration data

Config.	Phasing	Phase	Neutral	Spacing
		ACSR	ACSR	ID
601	B A C N	556,500 26/7	4/0 6/1	500
602	C A B N	4/0 6/1	4/0 6/1	500
603	C B N	1/0	1/0	505
604	A C N	1/0	1/0	505
605	C N	1/0	1/0	510

Table A.2 Underground line configuration data

Config.	Phasing	Cable	Neutral	Space ID
606	A B C N	250,000 AA, CN	None	515
607	A N	1/0 AA, TS	1/0 Cu	520

Table A.3 Line segment data

Node A	Node B	Length(ft.)	Config.
632	645	500	603
632	633	500	602
633	634	0	XFM-1
645	646	300	603
650	632	2000	601
684	652	800	607
632	671	2000	601
671	684	300	604
671	680	1000	601
671	692	0	Switch
684	611	300	605
692	675	500	606

Table A.4 Transformer data

	kVA	kV-high	kV-low	R - %	X - %
Substation:	5,000	115 - D	4.16 Gr. Y	1	8
XFM -1	500	4.16 – Gr.W	0.48 – Gr.W	1.1	2

Table A.5 Capacitor data

Node	Ph-A	Ph-B	Ph-C
	kVAr	kVAr	kVAr
675	200	200	200
611			100
Total	200	200	300

Table A.6 Regulator data

Regulator ID:	1		
Line Segment:	650 - 632		
Location:	50		
Phases:	A - B -C		
Connection:	3-Ph,LG		
Monitoring Phase:	A-B-C		
Bandwidth:	2.0 volts		
PT Ratio:	20		
Primary CT Rating:	700		
Compensator Settings:	Ph-A	Ph-B	Ph-C
R - Setting:	3	3	3
X - Setting:	9	9	9
Volltage Level:	122	122	122

Table A.7 Spot load data

Node	Load	Ph-1	Ph-1	Ph-2	Ph-2	Ph-3	Ph-3
	Model	kW	kVAr	kW	kVAr	kW	kVAr
634	Y-PQ	160	110	120	90	120	90
645	Y-PQ	0	0	170	125	0	0
646	D-Z	0	0	230	132	0	0
652	Y-Z	128	86	0	0	0	0
671	D-PQ	385	220	385	220	385	220
675	Y-PQ	485	190	68	60	290	212
692	D-I	0	0	0	0	170	151
611	Y-I	0	0	0	0	170	80
	TOTAL	1158	606	973	627	1135	753

Table A.8 Distributed load data

Node A	Node B	Load	Ph-1	Ph-1	Ph-2	Ph-2	Ph-3	Ph-3
		Model	kW	kVAr	kW	kVAr	kW	kVAr
632	671	Y-PQ	17	10	66	38	117	68

Appendix B: IEEE-123 bus test feeder

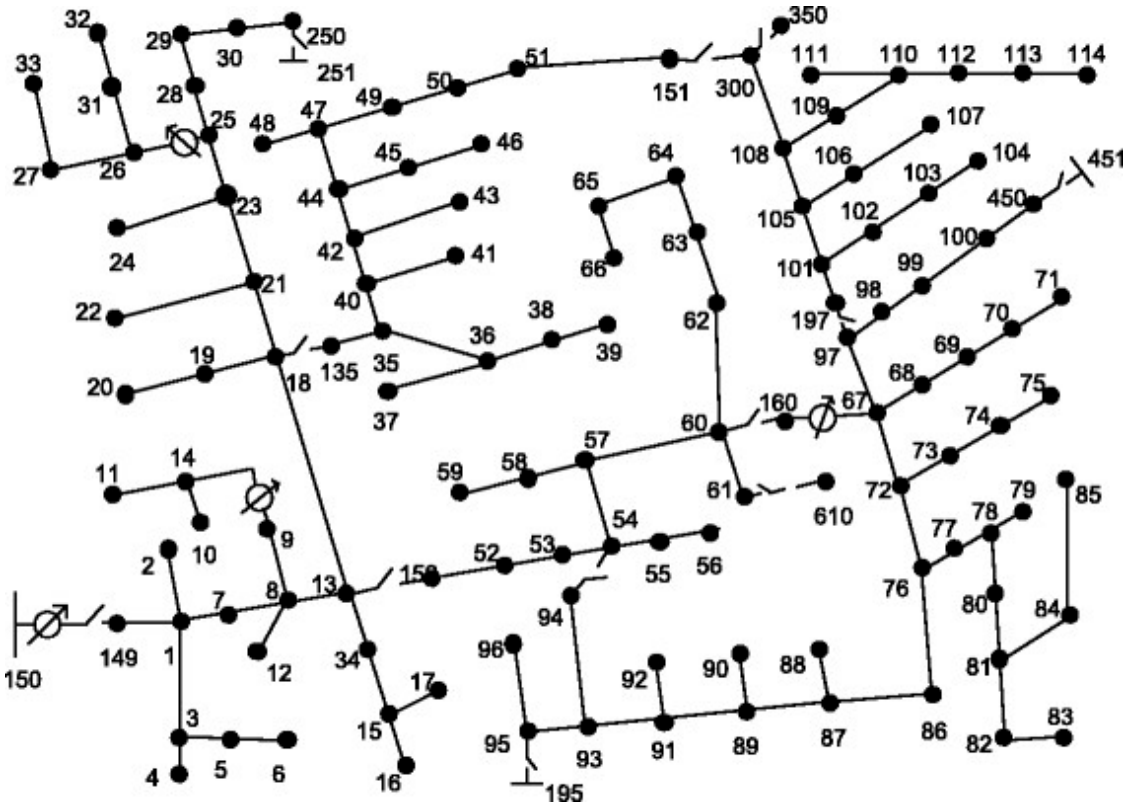


Fig. B.1 IEEE 123 bus test system

Table B.1(a) Line segment data

Node A	Node B	Length (ft.)	Config.
1	2	175	10
1	3	250	11
1	7	300	1
3	4	200	11
3	5	325	11
5	6	250	11
7	8	200	1
8	12	225	10
8	9	225	9
8	13	300	1
9	14	425	9
13	34	150	11
13	18	825	2
14	11	250	9
14	10	250	9
15	16	375	11
15	17	350	11
18	19	250	9
18	21	300	2
19	20	325	9
21	22	525	10
21	23	250	2
23	24	550	11
23	25	275	2
25	26	350	7
25	28	200	2
26	27	275	7
26	31	225	11
27	33	500	9

Table B.2(b) Line segment data

Node A	Node B	Length (ft.)	Config.
28	29	300	2
29	30	350	2
30	250	200	2
31	32	300	11
34	15	100	11
35	36	650	8
35	40	250	1
36	37	300	9
36	38	250	10
38	39	325	10
40	41	325	11
40	42	250	1
42	43	500	10
42	44	200	1
44	45	200	9
44	47	250	1
45	46	300	9
47	48	150	4
47	49	250	4
49	50	250	4
50	51	250	4
52	53	200	1
53	54	125	1
54	55	275	1
54	57	350	3
55	56	275	1
57	58	250	10
57	60	750	3
58	59	250	10

Table B.3(c) Line segment data

Node A	Node B	Length (ft.)	Config.
60	61	550	5
60	62	250	12
62	63	175	12
63	64	350	12
64	65	425	12
65	66	325	12
67	68	200	9
67	72	275	3
67	97	250	3
68	69	275	9
69	70	325	9
70	71	275	9
72	73	275	11
72	76	200	3
73	74	350	11
74	75	400	11
76	77	400	6
76	86	700	3
77	78	100	6
78	79	225	6
78	80	475	6
80	81	475	6
81	82	250	6
81	84	675	11
82	83	250	6
84	85	475	11
86	87	450	6
87	88	175	9
87	89	275	6

Table B.4(d) Line segment data

Node A	Node B	Length (ft.)	Config.
89	90	225	10
89	91	225	6
91	92	300	11
91	93	225	6
93	94	275	9
93	95	300	6
95	96	200	10
97	98	275	3
98	99	550	3
99	100	300	3
100	450	800	3
101	102	225	11
101	105	275	3
102	103	325	11
103	104	700	11
105	106	225	10
105	108	325	3
106	107	575	10
108	109	450	9
108	300	1000	3
109	110	300	9
110	111	575	9
110	112	125	9
112	113	525	9
113	114	325	9
135	35	375	4
149	1	400	1
152	52	400	1
160	67	350	6
197	101	250	3

Table B.5 Overhead line configurations (Config.)

Config.	Phasing	Phase Cond.	Neutral Cond.	Spacing
		ACSR	ACSR	ID
1	A B C N	336,400 26/7	4/0 6/1	500
2	C A B N	336,400 26/7	4/0 6/1	500
3	B C A N	336,400 26/7	4/0 6/1	500
4	C B A N	336,400 26/7	4/0 6/1	500
5	B A C N	336,400 26/7	4/0 6/1	500
6	A C B N	336,400 26/7	4/0 6/1	500
7	A C N	336,400 26/7	4/0 6/1	505
8	A B N	336,400 26/7	4/0 6/1	505
9	A N	1/0	1/0	510
10	B N	1/0	1/0	510
11	C N	1/0	1/0	510

Table B.6 Underground line configuration (Config.)

Config.	Phasing	Cable	Spacing ID
12	A B C	1/0 AA, CN	515

Table B.7 Three phase switch

Node A	Node B	Normal
13	152	closed
18	135	closed
60	160	closed
61	610	closed
97	197	closed
150	149	closed
250	251	open
450	451	open
54	94	open
151	300	open
300	350	open

Table B.8 Transformer data

	kVA	kV-high	kV-low	R - %	X - %
Substation	5,000	115 - D	4.16 Gr-W	1	8
XFM - 1	150	4.16 - D	.480 - D	1.27	2.72

Table B.9 Regulator data

Regulator ID:	1			**Regulator ID:**	2		
Line Segment:	150 - 149			**Line Segment:**	9 - 14		
Location:	150			**Location:**	9		
Phases:	A-B-C			**Phases:**	A		
Connection:	3-Ph, Wye			**Connection:**	1-Ph, L-G		
Monitoring Phase:	A			**Monitoring Phase:**	A		
Bandwidth:	2.0 volts			**Bandwidth:**	2.0 volts		
PT Ratio:	20			**PT Ratio:**	20		
Primary CT Rating:	700			**Primary CT Rating:**	50		
Compensator:	Ph-A			**Compensator:**	Ph-A		
R - Setting:	3			**R - Setting:**	0.4		
X - Setting:	7.5			**X - Setting:**	0.4		
Voltage Level:	120			**Voltage Level:**	120		
Regulator ID:	3			**Regulator ID:**	4		
Line Segment:	25 - 26			**Line Segment:**	160 - 67		
Location:	25			**Location:**	160		
Phases:	A-C			**Phases:**	A-B-C		
Connection:	2-Ph,L-G			**Connection:**	3-Ph, LG		
Monitoring Phase:	A & C			**Monitoring Phase:**	A-B-C		
Bandwidth:	1			**Bandwidth:**	2		
PT Ratio:	20			**PT Ratio:**	20		
Primary CT Rating:	50			**Primary CT Rating:**	300		
Compenator:	Ph-A	Ph-C		**Compensator:**	Ph-A	Ph-B	Ph-C
R - Setting:	0.4	0.4		**R - Setting:**	0.6	1.4	0.2
X - Setting:	0.4	0.4		**X - Setting:**	1.3	2.6	1.4
Voltage Level:	120	120		**Voltage Level:**	124	124	124

Table B.10(a) Spot loads

Node	Load	Ph-1	Ph-1	Ph-2	Ph-2	Ph-3	Ph-4
	Model	kW	kVAr	kW	kVAr	kW	kVAr
1	Y-PQ	40	20	0	0	0	0
2	Y-PQ	0	0	20	10	0	0
4	Y-PQ	0	0	0	0	40	20
5	Y-I	0	0	0	0	20	10
6	Y-Z	0	0	0	0	40	20
7	Y-PQ	20	10	0	0	0	0
9	Y-PQ	40	20	0	0	0	0
10	Y-I	20	10	0	0	0	0
11	Y-Z	40	20	0	0	0	0
12	Y-PQ	0	0	20	10	0	0
16	Y-PQ	0	0	0	0	40	20
17	Y-PQ	0	0	0	0	20	10
19	Y-PQ	40	20	0	0	0	0
20	Y-I	40	20	0	0	0	0
22	Y-Z	0	0	40	20	0	0
24	Y-PQ	0	0	0	0	40	20
28	Y-I	40	20	0	0	0	0
29	Y-Z	40	20	0	0	0	0
30	Y-PQ	0	0	0	0	40	20
31	Y-PQ	0	0	0	0	20	10
32	Y-PQ	0	0	0	0	20	10
33	Y-I	40	20	0	0	0	0
34	Y-Z	0	0	0	0	40	20
35	D-PQ	40	20	0	0	0	0
37	Y-Z	40	20	0	0	0	0
38	Y-I	0	0	20	10	0	0
39	Y-PQ	0	0	20	10	0	0
41	Y-PQ	0	0	0	0	20	10

Table B.11(b) Spot loads

Node	Load	Ph-1	Ph-1	Ph-2	Ph-2	Ph-3	Ph-4
	Model	kW	kVAr	kW	kVAr	kW	kVAr
42	Y-PQ	20	10	0	0	0	0
43	Y-Z	0	0	40	20	0	0
45	Y-I	20	10	0	0	0	0
46	Y-PQ	20	10	0	0	0	0
47	Y-I	35	25	35	25	35	25
48	Y-Z	70	50	70	50	70	50
49	Y-PQ	35	25	70	50	35	25
50	Y-PQ	0	0	0	0	40	20
51	Y-PQ	20	10	0	0	0	0
52	Y-PQ	40	20	0	0	0	0
53	Y-PQ	40	20	0	0	0	0
55	Y-Z	20	10	0	0	0	0
56	Y-PQ	0	0	20	10	0	0
58	Y-I	0	0	20	10	0	0
59	Y-PQ	0	0	20	10	0	0
60	Y-PQ	20	10	0	0	0	0
62	Y-Z	0	0	0	0	40	20
63	Y-PQ	40	20	0	0	0	0
64	Y-I	0	0	75	35	0	0
65	D-Z	35	25	35	25	70	50
66	Y-PQ	0	0	0	0	75	35
68	Y-PQ	20	10	0	0	0	0
69	Y-PQ	40	20	0	0	0	0
70	Y-PQ	20	10	0	0	0	0
71	Y-PQ	40	20	0	0	0	0
73	Y-PQ	0	0	0	0	40	20
74	Y-Z	0	0	0	0	40	20
75	Y-PQ	0	0	0	0	40	20
76	D-I	105	80	70	50	70	50

Table B.12(c) Spot loads

Node	Load	Ph-1	Ph-1	Ph-2	Ph-2	Ph-3	Ph-4
	Model	kW	kVAr	kW	kVAr	kW	kVAr
77	Y-PQ	0	0	40	20	0	0
79	Y-Z	40	20	0	0	0	0
80	Y-PQ	0	0	40	20	0	0
82	Y-PQ	40	20	0	0	0	0
83	Y-PQ	0	0	0	0	20	10
84	Y-PQ	0	0	0	0	20	10
85	Y-PQ	0	0	0	0	40	20
86	Y-PQ	0	0	20	10	0	0
87	Y-PQ	0	0	40	20	0	0
88	Y-PQ	40	20	0	0	0	0
90	Y-I	0	0	40	20	0	0
92	Y-PQ	0	0	0	0	40	20
94	Y-PQ	40	20	0	0	0	0
95	Y-PQ	0	0	20	10	0	0
96	Y-PQ	0	0	20	10	0	0
98	Y-PQ	40	20	0	0	0	0
99	Y-PQ	0	0	40	20	0	0
100	Y-Z	0	0	0	0	40	20
102	Y-PQ	0	0	0	0	20	10
103	Y-PQ	0	0	0	0	40	20
104	Y-PQ	0	0	0	0	40	20
106	Y-PQ	0	0	40	20	0	0
107	Y-PQ	0	0	40	20	0	0
109	Y-PQ	40	20	0	0	0	0
111	Y-PQ	20	10	0	0	0	0
112	Y-I	20	10	0	0	0	0
113	Y-Z	40	20	0	0	0	0
114	Y-PQ	20	10	0	0	0	0
Total		1420	775	915	515	1155	635

Table B.13 Shunt capacitor

Node	**Ph-A**	**Ph-B**	**Ph-C**
	kVAr	**kVAr**	**kVAr**
83	200	200	200
88	50		
90		50	
92			50
Total	250	250	250

Appendix C: Measurement Jacobian

The Jacobian elements corresponding to the real and reactive power injections are:

$$\frac{\partial P_i^k}{\partial \delta_i^l}_{l=k} = \sum_{\substack{j=1 \\ j\neq i}}^{n} V_i^k V_j^k [-G_{ij}^{k,k} \sin(\delta_i^k - \delta_j^k) + B_{ij}^{k,k} \cos(\delta_i^k - \delta_j^k)] + \sum_{\substack{l=1 \\ l\neq k}}^{3} \sum_{j=1}^{n} V_i^k V_j^l [-G_{ij}^{k,l} \sin(\delta_i^k - \delta_i^l) + B_{ij}^{k,l} \cos(\delta_i^k - \delta_j^l)] = -Q_i^k - (V_i^k)^2 B_{ii}^{k,k} \quad \text{(C.1)}$$

$$\frac{\partial P_i^k}{\partial \delta_i^l}_{l\neq k} = V_i^k V_i^l [G_{ii}^{k,l} \sin(\delta_i^k - \delta_i^l) - B_{ii}^{k,l} \cos(\delta_i^k - \delta_i^l)] \quad \text{(C.2)}$$

$$\frac{\partial P_i^k}{\partial \delta_j^l} = V_i^k V_j^l [G_{ij}^{k,l} \sin(\delta_i^k - \delta_j^l) - B_{ij}^{k,l} \cos(\delta_i^k - \delta_j^l)] \quad \text{(C.3)}$$

$$\frac{\partial P_i^k}{\partial V_i^l}_{l=k} = 2V_i^k G_{ii}^{k,k} + \sum_{\substack{j=1 \\ j\neq i}}^{n} V_j^k [G_{ij}^{k,k} \cos(\delta_i^k - \delta_j^k) + B_{ij}^{k,k} \sin(\delta_i^k - \delta_j^k)] + \sum_{\substack{l=1 \\ l\neq k}}^{3} \sum_{j=1}^{n} V_j^l [G_{ij}^{k,l} \cos(\delta_i^k - \delta_j^l) + B_{ij}^{k,l} \sin(\delta_i^k - \delta_j^l)] + P_n(c_2^P (1/V_n) + c_3^P (V/V_n^2)) = \frac{P_i^k}{V_i^k} + V_i^k G_{ii}^{k,l} + P_n(c_2^P (1/V_n) + c_3^P (V/V_n^2)) \quad \text{(C.4)}$$

$$\frac{\partial P_i^k}{\partial V_j^l} = V_i^k [G_{ij}^{k,l} \cos(\delta_i^k - \delta_j^l) + B_{ij}^{k,l} \sin(\delta_i^k - \delta_j^l)] \quad \text{(C.5)}$$

$$\frac{\partial Q_i^k}{\partial \delta_i^l}_{l=k} = -\sum_{\substack{j=1 \\ j\neq i}}^{n} V_i^k V_j^k [-B_{ij}^{k,k} \sin(\delta_i^k - \delta_j^k) - G_{ij}^{k,k} \cos(\delta_i^k - \delta_j^k)] - \sum_{\substack{l=1 \\ l\neq k}}^{3} \sum_{j=1}^{n} V_i^k V_j^l [-B_{ij}^{k,l} \sin(\delta_i^k - \delta_i^l) - G_{ij}^{k,l} \cos(\delta_i^k - \delta_j^l)] = P_i^k - (V_i^k)^2 G_{ii}^{k,k} \quad \text{(C.6)}$$

$$\frac{\partial Q_i^k}{\partial \delta_i^l}_{l\neq k} = -V_i^k V_i^l [B_{ii}^{k,l} \sin(\delta_i^k - \delta_i^l) + G_{ii}^{k,l} \cos(\delta_i^k - \delta_i^l)] \quad \text{(C.7)}$$

$$\frac{\partial Q_i^k}{\partial \delta_j^l} = -V_i^k V_j^l [B_{ij}^{k,l} \sin(\delta_i^k - \delta_j^l) + G_{ij}^{k,l} \cos(\delta_i^k - \delta_j^l)] \quad \text{(C.8)}$$

$$\frac{\partial Q_i^k}{\partial V_i^l}_{l=k} =$$

$$-2V_i^k B_{ii}^{k,k} - \sum_{\substack{j=1 \\ j\neq i}}^{n} V_j^k [B_{ij}^{k,k} \cos(\delta_i^k - \delta_j^k) - G_{ij}^{k,k} \sin(\delta_i^k - \delta_j^k)] - \sum_{\substack{l=1 \\ l\neq k}}^{3} \sum_{j=1}^{n} V_j^l [B_{ij}^{k,l} \cos(\delta_i^k -$$

$$\delta_j^l) - G_{ij}^{k,l} \sin(\delta_i^k - \delta_j^l)] + Q_n(c_2^Q \left({}^1/_{V_n}\right) + c_3^Q ({}^V/_{V_n^2})) \quad = -\frac{Q_i^k}{V_i^k} - V_i^k B_{ii}^{k,l} + Q_n(c_2^Q \left({}^1/_{V_n}\right) +$$

$$c_3^Q ({}^V/_{V_n^2})) \quad \text{(C.9)}$$

$$\frac{\partial Q_i^k}{\partial V_j^l} = -V_i^k [B_{ij}^{k,l} \cos(\delta_i^k - \delta_j^l) - G_{ij}^{k,l} \sin(\delta_i^k - \delta_j^l)] \quad \text{(C.10)}$$

The Jacobian elements corresponding to the real and reactive power flows between bus*i* and bus *j* are:

$$\frac{\partial P_{ij}^k}{\partial \delta_i^l}_{l=k} = -\sum_{l=1}^{3} V_i^k V_j^l [-g_{ij}^{k,l} \sin(\delta_i^k - \delta_j^l) + b_{ij}^{k,l} \cos(\delta_i^k - \delta_j^l)] = -Q_{ij}^k - \sum_{l=1}^{3} V_i^k V_i^l [b_{ij}^{k,l} + b_{si}^{k,l}]$$

(C.11)

$$\frac{\partial P_{ij}^k}{\partial \delta_i^l}_{l\neq k} = 0 \quad \text{(C.12)}$$

$$\frac{\partial P_{ij}^k}{\partial \delta_j^l} = -V_i^k V_j^l [g_{ij}^{k,l} \sin(\delta_i^k - \delta_j^l) - b_{ij}^{k,l} \cos(\delta_i^k - \delta_j^l)] \quad \text{(C.13)}$$

$$\frac{\partial P_{ij}^k}{\partial V_i^l}_{l=k} = V_i^k [g_{ij}^{k,k} + g_{si}^{k,l}] + \sum_{l=1}^{3} [V_i^l \{g_{ij}^{k,k} + g_{si}^{k,l}\} - V_j^l [g_{ij}^{k,l} \cos(\delta_i^k - \delta_j^l) + b_{ij}^{k,l} \sin(\delta_i^k - \delta_j^l)]]$$

$$= \frac{P_{ij}^k}{V_i^k} + V_i^k [g_{ij}^{k,k} + g_{si}^{k,l}] \quad \text{(C.14)}$$

$$\frac{\partial P_{ij}^k}{\partial V_i^l}_{l\neq k} = V_i^k [g_{ij}^{k,k} + g_{si}^{k,l}] \quad \text{(C.15)}$$

$$\frac{\partial P_{ij}^k}{\partial V_j^l} = -V_i^k [g_{ij}^{k,l} \cos(\delta_i^k - \delta_j^l) + b_{ij}^{k,l} \sin(\delta_i^k - \delta_j^l)] \quad \text{(C.16)}$$

$$\underset{l=k}{\frac{\partial Q_{ij}^k}{\partial \delta_i^l}} = -\sum_{l=1}^{3} V_i^k V_j^l \left[g_{ij}^{k,l} \cos\left(\delta_i^k - \delta_j^l\right) + b_{ij}^{k,l} \sin\left(\delta_i^k - \delta_j^l\right)\right] = P_{ij}^k - \sum_{l=1}^{3} V_i^k V_i^l \left[g_{ij}^{k,k} + g_{si}^{k,l}\right]$$

(C.17)

$$\underset{l\neq k}{\frac{\partial Q_{ij}^k}{\partial \delta_i^l}} = 0 \tag{C.18}$$

$$\frac{\partial Q_{ij}^k}{\partial \delta_j^l} = -V_i^k V_j^l \left[-g_{ij}^{k,l} \cos\left(\delta_i^k - \delta_j^l\right) - b_{ij}^{k,l} \sin\left(\delta_i^k - \delta_j^l\right)\right] \tag{C.19}$$

$$\underset{l=k}{\frac{\partial Q_{ij}^k}{\partial V_i^l}} = -V_i^k \left[b_{ij}^{k,l} + b_{si}^{k,l}\right] + \sum_{l=1}^{3} \left[-V_i^l \left[b_{ij}^{k,l} + b_{si}^{k,l}\right] - V_j^l \left[g_{ij}^{k,l} \sin\left(\delta_i^k - \delta_j^l\right) - b_{ij}^{k,l} \cos\left(\delta_i^k - \delta_j^l\right)\right]\right]$$

$$= \frac{Q_{ij}^k}{V_i^k} - V_i^k \left[b_{ij}^{k,l} + b_{si}^{k,l}\right] \tag{C.20}$$

$$\underset{l\neq k}{\frac{\partial Q_{ij}^k}{\partial V_i^l}} = -V_i^k \left[b_{ij}^{k,l} + b_{si}^{k,l}\right] \tag{C.21}$$

$$\frac{\partial Q_{ij}^k}{\partial V_j^l} = -V_i^k \left[g_{ij}^{k,l} \sin\left(\delta_i^k - \delta_j^l\right) + b_{ij}^{k,l} \cos\left(\delta_i^k - \delta_j^l\right)\right] \tag{C.22}$$

The Jacobian elements corresponding to the branch current flows between bus *i* and bus *j* are:

$$\underset{l=k}{\frac{\partial I_{ij}^k}{\partial \delta_i^l}} =$$

$$\frac{P_{ij}^k}{\sqrt{(P_{ij}^k)^2 + (Q_{ij}^k)^2}} \left[\sum_{l=1}^{3} -V_j^l \left\{-g_{ij}^{k,l} \sin\left(\delta_i^k - \delta_j^l\right) + b_{ij}^{k,l} \cos\left(\delta_i^k - \delta_j^l\right)\right\}\right] +$$

$$\frac{Q_{ij}^k}{\sqrt{(P_{ij}^k)^2 + (Q_{ij}^k)^2}} \left[\sum_{l=1}^{3} -V_j^l \left\{g_{ij}^{k,l} \cos\left(\delta_i^k - \delta_j^l\right) + b_{ij}^{k,l} \sin\left(\delta_i^k - \delta_j^l\right)\right\}\right] \tag{C.23}$$

$$\underset{l\neq k}{\frac{\partial I_{ij}^k}{\partial \delta_i^l}} = 0 \tag{C.24}$$

$$\frac{\partial I_{ij}^{k}}{\partial \delta_{j}^{l}} =$$

$$\frac{P_{ij}^{k}}{\sqrt{\left(P_{ij}^{k}\right)^{2}+\left(Q_{ij}^{k}\right)^{2}}}\left[-V_{j}^{l}\left\{g_{ij}^{k,l}\sin\left(\delta_{i}^{k}-\delta_{j}^{l}\right)-b_{ij}^{k,l}\cos\left(\delta_{i}^{k}-\delta_{j}^{l}\right)\right\}\right]+\frac{Q_{ij}^{k}}{\sqrt{(P_{ij}^{k})^{2}+(Q_{ij}^{k})^{2}}}\left[-V_{j}^{l}\left\{-g_{ij}^{k,l}\cos\left(\delta_{i}^{k}-\right.\right.\right.$$

$$\left.\left.\left.\delta_{j}^{l}\right)-b_{ij}^{k,l}\sin\left(\delta_{i}^{k}-\delta_{j}^{l}\right)\right\}\right] \quad \text{(C.25)}$$

$$\frac{\partial I_{ij}^{k}}{\partial V_{i}^{l}}=\frac{P_{ij}^{k}}{\sqrt{(P_{ij}^{k})^{2}+(Q_{ij}^{k})^{2}}}\left[g_{ij}^{k,l}+g_{si}^{k,l}\right]+\frac{Q_{ij}^{k}}{\sqrt{(P_{ij}^{k})^{2}+(Q_{ij}^{k})^{2}}}\left[-b_{ij}^{k,l}-b_{si}^{k,l}\right] \quad \text{(C.26)}$$

$$\frac{\partial I_{ij}^{k}}{\partial V_{j}^{l}}=\frac{P_{ij}^{k}}{\sqrt{(P_{ij}^{k})^{2}+(Q_{ij}^{k})^{2}}}\left[-\left\{g_{ij}^{k,l}\cos\left(\delta_{i}^{k}-\delta_{j}^{l}\right)+b_{ij}^{k,l}\sin\left(\delta_{i}^{k}-\delta_{j}^{l}\right)\right\}\right]+\frac{Q_{ij}^{k}}{\sqrt{(P_{ij}^{k})^{2}+(Q_{ij}^{k})^{2}}}\left[-\left\{g_{ij}^{k,l}\sin\left(\delta_{i}^{k}-\right.\right.\right.$$

$$\left.\left.\left.\delta_{j}^{l}\right)-b_{ij}^{k,l}\cos(\delta_{i}^{k}-\delta_{j}^{l})\right\}\right] \quad \text{(C.27)}$$

The Jacobian elements corresponding to the voltage magnitude measurements at bus *i* are:

$$\frac{\partial V_{i}^{k}}{\partial \delta_{i}^{l}}=0 \quad \text{(C.28)}$$

$$\frac{\partial V_{i}^{k}}{\partial \delta_{j}^{l}}=0 \quad \text{(C.29)}$$

$$\frac{\partial V_{i}^{k}}{\partial V_{i}^{l}}_{l=k}=1 \quad \text{(C.30)}$$

$$\frac{\partial V_{i}^{k}}{\partial V_{i}^{l}}_{l\neq k}=0 \quad \text{(C.31)}$$

$$\frac{\partial V_{i}^{k}}{\partial V_{j}^{l}}=0 \quad \text{(C.32)}$$

Where

n: the number of buses

l: the number of phases

$G_{ij}^{k,l} + B_{ij}^{k,l}$: the ij^{th} element of the bus admittance matrix between phase k and phase l

$g_{ij}^{k,l} + b_{ij}^{k,l}$: the admittance of the series branch connecting bus i and bus j between phase k and phase l

Appendix D: Robust Estimation

The M-estimators are class of robust estimators used in power system and are based on the maximum likelihood concept. The M- estimator minimise the following objective which is expressed as a function of the measurement residuals $\boldsymbol{\rho}(r)$ [39], [47]:

$$Minimize\ J = \sum_i^m \rho(r_i) \tag{D.1}$$

The various types of estimators that use function $\boldsymbol{\rho}(r)$ have been explored for power system state estimation. The following are some of choices of $\boldsymbol{\rho}(r)$ [39].

- Quadratic Constant (QC) estimator

The following shows the objective function for QC estimator.

$$\rho(r_i) = \begin{cases} r_i^2 & if\ |r_i| \le a \\ a^2 & otherwise \end{cases} \tag{D.2}$$

a: tuning parameter

The QC estimator has decent bad data rejection properties which can eliminate large errors more efficiently than other objectives. For example, if the cause of bad data is due to meter malfunction, QC objective provides better estimate to the meter failure. Some of the main features of this estimator are enhanced bad data rejection, superior performance indices, and robust convergence. However the main downside of QC objective is that it is not convex, which creates convergence and computational complications.

- Weighted Least Absolute Value (WLAV) estimator

The objective function of WLAV estimator can be defined as:

$$\rho(r_i) = |r_i| \tag{D.3}$$

The advantage of WLAV over WLS is that it can constantly identify and reject the bad data during the estimation process and replace them by the redundant measurements. However the performance of the WLAV estimator depends on the adequate redundancy in measurements

in order to replace the bad data. The downside of WLAV method in comparison to WLS is its complexity and longer computational time which makes it incompatible for real time state estimation application.

- Schweppe Huber Generalised M (SHGM) estimator

The objective function of SHGM estimator is expressed as:

$$\rho(r_i) = \begin{cases} \frac{1}{2} r_i^2 & if \ \ |r_i| \leq a w_i \\ a w_i |r_i| - \frac{1}{2} a^2 w_i^2 & otherwise \end{cases} \quad \text{(D.4)}$$

w_i: weighting factor

a: tuning parameter

The SHGM estimator is benefits from characteristics of both the WLS and WLAV estimators. It performs like WLS estimator for small values of errors which are below some specified threshold and for the points outside the threshold it behaves like the WLAV estimator. However the performance of this estimator highly depends on w_i and a parameters which is the drawback of this method over WLS method.

- Square Root (SR) estimator

The objective function of SR estimator is shown as follow:

$$\rho(r_i) = \begin{cases} r_i^2 & if \ \ |r_i| \leq a \\ 4a^{3/4}\sqrt{r_i} - \ 3a^2 & otherwise \end{cases} \quad \text{(D.5)}$$

The SR estimator behaves like the WLS estimator computationally. It could detect and reject faulty measurements at around twice the computational cost of least squares without bad data rejection. Its bad data rejection characteristics lie between the SHGM and QC estimators. SR estimator doesn't require more computer time or complexity than the WLS estimator does.

In conclusion, although the bad data rejection properties of the robust estimators are very attractive, they could suffer from the possible existence of local minima. Other disadvantages of these estimators are their slow convergence or occasionally divergence, numerically unobservable situation due to the rejection of several measurements particularly in the case of poor local redundancy, high risk of wrong identification and partial rejection of bad data,

except for QC. In contrast the WLS can perform well under limited redundancies and large errors if the errors are Gaussian and their characteristics are known. Moreover the WLS method is computationally fast and provides optimal results due to the global convexity of the WLS objective.